UNIVERSITY OF LIVERPOOL

Department of Mathematical Sciences

Ph. D. Thesis

Submitted in fulfillment of the requirements of the degree of

Doctor of Philosophy

Temperature-based Weather Derivatives Modeling and Contract Design in Mainland China

Author: Lu Zong

June 2015

University of Liverpool

Temperature-based weather derivatives modeling and contract design in Mainland China

Lu Zong
Doctor of Philosophy

June 2015

Thesis Summary

In the presented thesis, we build the theoretical framework for the development of temperature-based weather derivatives market in China. Our research is divided into two separate studies due to their different scopes.

In the first study, we focus on the determination of the most precise model for temperature-based weather derivative modeling and pricing in China. To achieve this objective, a heuristic comparison of the new stochastic seasonal variation (SSV) model with three established empirical temperature and pricing models, i.e. the Alaton model [1], the CAR model [2] and the Spline model [3] is conducted. Comparison criteria include residual normality, residual auto-correlation function (ACF), Akaike information criterion (AIC), relative errors, and stability of price behaviors. The results show that the SSV model dominates the other three models by providing both a more precise fitting of the temperature process and more stable price behaviors.

In the second study, novel forms of temperature indices are proposed and analyzed both on the city level and the climatic zone level, with the aim to provide a contract-selecting scheme that increases the risk management efficiency in the agricultural sector of China. Performances of the newly-introduced indices are investigated via an efficiency test which considers the root mean square loss (RMSL), the value at risk (VaR) and the certainty-equivalent revenues (CERs). According to the results, agricultural risk management on the city scale can be optimized by using the absolute-deviation growth degree-day (GDD) index. On the other hand, it is suggested that climatic zone-based contracts can be more efficient compared with city-based contracts. The recommended contract-selection scheme is to purchase climatic zone-based average GDD contracts in climatic zone II, and to purchase climatic zone-based optimal-weighted GDD contracts in climatic zone I or III.

Keywords: Weather derivatives, China, stochastic modeling, Monte Carlo simulation, risk management, agricultural risk.

Contents

List of Figures

List of Tables

Chapter 1

Introduction

Weather risks arise due to the unpredictability of weather variations. Regarding to the world's economy, the majority of market participants is affected by weather risks. Especially industries in the sector of energy, agriculture, retail, construction and transportation are claimed to be with the highest degree of weather sensitivities [4]. As a possible hedging instrument, weather derivatives were first traded in the US in 1996 and 1997 in the form of insurance [5]. In the year of 1999, weather derivatives were officially launched by Chicago Mercantile Exchange (CME). At this moment, a variety of weather products are being traded on the CME which cover weather derivative contracts written on temperature, precipitation, frost, hurricane and snowfall. As the most original type of weather products, temperature-based derivatives are considered to be the most widely traded and with the most mature market. So far, temperature contracts on the CME cover the United States, Canada, Europe, Japan and Australia.

Despite of the booming markets in the USA and Europe, weather derivatives in Asian countries are still underdeveloped. So far, Japan is the only country where there are weather derivative deals taking place in the Asia pacific zone. However, studies suggest that weather risk management tools, like weather derivatives, are in great demand in developing countries, like China, from different aspects [6, 7]).

Among all the economic sectors that are exposed under weather uncertainties, agriculture is always the priority to be considered when it comes to weather risk management in China [8–10]. The importance of the agriculture industry is recognized for three reasons. First, agriculture is one of the most important sectors in terms of the contribution of the GDP in China. Second, 45.23% of the population of China live on farms [11]. Finally, agriculture in China is more sensitive upon weather risks than in developed countries due to its extremely large rural population and underdevelopment.

The major purpose of this thesis is to offer valuable information to those who are interested in issuing temperature-based weather derivatives in China.

1.1 Thesis structure and objectives

The essential barrier of studying temperature-based weather derivatives in China is due to the absence of real market, where weather derivative transactions take place. In this case, market-based researches and analyzes have to be discarded. In this thesis, an attempt is made to build a systematic framework of temperature-based weather derivative modeling in China as a foundation of opening the Chinese weather derivative market.

Empirical analyzes are conducted based on the existing theory of temperature-based derivative modeling, along with original approaches adopted to the reality of Chinese market. Meanwhile, different possibilities of pricing methods are discussed, considering that there is no accessible data of the market price. Through this study, we hope to gain a comprehensive understanding of the temperature evolution, the price and the market behavior towards weather risks. Further, we propose a range of novel temperature-based indices, aiming to increase the efficiency of agricultural risk management. The risk hedging efficiency of the proposed indices are investigated empirically in order to test for their practical values.

The thesis is organized as follows.

In Chapter 2, an overview on different forms of temperature-based derivatives and on relevant studies of temperature-based derivative modeling is provided. Structures of the most common valuation frameworks of temperature-based derivative contracts are outlined. The objective of Chapter 2 is to introduce the research background and preliminaries for the following chapters of temperature modeling and pricing.

According to the scopes of the researches, the thesis is divided into two parts from Chapter 3, namely the temperature modeling and pricing part (Chapter 3 and 4) and the contract design and agricultural risk management part (Chapter 5) . In Chapter 3, we propose an new temperature model with temperature volatility expressed by a stochastic process. The new stochastic seasonal variation (SSV) model is then employed to fit the temperature data of twelve Chinese cities. Further, a discussion on the possible pricing approaches is provided regarding to the price risk that comes along with the stochastic process of the volatility. The objective of Chapter 3 is to increase the preciseness of temperature modeling on the basis of established temperature models, by removing heteroskedasticity via stochastic volatilities.

In Chapter 4, we carry out a heuristic analysis on the model performances of the proposed SSV model along with other three existing temperature models, i.e. the Alaton model [1], the CAR model [2], the Spline model [3], in capturing Chinese temperature fluctuation and in price behaviors. Recommendations on the application of different models are made taking into account the residual normality, autocorrelation functions (ACF), the Akaike Information Criterion (AIC), monthly relative errors (MRE) and contract prices. The major goal of this chapter is to examine the SSV model, and to find a most suitable model for temperature modeling and derivative pricing in China.

In Chapter 5, we look into the practical value of temperature-based derivatives in reducing yield-variation risks for Chinese farm households. We first define a variety of temperature indices based on both the city scale and the climatic-zone scale. Next, an efficiency investigation on weather derivatives [12] are applied to the new temperature indices. Through Chapter 5, we hope to increase the efficiency of agricultural risk management in China. Meanwhile, we aim to reduce the model dimension of temperature-based derivative pricing, and diverse the basis risk via spatial aggregation with climatic zone-based contracts.

Contributions of the current study are fourfold. First, a novel temperature model is developed, which takes into account the stochastic properties of the volatility process. Second, the study investigates modeling performances of the proposed temperature model along with other three standard existing temperature models, targeting on determining the most precise model for Chinese temperature data. Numerical studies based on thirty years of daily average temperature (DAT) data of twelve Chinese cities are conducted in order to examine the goodness-of-fit and the forecasting power of the temperature models. We hope to increase the reliability and robustness of our conclusion via a larger DAT sample size in the empirical analysis. Third, for the purpose of investigating the risk management scheme in agriculture-related sectors, we present three new types of temperature-based growth degree-day (GDD) indices. Efficiency tests on reducing agricultural yield-variation risks are conducted, aiming to find the type of GDD indices with the highest risk reducing power. Fourth, this study presents a novel type of temperature-based contracts, i.e. the climatic zone-based GDD contract, which gives identical prices to all the cities in the same climatic zone. The performance of the climatic zone-based GDD contract is examined in order to verify its practical value.

Chapter 2

Review of temperature-based weather derivatives

In this chapter, an overview of temperature-based derivative contracts is presented. In Section 2.1, we introduce temperature-based derivatives in a general scope, with particular focus on underlying temperature indices, contract specifications and pay-off styles. In Section 2.2, we provide a literature review on the existing valuation frameworks of temperature-based derivative contracts, where the advantages and the disadvantages of each method are discussed.

2.1 Introduction of temperature-based derivative contracts

Among all the weather derivative contracts that exist so far, temperature-based contracts are by far the most popular and the most widely traded. There are three reasons explaining why weather contracts written on temperature are more preferred. First, temperature is one of the crucial factors for a broad range of sectors, including agriculture, energy and retail, and has direct impacts on the profit of the business. Second, adequate financial risks associated with weather changes can be reflected by temperature changes. That is to say, even those sectors that are influenced by other weather factors, such as frost, hail, and fog, can possibly control their risk exposure via a temperature-based derivative contract. Typical examples of this type of industries are transportation and aviation. Third, compared to derivatives written on other weather factors, temperature-based derivatives cover an extensive diversity of contracts (see Section 1.2 and 1.3), which are designed to satisfy the needs of market participates facing all sorts of temperature-associated risks.

Apart from temperature-based derivatives, weather contracts written on precipitation, frost, hurricane and snowfall are traded in the CME as well. Second to temperature, precipitation is another common of weather factor to be considered, while dealing with weather risks, with respect to its great influence on a variety of market sectors. Moreover, among the sectors that depends upon the precipitation

conditions, there is a considerable amount of them affected by temperature at the same time. However, low correlation between the temperature and the precipitation behaviors requires risk hedging schemes combining the two types of weather risks. According to Pelka and Musshoff [13], it is actually better off to hold weather derivative contracts written on a single weather index, i.e. the temperature index and the precipitation index, and hedge associated risks separately, other than to hold a single complex contract written on a mixed index based on multiple weather indices. This argument arises as it is indicated in Pelka and Musshoff's study [13]that the mixed-index contract comes along with higher basis risks than the conventional single-index contract.

In this section, we give a general introduction of temperature-based derivative contracts from different angles. We first discuss the differences between weather derivatives and weather insurances. Next, a list of temperature underlyings are introduced together with a presentation of common payoff schemes of the temperature-based contract.

2.1.1 Weather derivatives or weather insurance?

Weather derivatives are sometimes referred as weather index-based insurances in the literature. However, the differences between insurances and derivatives cover multiple aspects. One of the most fundamental differences is the payoff of a derivative claim is calculated from the market price of its underlying, while the payoff of an insurance is calculated from the loss which is caused by the occurrence of a particular (pre-specified) event. Furthermore, typical types of derivative contracts include swaps, futures, options, etc..

Technically, weather derivatives and insurances play different roles in hedging weather related risks. That is, weather derivatives are targeted on those weather risks associated with higher probabilities and lower losses. For instance, a right temperature-based derivative contract allows agricultural producers to hedge yield risks resulted from adversely long cold period during the growing phase of a particular crop. Another example takes place in the energy sector, where weather changes would lead to the volumetric risk, which is recognized as the most fundamental risk of the industry. To be specific, as the demand of energy products fluctuates according to the change of weather conditions, so does the price. From the perspective of producers in the energy business, higher demands are often linked with higher profits, while lower demands are related with lower profits, or even loss. Such uncertainty of the profit forms the so-called volumetric risk. To address this problem, one possible mechanism is to purchase a weather derivative contract that describes the opposite situation to his favorable weather condition, thus to hedge the risk.

On the other hand, weather insurances are mainly targeted on more vital risks that are related to weather catastrophes, which cause huge damages, such as flood, hurricane, etc.. Moreover, weather-related insurances are usually devised in more general forms which covers all possible risks that might be faced by a particular market sector, which includes the weather risk. Most of the time, such insurance

contracts are named after the particular sector that they are designed for, such as the agricultural product insurance. In this sense, weather insurances tend to generate higher transaction costs compared to weather derivatives.

2.1.2 Common underlyings of temperature-based weather derivatives

Different from traditional financial derivatives, underlyings of temperature-based weather derivatives are temperature indices which are non-tradable. So far, the most frequently discussed and commonly traded temperature underlyings are the cumulative average temperature (CAT), the cooling degree-day (CDD) and the heating degree-day (HDD). Contracts written on different temperature indices hedge temperature-associated risks from different angles.

Cumulative average temperature (CAT)

Generally speaking, the most fundamental temperature variable which temperature indices are calculated from is the so-called "daily average temperature (DAT)". The definition of the DAT varies from country to country. In China, the DAT is defined to be the mean value of the temperatures measured at four time point of the day, namely 2:00, 8:00, 14:00, and 20:00 [14]. However, the most commonly-used definition of a DAT is the average of the daily maximum and minimum temperatures.

Given the contract period, the cumulative average temperature (CAT) is define as:

$$CAT(0,t) = \sum_{i=1}^{t} T(i), \tag{2.1}$$

where $T(i)$ stands for the DAT of day i.

On the Chicago Mercantile Exchange (CME), where weather derivative transactions are organized, contracts written on the CAT are open to the Canadian and the European markets.

Cooling degree-day (CDD) and heating degree-day (HDD)

Compared with CAT indices, degree-day indices are even more widely traded around the world. Markets that have access to contracts written on degree-day indices, are in the U.S, Canada, Europe, and Australia. Degree-day indices measure temperature differences between the DAT and a pre-specified threshold (18 °C in Canada, Europe, and Australia, and 65 °F in the U.S). On the daily scale, the definitions of the HDD and of the CDD are respectively given by Eq. 2.2 and 2.3:

$$HDD(i) = max(18 - T(i), 0), \tag{2.2}$$

$$CDD(i) = max(T(i) - 18, 0), \tag{2.3}$$

where $T(i)$ denotes the DAT of day i.

With the contract period $(0, t]$, the accumulated HDD and CDD indices follow:

$$HDD(0,t) = \sum_{i=1}^{t} max(18 - T(i), 0), \tag{2.4}$$

$$CDD(0,t) = \sum_{i=1}^{t} max(T(i) - 18, 0). \tag{2.5}$$

Considering different risk managing demands, temperature-based derivative transactions divide the year into two seasons, i.e. the cold season and the warm season. CDD contracts are generally issued in a warm season in order to hedge the risks caused by the over-high temperatures, and the HDD contracts are issued in the cold season to hedge the risks due to the over-low temperatures. However, applications of HDD and CDD can be rather flexible. Technically, by changing the combination of contract types (futures, put or call options) and indices (HDD or CDD) accordingly, different sorts of temperature risks can be hedged in an efficient manner.

2.1.3 Temperature-based weather derivative contract types

To satisfy a variety of market participants with different financing purposes, temperature-based weather derivatives are traded in multiple forms. Unlike weather insurances, weather derivatives aim at reducing weather risks with a lower degree of damage, but higher probability. For instance, holding a HDD derivative contract before winter can help farm households offset the loss due to low yields under the forthcoming low temperature.

Technically, transactions of weather derivatives are of the same dynamics with the conventional commodity-based derivatives. To be specific, weather derivative contracts are built between two parties, i.e. the buyer and the seller. The buyer, who is also known as the portfolio holder, takes the short position in the transaction. Note that when a risk-neutral method is applied to valuate a weather derivative contract, one shall pursue from the buyer's point of view.

Basically, the most widely-traded temperature-based weather derivative contracts are futures, options written on the futures, and swaps. In the following part of this section, brief explanations to the three types of temperature-based derivative contracts are provided.

Temperature futures

Table 2.1 lists the major features of a temperature future contract. As it is discussed in the previous section, common underlyings of temperature futures are the CAT, the CDD and the HDD. In a temperature future contract, the contract size and the

tick size specify the fundamental measures for the contract valuation. On the CME, the contract size of temperature-based derivatives varies from country to country, but the tick size stays one index point for all the regions. Basically, the contract period of temperature futures can be either a month or a season (three months). Further, it is claimed by CME that for the degree-day contract, market participants can only have access to the CDD contracts during the warm months, and the HDD contracts during the cold months.

Table 2.1: Contract specifications of temperature futures

Underlying	Temperature index
Contract size	The unit price of the underlying index
Tick size	The minimum fluctuation
Contract period	Monthly or seasonally

By holding a temperature future, one has the obligation to buy a particular volume of temperature indices with a particular price on the expiration date. Note that the volume and the price are pre-specified by the future contract. Wherefore the holder of a future contract has the possibility of suffering from negative payoffs, if the price of the temperature index is below his expectation at the expiration data. In order to constrain the payoff deviation, there always exist upper and lower limits on the payoffs in the real world transactions.

To mathematically express the payoff of a future contract, we let $X(0,T)$ denote the value of the temperature index value during the contract period $[0,T]$, K denote the strike level, α denote the tick size and L_1 and L_2 respectively denote the upper and the lower limit of the temperature index value. Thus, the payoff P satisfies:

$$P = \begin{cases} \alpha \times (L_2 - K), & X(0,T) < L_2 \\ \alpha \times (X(0,T) - K), & L_2 \leqslant X(0,T) \leqslant L_2 \\ \alpha \times (L_1 - K), & X(0,T) > L_1 \end{cases} \tag{2.6}$$

Theoretically, for the purpose of hedging risks, buyers shall purchase the temperature future that is contrary to the favorable weather condition of their commercial activities in the spot market.

Temperature options

Temperature-based options are traded in a close way with temperature futures. The key difference between the two weather products is that temperature-based options also give holders the right to give up exercising the option, which enables the holder to avoid losses. As a result, the payoff of a temperature call option P_C and of a temperature put option P_P respectively can be expressed as:

$$P_C = \begin{cases} \alpha * max[(X(0,T) - K), 0], & X(0,T) \leqslant L_1; \\ \alpha * (L_1 - K), & X(0,T) > L_1 \end{cases} \tag{2.7}$$

$$P_P = \begin{cases} \alpha * (K - L_2), & X(0,T) < L_2 \\ \alpha * max[(K - X(0,T)), 0], & X(0,T) \geqslant L_2, \end{cases} \tag{2.8}$$

where the denotations follow the same specifications as those for future contracts.

With respect to the different payoff schemes of future and option contracts, Figure 2.1 gives an example of payoff changes of a future contract, a call option contract and a put option contract in response to different values of the temperature index.

Figure 2.1: Temperature contract payoff diagrams

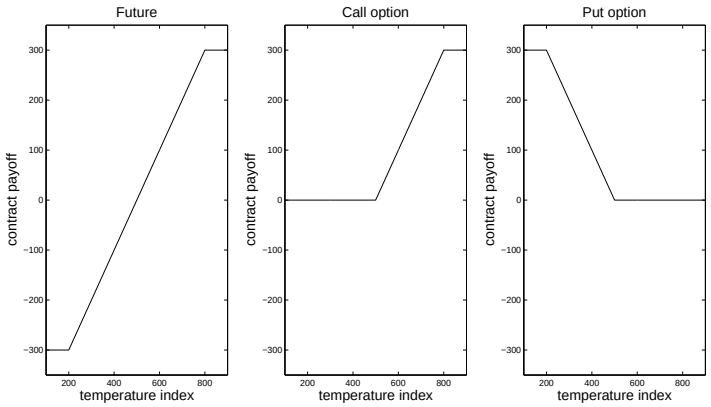

Note that the strike prices of the temperature contracts in Figure 2.1 are all set to be 500. Further, we let the tick size equal to one, and the upper and the lower limits of the temperature index respectively equal to 800 and 100.

Temperature basket options

A temperature basket option is written on temperature indices of multiple regions. This type of derivative contracts reduces the transaction cost of cross-regional weather risk management. Market participates whose business is spread in multiple locations and influenced by temperature risks are the major group of people benefited from temperature basket options. On the other hand, issuers of temperature basket options increase the market liquidity by encouraging transactions between people from different places.

From the modeling point of view, basket options could be the solution of the model dimension reduction problem in pricing temperature-based derivatives [15]. Furthermore, the way that basket options are structured incorporates the idea of spatial aggregation, which is claimed to be a possible resolution for diminishing the basis risk of weather derivatives [16].

2.2 Temperature-based derivative contract valuating

The major barrier of valuating temperature-based derivative contracts arises as the underlying is non-tradable. To be specific, since there is no observable market price for temperature, one cannot apply the classic non-arbitrage method, such as the Black-Scholes model, which is commonly used for equity-based derivative pricing. Generally, methods of valuating temperature-based derivatives can be grouped into three categories.

2.2.1 Burn analysis and index modeling

The first category is the so-called burn analysis, which estimates temperature-based derivative prices basing on historical payoffs of the contract. To apply burn analysis to derive the fair price of a temperature-based contract, one needs to make sure that the historical payoff data is properly detrended to be time-stationary before looking into its distribution. For instance, a detrending process regarding to global warming is needed in most cases in order to achieve the data stationarity, as temperature increases year by year. After the detrending process, the fair price of the contract theoretically equals to the expectation of historical payoffs. Further, an additional risk loading might be added to the price in some cases, taking into account the risk taken by the seller who has the probability of paying out [5, 17]. Technically, one of the vital disadvantages of burn analysis is the loss of information, as it only considers the overall payoff instead of the underlying itself, which may cause large biases in the price prediction. Moreover, in markets without accessible payoff data, such as China, burn analysis cannot be applied.

As an extension of burn analysis, index modeling models the distribution of the underlying index, instead of the payoff. By employing different statistics of the index distribution, index modeling provides a more accurate and more comprehensive understanding to the temperature evolution than burn analysis. However, it is claimed in some literature that index modeling is not necessarily a more advanced model than burn analysis, as in reality, it can be rather difficult to find a suitable known distribution to fit the data, especially when the size of the data is limited [5].

Generally, the most attractive advantage of burn analysis and index modeling is their simplicity, since there is no simulation, or complex mathematics required in order to find out the contract price.

2.2.2 Utility-based modeling

The second class of temperature-based derivative pricing methods is based on the argument of constructing equilibrium using the Utility Theory. Practically, utility-based approaches are more commonly used for economical purposes, other than financial engineering, as this type of approaches is built on a more macroscopical base which usually draws emphasis on the achievement of economical equilibrium. On the other hand, financial engineers tend to believe that prices of financial derivatives can be reflected by the historical prices of the underlying asset, in which case no-arbitrage models, or actuarial pricing approaches are more frequently adopted.

Generally speaking, in the valuation of temperature-based derivative contracts, the most significant advantage of utility-based models is that they provide a possible access to the derivation of the market price of temperature risk [18]. However, utility-based approaches usually heavily rely on sophisticated assumptions on the economical environment and on the utility function, which restricts the models' performance in practice.

In this subsection, we provide overviews of three typical utility-based models proposed to price temperature-based derivatives. The advantages and disadvantages of each model will be discussed accordingly.

Cao and Wei model [18]

The first utility-based method is proposed in Cao and Wei's study [18]. To determine the fair price of temperature variables, Cao and Wei [18] build their model under the framework of the Lucas model [19], in which a pure-exchange economy is assumed. According to Lucas [19], a pure-exchange economy is formed when all goods in the economy are produced costlessly by several productive units y_i, $i = 1, ..., n$, and traded among consumers. Equilibrium occurs when the total consumption equals to the total output. Cao and Wei [18] adopts temperature variables Y_t into this case as the output of one productive unit, equivalently an asset, and the aggregate dividend δ_t is recognized as the total output/consumption. Thus, the equilibrium exists when:

$$X(t,T) \times U_c(\delta_t, t) = E(U_c(\delta_t, T))q_T, \forall t \in (0,T). \tag{2.9}$$

where $X(t,T)$ denotes the contract price at time t, given that the future payoff at time T is q_T. $U_c(\delta_t, t)$ denotes the first order derivative of the utility function at time t and consumption equals to δ_t. With repect to Eq. 2.9, in order to compute the price of a temperature-based derivative contract, one needs to determine the time dependent processes respectively of the payoff q_t and of the dividend δ_t, together with the utility function $U(c_t, t)$.

Starting off with the payoff process, contract payoffs can be derived from underlying temperature indices, which are driven by the temperature evolution. According to Cai and Wei [18], the daily average temperature of day t can be expressed as:

$$Y_t = (\frac{\beta}{365}(t - \frac{T}{2}) + \bar{Y}_t) + R_t, \tag{2.10}$$

where $\bar{Y}_t$ represents the N-year historical average temperature for each day of the year which satisfies:

$$\bar{Y}_t = \bar{y}_{365\times 1} \otimes l_{N\times 1}, \tag{2.11}$$

$$\bar{y}_d = \frac{1}{N}\sum_{yr=1}^{N} y_{yr,d}, \tag{2.12}$$

where $d = 1, 2, ..., 365$, and $l_{N\times 1}$ is a $N \times 1$ vector of ones.

Further, R_t in Eq.2.10 is the residual of daily temperature which follows an auto-correlation process with lag k:

$$R_t = \sum_{i=1}^{k} a_i R_{t-i} + \sigma_t * \xi_t, \tag{2.13}$$

where

$$\sigma_t = \sigma_0 - \sigma_1 |sin(\pi t/365 + \phi)|, \tag{2.14}$$

and $\xi_t \sim i.i.dN(0, 1)$.

The aggregate dividend follows a Markov process correlated with the temperature process, which is expressed as:

$$\ln \delta_t = \alpha + \mu \ln \delta_{t-1} + \upsilon_t, \tag{2.15}$$

where

$$\upsilon_t = \sigma\epsilon_t + \sigma[\frac{\varphi}{\sqrt{1-\varphi^2}}\xi_t + \sum_{i=1}^{m}\eta_m \xi_{t-m}]. \tag{2.16}$$

In the preceding formulae, μ is the mean-reverting parameter which satisfies $\mu \leqslant 1$, and $\epsilon_t \sim i.i.dN(0, 1)$. Note that φ represents the contemporaneous correlation between the temperature and the dividend processes.

Finally, Cao and Wei [18] specify the utility function as:

$$U(c_t, t) = e^{(-\rho t)}\frac{c_t^{\gamma+1}}{\gamma + 1}, \tag{2.17}$$

with the rate of time preference $\rho > 0$, and the risk parameter $\gamma \leqslant 0$.

Therefore, one can valuate temperature-based weather derivative contracts by applying temperature and consumption data to Eq. 2.11-2.17.

The most outstanding contribution of the Cao and Wei model [18] is that it provides a solution to the estimation of the market price of risk (MPR). First of all, it is a general consensus that temperature-related risks that stem from production

variations are resulted from temperature fluctuations. However, to derive the price of such risk mathematically is another story. Cao and Wei [18] argue that the inherent risk premium of temperature contracts can be fully reflected by the correlation between the aggregated dividend and the underlying temperature index. In this way, the risk premium equals to zero only when the temperature and the dividend processes are "completely independent".

The major drawbacks of Cao and Wei's method [18] are twofold. First, the model is built on an ideally specified environment with many assumptions, which increases the level of the model risk. For instance, the pure exchange economy described in the study can hardly be adopted to the real market. Further, the utility function, the risk parameters, i.e. γ and ρ, and the mean-reverting parameter μ are specified without empirical calibration, which may lead to large biases to the fair price. Second, the utility function that is employed in the Cao and Wei model [18] requires the consumption data, which complicates the valuation procedure. The overall complexity of the Cao and Wei model [18] tends to generate greater model risks than those straight-forward methods, namely burn analysis, index modeling, and daily average temperature (DAT) models. Moreover, the complexity makes the valuation more time-consuming and more costly.

Davis model [20]

Davis (2001) [20] proposes to price temperature-based weather derivatives basing on the argument of utility maximization. The fundamental difference between the Davis model [20] and the Cao and Wei model [18] is their basic assumptions on the economic environment. Cao and Wei [18] argue ideally that the market participates are affected by weather risks in an identical way, while Davis suggests that agents in different sectors of the market face specific weather risks with different levels, and will only purchase weather contracts if the purchase increases their utility.

To begin with, the underlying temperature variable X_t, i.e the accumulated degree-day index, and the commodity price S_t are assumed to be log-normal with correlation parameter ρ, thus:

$$dX_t = \nu X_t\, dt + \gamma X_t\, dw_1(t), \tag{2.18}$$

$$dS_t = \mu S_t\, dt + \sigma S_t\, dw_2(t). \tag{2.19}$$

Now assume the sales volume of the commodity $v(t)$ is linearly affected by the temperature variable X_t. Therefore, $v(X_t)$ is given by:

$$v(X_t) = \alpha X_t. \tag{2.20}$$

Thus, the profit Y_t satisfies:

$$Y_t = \alpha X_t S_t. \tag{2.21}$$

Substitute Eq. 2.18 and 2.19 into Eq. 2.21, the profit Y_t can be written as:

$$Y_t = \theta Y_t \, dt + \xi Y_t \, dw(t), \tag{2.22}$$

where

$$\theta = \nu + \mu + \gamma\sigma\rho, \tag{2.23}$$

$$\xi = \sqrt{\nu^2 + \mu^2 + 2\gamma\sigma\rho}, \tag{2.24}$$

and dw is a new Brownian motion, which follows:

$$dw = \frac{1}{\xi}(\gamma \, dw_1 + \sigma \, dw_2). \tag{2.25}$$

Given that the objective is to maximize the utility, Davis assumes that the value of the optimal portfolio at time T equals to the net profit Y_T. Thus, the temperature-based contract price in an equilibrium condition satisfies:

$$P_T = \frac{E[U'(Y_T)B(X_T)]}{E[U(Y_T)]}, \tag{2.26}$$

where $B(X_T)$ denotes the contract payoff at time T, and $U(*)$ is the utility function.

Further, Davis species the utility function to be logarithmic:

$$U(y) = \log y. \tag{2.27}$$

Consequently, the pricing formula under the Davis model (2001) follows:

$$P_T = E[\frac{Y_0}{Y_T}B(X_T)], \tag{2.28}$$

where $Y_0 = \alpha X_0 S_0$.

Compared with the Cao and Wei model [18], the improvement of Davis's method is that it provides an access to the estimation of the risk parameters, which theoretically increases the model accuracy. However, the Davis model inevitably displays two typical weaknesses as an utility-based model. First, it is rather difficult and time-consuming to acquire complete data sets of commodity prices. Second, there is no solid evidence suggesting that the utility function employed is appropriately specified and suitable for the considered situation. Besides the drawbacks as an utility-based model, the major weaknesses of Davis model itself are twofold. In the first place, according to Davis [20] , the contract price changes from sector to sector, which brings up the transaction cost, in terms of both time and money. Next, the model is loaded with simplified assumptions which restricts the practical value of the model, and increases the model risk. For instance, the underlying index tends to show heavy tails and residual heteroscedasticity [27] in reality, instead of being log-normal as it is specified by Davis. Further, it is still arguable to simply presume

the sales volume $v(t)$ to follow a linear function of the temperature index X_t without any analytical evidence.

Platen and West model [17]

Platen and West derive their pricing model of temperature-based weather derivatives basing on the argument of the growth optimal portfolio (GOP) via the so-called "benchmark approach" [21]. The most significant difference between the Platen and West model [17] and other utility-based models is that Platen and West include actuarial pricing schemes to their model. In detail, suppose that there exists a portfolio containing different volumes of different assets. Let $S_i^{(j)}$ denote the price of the security account for the j^th asset at time t_i, the corresponding price ratio $h_i^{(j)}$ is defined as:

$$h_i^{(j)} = \begin{cases} \frac{S_i^{(j)}}{S_{i-1}^{(j)}}, & S_{i-1}^{(j)} > 0 \\ 0, & otherwise \end{cases} \tag{2.29}$$

for $i = 1, 2, ..., n$ and $j = 0, 1, ..., d$, where $S_i^{(0)}$ denotes the value of the domestic saving account at time t_i.

Thus, $S_i^{(j)}$ can be expressed as:

$$S_i^{(j)} = S_0^{(j)} \prod_{m=1}^{i} h_m^{(j)}. \tag{2.30}$$

Next, Platen and West [17] make an attempt to construct the so-called self-financing portfolio, which assumes that changes of the value of the portfolio are exclusively caused by changes of the value of the security accounts that forms the portfolio. The proportion of each asset in the portfolio is expressed as a vector process of π where $\pi = \pi_i = (\pi_i^{(1)}, ..., \pi_i^{(d)}), i = 0, 1, ..., n$, and

$$\sum_{j=0}^{d} \pi_i^{(j)} = 1. \tag{2.31}$$

Therefore, the price ratio of the self-financing portfolio $S^{(\pi)}$ is given by:

$$h_m^{(\pi)} = \frac{S^{(\pi)_m}}{S^{(\pi)_{m-1}}}. \tag{2.32}$$

To determine the growth optimal portfolio (GOP), Platen and West [17] first let the growth rate $g_i^{(\pi)}$ of a given portfolio process $S^{(\pi)}$ be defined as:

$$g_i^{(\pi)} = E[\ln(h_{i+1}^{(\pi)})|\mathcal{A}_{t_i}], \tag{2.33}$$

Thereby, the optimal growth rate g_i is the essential supremum which satisfies:

$$\underline{g_i} = ess\ sup_{S^{(\pi)} \in \mathcal{V}}\ g_i^{(\pi)}, \tag{2.34}$$

where $\mathcal{V}$ refers to the class of all self-financing portfolio processes that are strictly positive. Assume that there exists a portfolio $S^{(\underline{\pi})} \in \mathcal{V}$ satisfying:

$$g(\underline{\pi})_i = \underline{g_i} < \inf. \tag{2.35}$$

Such a portfolio can be recognized as the GOP if it is strictly positive for all π. Next, by assuming that the payoff H_{t_n} of an European contingent claim, such as a temperature-based weather derivative contract, is independent with the GOP value $S_n^{(\pi)}$, the fair pricing of the contingent claim satisfies:

$$C_{H_{t_n}} = E[\frac{S_i^{(\pi)}}{S_n^{(\underline{\pi})}}|\mathcal{A}_{t_i}]E[H_{t_n}|\mathcal{A}_{t_i}], \tag{2.36}$$

where t_n is the expiration date, and $i = 1, 2, ..., n$. Let

$$P(t_i, t_n) = E[\frac{S_i^{(\underline{\pi})}}{S_n^{(\underline{\pi})}}|\mathcal{A}_{t_i}], \tag{2.37}$$

and $P(t_i, t_n)$ is the fair price of a zero coupon bond [17] at time t_i which expires on t_n. Thus, the general pricing formula of the European contingent claim is given by:

$$C_{H_{t_n}} = P(t_i, t_n)E[H_{t_n}|\mathcal{A}_{t_i}]. \tag{2.38}$$

With the fair pricing formula Eq. 2.38, the price of a temperature-based weather derivative contract can be determined by the distribution of the contract payoff with respect to the temperature process. Platen and West [17] incorporate the actuarial idea to their model, which allows an emphasis on the risk neutral environment, while pricing temperature-based derivative contracts. Therefore, the Platen and West model [17] should be theoretically more accurate than other utility models, as its result reflects more information of the temperature evolution. Further, Platen and West [17] present their work in a more general case, which avoids assumptions on the utility function and on the dividend/asset price behavior, which increases the practical value of their model. Despite that the Platen and West model [17] provides pronounced improvements in the theory of utility-based models, the absence of considerations on the market price of temperature risk leaves the model in a less robust position.

2.2.3 Daily average temperature (DAT) modeling

The third class of temperature-based contract pricing methods starts off with modeling daily average temperature (DAT). Contract prices are then derived with respect to the distribution of the underlying temperature index. This type of methods also allows Monte Carlo simulation of contract prices. At this moment, contract valu-

ation based on daily temperature modeling has become the most popular method in the field, and is being developped both theoretically and empirically by a great number of studies.

The initial development of DAT models takes place in 2000 by Dornier and Queruel [22], who propose to use a continuous-time Ornstein-Uhlenbeck (OU) process to express the temperature evolution. The temperature volatility is assumed to be constant in the Dornier and Queruel model [22]. Subsequentially, as temperature data shows heteroskedasticity due to the volatility, an improvement is made by Alaton et al. [1] who introduce the monthly-constant volatility. Considering the OU process itself cannot model auto-correlation, Brody et al. [23] introduce a fractional Brownian motion to the DAT OU process. Furthermore, Benth and Saltyte-Benth [24] use a hyperbolic Levy-process to model the residual instead of a Brownian motion.

Beside DAT models built on stochastic processes, a wide range of auto-regressive models are applied to temperature data as well. For instance, Caballero et al. [25] suggest to use ARMA and ARFIMA models. Jewson and Caballero [26] propose a model called AROMA to process the slow decay of the autocorrelation function. An ARCH model is suggested by Campbell and Diebold [27]. Additionally, in Benth et al.'s study [28], the OU process is combined with an discrete autoregressive (AR) process to get a continuous-time AR process which has higher orders, namely the CAR model. Theoretically, there always exists a stochastic process to correspond the econometric process, as the latter one can be considered as the representation of a discretized form of the former one.

In the following part of this section, we introduce four typical temperature models and their pricing schemes. We then discuss in detail about the strengthes and the weaknesses of each model.

Dornier and Querel model [22]

Dornier and Querel [22] propose in their model to separate the DAT evolution into two parts, i.e. the seasonal trend and the random walk. The first part, namely the seasonality, is written as a sine function measuring both, the seasonal change and the global warming, which follows:

$$\mu(t) = A + Bt + C\sin(\omega t + \varphi), \tag{2.39}$$

where t denotes the time measured daily and $\omega = 2\pi/365$.

Meanwhile, Dornier and Querel [22] employ an Ornstein-Uhlenbeck (OU) process to express the random walk of the DAT fluctuation. The OU process by nature ensures that DAT moves around the mean function given in Eq. 2.39, and does not allow any drastic jump which leads to huge biases. Now the DAT process is expressed as:

$$dT(t) = -\alpha(\mu(t) - T(t))\,dt + \sigma\,dB(t), \tag{2.40}$$

where $\mu(t)$ is defined in Eq. 2.39. Further, α and σ denote respectively the mean-reverting rate and the temperature volatility, which are both assumed to be constant [22]. Solving Eq.2.40 by the Itō's Lemma, the DAT of day t satisfies:

$$T(t) = (T(s) - \mu(s))e^{-\alpha(t-s)} + \mu(t) + \int_s^t e^{-\alpha(t-\tau)}\sigma \, dW_\tau, t > s. \tag{2.41}$$

where T_s^m is given by Eq.2.39 and W_t refers to a Brownian motion.

The most pronounced contribution of Dornier and Querel [22] is their application of the OU process to the time series of daily temperature. However, the Dornier and Querel model [22] fails to take several components of the temperature process, such as the volatility evolution, the seasonality of the mean-reverting rate, and the daily temperature autocorrelation, etc., into account which causes comparatively large biases towards the real temperature distribution. More importantly, such bias in the temperature distribution can reduce the reliability of pricing results through the pricing machanism.

Alaton model [1]

The Alaton model [1] follows fairly similar dynamics with the Dornier and Querel model [22]. Generally speaking, Alaton et al. [1] keep the OU process driven by a mean sine function. At the same time, they modify the specification of the volatility parameter σ_t to be monthly constant. The DAT process under the Alaton model [1] satisfies:

$$dT(t) = -\alpha(\mu(t) - T(t)) \, dt + \sigma_t \, dB(t), \tag{2.42}$$

where $\mu(t)$ is the temperature mean function (see Eq. 2.39).

According to Alaton et al. [1], a seasonal trend of the temperature volatility is indicated when they analyze the DAT data of Stockholm. As a resolution, Alaton et al. [1] propose to assume σ_t to be constants that change every month. It is suggested by Alaton et al. [1] to estimate monthly volatilities with the mean value of the temperature quadratic variation and the regressed estimation, aiming to achieve a greater level of preciseness.

As it is explained by the Dornier and Querel model [22], the OU process models temperature deviations from the mean seasonal function μ_t with a reverting rate α, which can be solved by the Itō's Lemma:

$$T(t) = (T(s) - \mu(s))e^{-\alpha t} + \mu(t) + \int_0^t e^{-\alpha(t-\tau)}\sigma(\tau) \, dB(\tau). \tag{2.43}$$

Meanwhile, Alaton et al. [1] derive the approximation formula of temperature-based option prices basing on the Martingale measure Q, given that the Black-Scholes model cannot be applied in this case. Taking CDD call options as an example, its payoff can be written as:

$$X_n = \sum_{t=1}^{n} \max(T_t - 18, 0) = \sum_{t=1}^{n} T_t - 18n. \tag{2.44}$$

With the assumption that $X_n \sim N(\mu_n, \sigma_n^2)$, the strike price and the risk free rate are denoted by K and r, the CDD call option price follows:

$$C_{CDD}(t_0, t_n) = e^{-r(t_n - t_0)} \left[(\mu_n - K)\Phi\left(\frac{K - \mu_n}{\sigma_n}\right) + \frac{\sigma_n}{\sqrt{2\pi}} e^{\frac{-(K-\mu_n)^2}{2\sigma_n^2}} \right], \tag{2.45}$$

where Φ represents the cdf. of the standard normal distribution.

Compared with the Dornier and Querel model [22], Alaton et al. [1] provide a more comprehensive valuation framework of temperature-based derivative contracts, with monthly volatilities and approximation pricing formulae derived from the temperature process. In their empirical study of Stockholm temperature data, the result shows that the model performs in an arguably precise manner, with high goodness-of-fit to temperature data and reasonable contract prices. Further, Alaton et al. [1] look into the estimation of the market price of risk (MPR) by calibrating their model to real prices of HDD option contracts. The result indicates that the MPR is not necessarily constant.

Despite of the advantages in terms of simplicity and accuracy, the Alaton model [1] fails to capture daily temperature fluctuations in the Monte Carlo simulation in several empirical studies [7, 29], as only smooth trajectories are displayed. Technically, the fitting performance of the Alaton model [1] could be improved with more sophisticated autocorrelation and volatility components.

Continuous auto-regressive (CAR) model [2]

The CAR model keeps the framework of the Alaton model [1] . Different from the Alaton model [1], Benth et al. [2] add an CAR(p) process to the mean function solved by the multidimensional Itō's Lemma. Therefore, the daily temperature of day t satisfies:

$$T(t) = \mu(t) + X(t), \tag{2.46}$$

where $\mu(t)$ is defined by Eq. 2.39,
and

$$X(s) = exp(A(s-t))X(t) + \int_t^s exp(A(s-u))e_p\sigma(u)\, dB(u), \tag{2.47}$$

e_q is the q_{th} unit vector in $\mathbf{R}_p, q = 1, \ldots, p$.

The parameter A is a $p \times p$ matrix given by:

$$\mathbf{A} = \begin{bmatrix} 0 & 1 & 0 & \dots & 0 \\ 0 & 0 & 1 & \dots & 0 \\ \vdots & \vdots & \ddots & \vdots & \\ -\alpha_p & -\alpha_{p-1} & -\alpha_{p-2} & \dots & -\alpha_1 \end{bmatrix}, \tag{2.48}$$

where $\alpha_q, q = 1, \dots p$, are assumed to be constants.

Meanwhile, the temperature variance is modeled with a truncated Fourier series which is expressed as:

$$\sigma^2(t) = c_1 + \sum_{k=1} n(c_{2k} cos(2k\pi t/365) + c_{2k+1} sin(2k\pi t/365)). \tag{2.49}$$

According to Benth et al (2008), the optimal orders of the CAR process and of the truncated Fourier volatility process are respectively three and four.

With the determined temperature process, Benth et al. [2] derive the non-arbitrage approximation pricing formula under the CAR model. For a CDD future with $c = 18$ at time $t \leqslant t_0$, its prices follows:

$$F^{CAR}_{CDD}(t, t_0, t_n) = \sum_{t_0}^{t_n} \max(T(s) - c, 0) = \int_{t_0}^{t_n} v(t,s) \Psi \left(\frac{m(t, s, e_1' exp(A(s-t)X(t)))}{v(t,s)} \right) ds, \tag{2.50}$$

where

$$m(t, s, x) = \Lambda(s) - c + \int_t^s \sigma(u)\theta(u) e_1' exp(A(s-u)) e_p \, du + x, \tag{2.51}$$

$$x = e_1' exp(A(s-t))X(t), \tag{2.52}$$

$$v^2(t,s) = \int_t^s \sigma^2(u) (e_1' exp(A(s-u))e_p)^2 \, du, \tag{2.53}$$

$$\Psi(x) = x\Phi(x) + \Phi'(x). \tag{2.54}$$

Thus, the price of a CDD option contract under the CAR model can be obtained by:

$$C^{CAR}_{CDD}(t, \tau, t_0, t_n) = e^{-r(\tau - t)} [\max(F^{CAR}_{CDD}(\tau, t_0, t_n) - K, 0)]. \tag{2.55}$$

One of the most significant contribution of the CAR model is its prevailing accuracy in capturing the heteroskedasticity of temperature residuals, as it tends to achieve a higher degree of residual normality [7]. According to Zong and Ender [7], the CAR model demonstrates a substantial improvement on residual normality and error measures from the Alaton model [1] while being applied to Chinese DAT data. Moreover, Schiller et al. [3] conclude that the CAR model is more powerful

in temperature predictions than the Alaton model [1] in their study of the US DAT data.

Further, using the CAR model, Benth et al. [30] calibrate the MPR for temperature-based futures and options basing on the price data of Tokyo. Benth et al. [30] state that by assuming the MPR to be zero, one actually underestimates the real price of temperature risks. Instead, Benth et al. [30] suggest a seasonal MPR which is reversed to the seasonal variation of the temperature process.

Spline model [3]

The Spline model [3] is proposed by Schiller et al. and is applied to the DAT data of 35 US weather stations. Different from the two stochastic models introduced above, Schiller et al. [3] models the seasonal mean and the variance of DATs with two bivariate surfaces obtained from their corresponding tensor product splines.

To be specific, let $T_{d,y}$ denotes the temperature at day $d \in 1, 2..., 365$ of year $y \in 1, 2..., n$, which is given by:

$$T_{d,y} = \mu_{d,y} + \sigma_{d,y} R_t. \tag{2.56}$$

Schiller et al. [3] argue that both the mean temperature μ and the variance σ^2 can be modeled with a tensor product spline. In general, let $X_{d,y}$ be the tensor product spline we are interested in, namely the seasonal mean temperature or the DAT variance. $X_{d,y}$ follows

$$X_{d,y} = Y_{Dd,Kd} \otimes Y_{Dy,Ky}, \tag{2.57}$$

where $Y_{Dd,Kd}$ denotes the vector space of all splines with degree Dd and knot sequence Kd in the day direction, and $Y_{Dy,Ky}$ is the vector space of all splines with degree Dy and knot sequence Ky in the year direction.

Schiller et al. next model the residual R_t with an auto-regress on moving average (AROMA) process [26] which is given by:

$$R_t = \phi_1 \bar{R}_{m1,t} + \phi_2 \bar{R}_{m2,t} + ... + \phi_r \bar{R}_{mr,t} + B_t, \tag{2.58}$$

where B_t is the Brownian motion and $\bar{R}_{m,t}$ stands for the mean of the residuals in the past m days:

$$\bar{R}_{m,t} = \sum_{i=1}^{m} R_{t-i}. \tag{2.59}$$

Despite of the fact that the Spline model displays an exclusive strength in fitting the US temperature data [3] in the comparison with the index modeling, the Alaton model [1], and the CAR model [2]. In Zong and Ender's study [7], the Spline model [3] yields a lower rate of residual normality than the Alaton model [1] and the CAR model [2] while being used to Chinese DAT data. For the reason that temperature processes are highly localized, in Chapter 4, we are going to discuss the performance

of the Spline model in fitting Chinese DAT data in a more elaborate manner.

Generally speaking, the Spline model [3] prevails other stochastic DAT models with its prominent simplicity, which comes along with time-saving computation. However, the usage of the Spline model [3] on the modeling of temperature-based derivatives should be treated with caution, as one can hardly determine the distribution of temperature indices since temperature estimations are made by tensor product splines. As a result, it is rather difficult to derive an analytical pricing formula for temperature-based derivatives basing on the Spline model [3].

2.2.4 Modeling and pricing weather derivatives in China

Since there is no weather derivative market in China yet, one can neither calibrate the market price of weather risk, nor adjust the model risk of different weather models. Consequently, researches based on modeling and pricing weather derivatives in China can only build their arguments on the models' performances in terms of modeling underlying weather factors.

Despite that the absence of trading data is restrictive, there still exist plenty of studies aiming to provide precise modeling for weather derivatives in China. To be specific, Goncu [29] applies a seasonal volatility model to capture the fluctuations of the DAT data of Beijing, Shanghai and Shenzhen, thus to price the temperature-based weather derivatives for those three cities. It is claimed that for degree-day options of Beijing and Shanghai, price approximation formulae under the seasonal volatility model tend to produce very close prices with the Monte Carlo simulation. However, HDD option prices of Shenzhen obtained by the two methods tend to diverge in Goncu's study [29]. Meanwhile, Zong and Ender [7] carry out a model comparison including two temperature models, namely the Alaton model [1] and the CAR model [2], based on the DAT data of twelve Chinese cities. The result indicates that the CAR model provides better fittings to the Chinese DAT data. Further, Sun and Van Kooten [31] apply three different types of models, including Burn Analysis, a stochastic mean-reverting model, and an autoregressive (AR) model, to price derivative contracts written on growth degree-day indices for the Chinese city Etuokeqi. It is argued by Sun and Van Kooten [31] that AR(1) process with a sine function produces the most accurate result in temperature modeling, and the lowest risk premiums of GDD options in Etuokeqi.

Besides studies of modeling temperature-based weather derivatives, Goncu [32] uses a Markov Chain with jumps model for the precipitation time of Chongqing. Additionally, Zhu et al. [33] introduce a drought option, which is written on the temperature-precipitation joint index, for the purpose of hedging agricultural risks caused by droughts. Zhu et al. [33] then price drought options hypothetically using the DAT and the precipitation data of Ji'nan. Furthermore, Lou and Sun [34] suggest to use agricultural insurance contracts written on precipitation and temperature indices to hedge the freezing-damage risk of tea trees. Employing the data of economic losses caused by freezing damage, precipitation and temperature of Zhejiang Province, Lou and Sun [34] estimate the insurance premium rate basing on

the information diffusion theoretical model, and design the tea tree freezing damage insurance contract with the analytical result.

Chapter 3

A new temperature model with stochastic volatility

In this chapter, we introduce an innovative type of stochastic temperature models with the attempt to fill in the gap of stochastic volatility modeling of daily average temperature (DAT). The objective is to provide a higher level of goodness-of-fit to the temperature data of Chinese cities, by achieving the normality of model residuals. In detail, we propose to model the temperature volatility with an Ornstein-Uhlenbeck (OU) process as an extension of Benth and Šaltynė-Benth's work [24]. Subsquentially, we apply the so-called stochastic seasonal variation (SSV) model to the DAT data of twelve Chinese cities, thus to investigate the model performance. To the best of our knowledge, this model has not been discussed in the literature.

This chapter proceeds as follows. In the next section, we give a brief overview of the DAT data applied in our study of temperature models. In the second section, we explain the model dynamics of the SSV model with the presentation of its mathematical framework. In the third section, we explain the parameter estimation procedure of the SSV model. In the last section, we discuss possible pricing approaches that could be applied based on the SSV model.

3.1 Data overview

In this chapter, we select twelve Chinese cities regarding to the Standard of Climatic Zone Partition of China. It is a typical partition method used by Chinese architects for the purpose of distinguishing construction standards among regions with different climate characteristics. As it is displayed in Figure 3.1, the standard divides the mainland of China into seven climatic zones.

Since the major factors of the partition method are temperature and precipitation, we suppose the possibility that it is also valid for our joint modeling of temperature derivatives. We are more interested with the four coastal climatic zones I, II, III and IV, as they constitute the eastern part of China which is more economically developed and with a higher chance of issuing weather derivative contracts first. In this study, we select two to three cities from each of these four climatic zones. For

Figure 3.1: Standard of Climatic Zone Partition of China

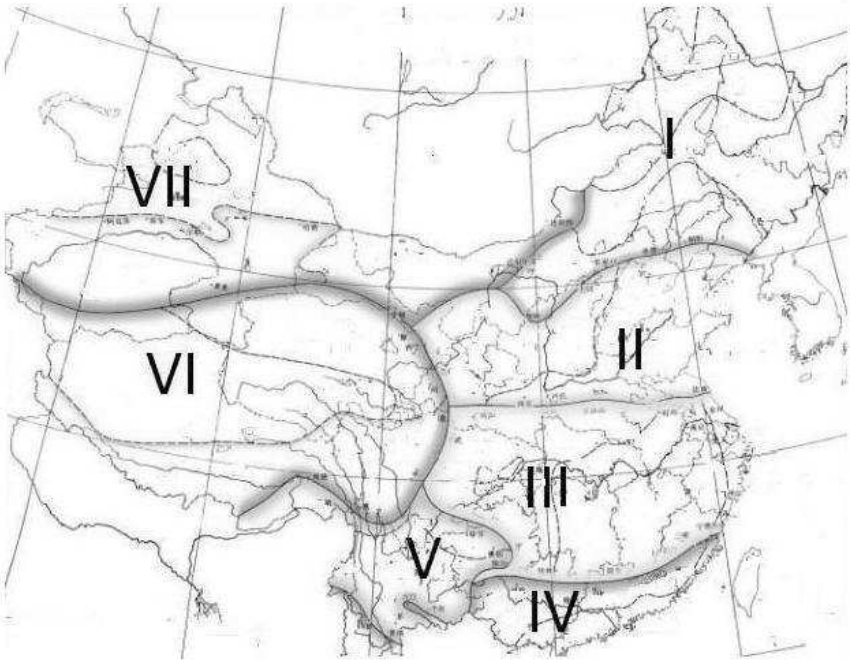

the rest of the climatic zones, namely V, VI, and VII, that cover the less developed regions of China, we only include one city per climatic zone. Generally, the climate of the four eastern climatic zones tends to be more humid with a greater amount of precipitation than the three inland climatic zones in the west.

Table 3.1 gives an overview of the DAT samples of the twelve cities considered in this study. Apart from Shanghai, the duration of the data is thirty years from January 1983 to December 2012. Due to the change of meteo-stations, we only obtain twenty years of Shanghai DAT data, which is from January 1993 to December 2012.

3.2 Model dynamics

Despite that the CAR model [2] outperforms the Alaton model [1] and the Spline model [3] while being applied to Chinese temperature data [7], one can still observe heteroskedasticity existing in the model residual. Further, for long-term temperature forecasts, the CAR model still tends to generate large biases. Even if the temperature volatility can be adjusted every day, the volatility remains deterministic. As a result, we propose a new temperature model under which the temperature variation is expressed as a stochastic process.

Similar with Alaton et al.'s work [1], we model the mean temperature process with an OU process driven by a sine function. Hence, the temperature process is expressed as:

Table 3.1: Mean, standard deviation, max and min values of twelve cities' daily temperature (May 1983 - June 2013)

	Climatic zone	Mean	Standard deviation	Max	Min
Harbin	I	4.95	14.91	30.9	-30.9
Changchun	I	6.20	14.07	30.4	-30.1
Beijing	II	12.96	11.03	34.5	-12.5
Tianjin	II	12.96	11.15	32.9	-14.1
Shanghai	III	16.38	8.75	34.2	-4.8
Hangzhou	III	17.01	8.93	35.0	-4.7
Nanjing	III	15.95	9.38	34.5	-7.8
Guangzhou	IV	22.43	6.17	34.2	3.3
Hainan	IV	25.28	4.35	32.6	9.8
Kunming	V	15.53	4.85	24.6	-3.0
Lhasa	VI	8.54	6.70	22.6	-10.5
Urumchi	VII	7.41	13.71	33.1	-27.2

$$dT(t) = -\alpha(\mu(t) - T(t))\,dt + \sigma_t\,dB(t), \tag{3.1}$$

where

$$\mu(t) = A + Bt + C\sin(\omega t + \varphi), \tag{3.2}$$

Next, instead of using a deterministic function to express the volatility as the Alaton model [1] and the CAR model [2], we employ another OU process to model the temperature volatility σ^2. That is:

$$d\sigma^2(t) = -\kappa(\theta(t) - \sigma^2(t))\,dt + \eta(t)\,dB_2(t), \tag{3.3}$$

where $B_2(t)$ is a Brownian motion which is assumed to be independent with the Brownian motion of the temperature process, and $\eta^2(t)$ is the volatility of the temperature volatility. As the mean squared residual of the volatility process tends to be more fluctuant in the cold season than in the warm season, seasonality exists in the volatility of temperature variations. As a result, we assume that $\eta^2(t)$ is piecewise-constant and takes different values in the cold season (November to April) and in the warm season (May to October).

We build the SSV model on the argument that the temperature volatility fluctuates over a particular mean $\theta(t)$ with a reverting rate κ. In this manner, the selection of the mean $\theta(t)$ is crucial. In the early work of Mraoua and Bari [35], the mean is set to be a constant. However, as seasonality can still be observed in the volatility of Chinese DAT data [7], we let $\theta(t)$ be a truncated Fourier series which is inspired by the CAR model [2], thus

$$\theta(t) = c_1 + \sum_{k=1}^{4}(c_{2k}cos(2k\pi t/365) + c_{2k+1}sin(2k\pi t/365)). \tag{3.4}$$

Note that the truncated Fourier series is specified with order four, which is suggested by Zong and Ender [7] in their study of Chinese DAT data.

Solved by the Itō's Lemma, Eq. 3.3 can be transformed as:

$$\sigma^2(t) = (\sigma^2(0) - \theta(0))e^{-\kappa t} + \theta(t) + \int_0^t e^{-\kappa(t-s)}\eta(s)\, dB_2(s). \tag{3.5}$$

Mathematically, the SSV model follows rather similar dynamics with the Heston model [41] which is a classic stochastic volatility model used in the stock (option) pricing. Apart from the independent Brownian motions and the functional mean of the volatility OU process, the SSV model allows negative volatility as well as the Heston model. Nevertheless, we consider the SSV model to be a suitable candidate to capture the temperature volatility process for two reasons. In the first place, the temperature volatility exhibits a seasonality in its random walk, and it is reasonable to believe that the daily volatility evolutes around the mean seasonal function, which consents to the idea of the OU process. Second, compared with other stochastic processes, the OU process has less parameters, which ensures the simplicity of the model and lower computational cost.

3.3 Parameter estimation

In this section, we explain the procedure of estimating unknown parameters in the SSV model.

To begin with, We employ the ordinary least squares (OLS) approach to estimate the parameters in the sine function in Eq. 3.2, which contains parameter A, B, C and φ. Table 3.2 gives the estimated value of the four parameters of the twelve Chinese cities.

After determining the mean function of temperature seasonality, the time series of the volatility is obtained by substituting the observed DAT $T(t)$ and its corresponding estimated values of $\mu(t)$ to the following equation:

$$\hat{\sigma}^2(t) = [T(t) - \mu(t)]^2. \tag{3.6}$$

Now we move on to the next step in which the parameters in the volatility Fourier series (see Eq. 3.4) , namely $c_i, i = 1, 2, ..., 9$, are estimated. We conduct the OLS regression basing on the volatility estimator $\hat{\sigma}^2(t)$ obtained from Eq. 3.6. Table 3.3 gives the results of the estimation.

Meanwhile, let quadratic variation be the estimator of $\eta(t)$, we have

$$\eta(t) = \frac{1}{t}\sum_{j=0}^{t-1}(\hat{\sigma}^2_{j+1} - \hat{\sigma}^2_j)^2. \tag{3.7}$$

Table 3.2: Estimated values of A, B, C, and φ of twelve cities in Mainland China

	A	B	C	φ
Harbin	3.986	$1.776 * 10^{-4}$	20.165	-1.851
Changchun	5.527	$1.25 * 10^{-4}$	18.876	-1.863
Beijing	12.406	$1.022 * 10^{-4}$	15.017	-1.852
Tianjin	12.814	$0.278 * 10^{-4}$	15.205	-1.874
Shanghai	16.29	$2.212 * 10^{-4}$	11.703	-2.071
Hangzhou	15.951	$1.937 * 10^{-4}$	11.82	-2.015
Nanjing	14.999	$1.75 * 10^{-4}$	12.561	-1.974
Guangzhou	21.819	$1.123 * 10^{-4}$	7.649	-2.021
Hainan	24.916	$0.673 * 10^{-4}$	5.237	-1.86
Kunming	14.505	$1.872 * 10^{-4}$	5.898	-1.739
Lahsa	8.060	$1.441 * 10^{-4}$	8.496	-1.84
Urumchi	5.942	$3.241 * 10^{-4}$	17.81	-1.839

Table 3.3: Estimated parameters of the truncated Fourier series of the SSV model

	c_1	c_2	c_3	c_4	c_5	c_6	c_7	c_8	c_9
Harbin	18.8545	9.4615	6.5011	-0.0145	-2.5202	0.6006	-2.7075	2.3878	0.3556
Changchun	19.9299	11.5163	5.4403	-0.4327	-2.7339	-0.1373	-1.9830	1.5268	1.2060
Beijing	8.9580	1.7619	3.3921	-0.6485	-1.2152	-0.2747	-1.5019	0.9502	0.0569
Tianjin	18.8545	9.4615	6.5011	-0.0145	-2.5202	0.6006	-2.7075	2.3878	0.3556
Nanjing	8.8268	2.4156	2.5868	-0.0586	-0.6045	-0.3277	-1.3580	0.1160	-0.1427
Hangzhou	9.5552	2.1217	3.3875	-0.2195	-0.1430	-0.2302	-0.7634	0.3357	-0.3379
Shanghai	8.8197	4.0621	2.2694	1.2786	-0.2947	0.3805	-1.3606	0.7884	-0.5382
Guangzhou	8.6944	5.7114	4.6297	-0.1766	1.9698	-0.6841	-0.4102	-0.3169	0.0885
Hainan	5.2052	3.2284	3.0350	-0.0927	1.1127	-0.2706	-0.4466	-0.5313	0.2545
Kunming	5.8087	1.4335	2.4915	-1.0379	-0.8924	-0.0415	0.0055	0.2688	0.0564
Lhasa	6.8182	1.9545	2.2312	1.6025	-0.2588	0.4893	-0.2447	0.5171	-0.5680
Urumchi	21.0326	5.4778	4.9290	-1.6419	-2.1118	3.5296	-1.7058	1.0004	0.9036

The estimated values of $\eta(t)$ in the cold and the warm seasons are listed in Table 3.3.

The final step to estimate parameters of the SSV model is to calibrate the mean reverting parameters of the OU processes, that is α and κ. As it is argued by Alaton et al. [1], methods based on martingale estimation functions can be employed as time intervals between two consecutive DAT observations are bounded away from zero. As a result, approximations of the mean-reverting rates α and κ of the temperature and the volatility processes respectively follow:

$$\alpha = -\log\left(\frac{\sum_{i=1}^{n}\frac{\mu_{i-1}-T_{i-1}}{\sigma_{i-1}^2}\left(T_i-\mu_i\right)}{\sum_{i=1}^{n}\frac{\mu_{i-1}-T_{i-1}}{\sigma_{i-1}^2}\left(T_{i-1}-\mu_{i-1}\right)}\right), \tag{3.8}$$

$$\kappa = -\log\left(\frac{\sum_{i=1}^{n}\frac{\theta_{i-1}-\hat{\sigma}_{i-1}^2}{\eta_{i-1}^2}\left(\hat{\sigma}_i^2-\theta_i\right)}{\sum_{i=1}^{n}\frac{\theta_{i-1}-\hat{\sigma}_{i-1}^2}{\eta_{i-1}^2}\left(\hat{\sigma}_{i-1}^2-\theta_{i-1}\right)}\right). \tag{3.9}$$

Table 3.5 gives the values of α and κ obtained from the equations above.

Table 3.4: Estimated values of $\eta(t)$ in the cold and the warm seasons

	Cold season	Warm season
Harbin	5.9868	2.8884
Changchun	6.2205	2.7228
Beijing	2.5804	1.5107
Tianjin	5.9868	2.8884
Nanjing	2.7651	1.7152
Hangzhou	3.5856	2.1353
Shanghai	4.2581	1.7826
Guangzhou	2.6469	0.9445
Hainan	2.0417	0.5547
Kunming	2.0556	1.3460
Lhasa	2.0592	1.3903
Urumchi	6.6500	4.0239

3.4 Pricing temperature-based contract with the SSV model

As the SSV model determines the underlying process of a temperature-based derivative contract, theoretically all the existing pricing schemes for temperature-based derivatives can be applied. However, due to the fact that there is no existing weather derivative market in China, it is unlikely to use the market-based pricing approaches [5] which require the historical price data. Nevertheless, it is never a simple multiple choice question to select the most suitable pricing approach, as a broad range of factors, including costs, feasibility, accuracy, and model risks, need to be considered. In this section, we give a discussion on the possible pricing schemes of temperature-based derivative pricing in the context of the SSV model.

3.4.1 Utility Theory

One of the feasible approaches to price temperature-based derivative contracts in China is to apply the Utility Theory, which skips the computation of the market price of risk. To implement the valuation, one needs to be able to forecast the future payoff of the derivative contract, which can be done by employing the SSV model. Therefore, existing Utility Theory-based models, such as the Cao and Wei model [18], can be improvised by replacing the payoff processes described in the models with payoffs determined by the SSV model. The advantage of incorporating the SSV model with the Utility Theory is that it reduces model risks of the existing Utility Theory-based models by providing a better fitting to the temperature, thus to increase the accuracy of the payoff forecasting. On the other hand, such method remains the disadvantages of those utility-based models, of which the price uncertainty due to the altering selections of utility functions is the major concern that

Table 3.5: Estimated values of mean-reverting parameters α and κ in the SSV model

	α	κ
Harbin	0.2600	0.7791
Changchun	0.2732	0.8310
Beijing	0.3034	0.7117
Tianjin	0.3360	0.7791
Nanjing	0.2880	0.5380
Hangzhou	0.3061	0.5198
Shanghai	0.4108	0.8383
Guangzhou	0.1825	0.5394
Hainan	0.1356	0.5199
Kunming	0.3102	0.5765
Lhasa	0.3458	0.5017
Urumchi	0.1579	0.4150

may affect the reliability of the pricing result.

3.4.2 Self-financing portfolio theory

Another possible approach to derive the pricing formula based on the SSV model is to apply the self-financing portfolio theory, which is a broadly-used method for derivative pricing in the complete market. One typical example is the Black-Scholes model. However, underlyings of weather derivatives are weather factors that are not tradable in the capital market. In this case, the most fundamental assumption of non-arbitrage in the self-financing portfolio theory breaks down. As a result, due to the market incompleteness that pertains to weather derivatives, improvisations on the original method of the self-financing portfolio theory are required.

As it is described by Jewson et al. [5], one resolution of building non-arbitrage to price temperature-based options is to consider the option contracts are written on the temperature-based swaps which have accessible market prices. Let along the limitation on the liquidity of the swap market [5], this method cannot be applied in China as there has been no temperature-based swap transaction taken place so far.

To address the problems described above, tradable assets that are correlated with price uncertainties of temperature-based derivatives shall be introduced. Given the process of the correlated asset's price, dynamic hedging can be adopted by using the asset, the temperature-based derivative contract, and a bond to construct a non-arbitrage portfolio, thus to solve the partial differentiation equation (PDE) of the option price. An exposition of this method is provided by Broni-Mensah [36] based on the Alaton model [1].

In the case of the SSV model, since the temperature volatility follows a stochastic process as well as the DAT process, risks that come together with the uncertainty of the volatility need to be considered while valuating temperature-based derivatives.

Therefore, in order to derive option prices based on the SSV model, two tradable assets, which are respectively correlated with temperature and temperature volatility, need to be introduced. However, we can hardly consider the pre-discussed approach to be realistic, as problems come along with the determination of the volatility-correlated asset, which is even a tough issue in the equity-derivative market.

In conclusion, as neither the market-based pricing nor the derivation of PDE is feasible to be applied to valuate temperature-based derivatives in China, we infer that the self-financing portfolio theory is not the most suitable method under the SSV model in this case.

3.4.3 Monte Carlo simulation

Compared to the pricing approaches described in the preceding sections, the Monte Carlo simulation is considered to be the most straightforward method to price temperature-based derivatives, as no further variable or assumption needs to be incorporated. Technically, to apply the Monte Carlo simulation to financial derivatives, a closed-form solution of the stochastic differentiation equation (SDE) is always preferred as it gives precise simulation results. However, it is unlikely to solve the price of temperature-based derivatives explicitly under the SSV model given that both the temperature and the volatility are modeled stochastically. As a consequence, the Monte Carlo estimator can only be obtained after the continuous temperature and volatility processes are discretized. Analogue to the Heston model (1993), there exist a variety of simulation schemes when the volatility process is modeled by an OU process [37–40]. In this section, we discuss briefly four typical methods used to simulate the Heston model, after which, we introduce our improvised simulation scheme for the SSV model.

To begin with, we explain analytically the volatility process under the Heston/SSV model, whose transition density is driven by a non-central chi-square distribution. To be specific, conditional on the volatility V_s at time s, the volatility V_t at time t can be expressed as:

$$V_t = \frac{\eta_s^2(1 - e^{-\kappa(t-s)})}{4\kappa}\chi_d'^2(\lambda), \tag{3.10}$$

where κ and η_s^2 respectively denote the mean-reverting rate and the volatility of the temperature volatility process, and $\chi_d'^2(\lambda)$ denotes a non-central chi-square distributed random variable with d degrees of freedom and non-centrality parameter λ. d and λ respectively follows:

$$d = \frac{4\theta\kappa}{\eta_s^2}; \tag{3.11}$$

$$\lambda = \frac{4\kappa e^{-\kappa(t-s)}}{\eta_s^2(1 - e^{-\kappa(t-s)})}V_s, \tag{3.12}$$

where θ is the mean function of temperature volatility that is given by Eq. 3.4.

Besides the convenience of few assumption, the major concern of employing the Monte Carlo simulation stems from the trade-off between the computational cost and the accuracy of price estimators. That is to say, a more accurate Monte Carlo estimator requires a larger number of simulation paths and a smaller size of time increments, both of which will result in a higher cost. Among the existing simulation schemes of the Heston model [41], Broadie and Kaya's method [37] guarantees exact results from the volatility distribution. However, the limitations of the method are widely recognized from a practical point of view. First, it is rather complex and computationally expensive when the Fourier inversion of the conditional characteristic function of the integrated volatility is involved in the simulation. Second, Broadie and Kaya [37] hire an acceptance-rejection scheme to fix negative values of the volatility, which can introduce significant biases during the parameter perturbation. Basing on the Broadie and Kaya's work [37], Andersen [39] simplifies the simulation scheme by employing a substitute distribution to replace the original volatility distribution. The proposed distribution has matching moments with a non-central chi-square distribution, but can be obtained by affine transformations of uniform and normal random variables. Another simpler class of methods, that is designed to implement the Monte Carlo simulation under the Heston volatility model [41], are built on basic discretizing theories, other than the volatility distribution. For instance, Kahl and Jackel [38] discretize the stock price and the volatility processes basing on the Balanced Implicit Method of Milstein et al. [42]. Moreover, Lord et al. [40] apply the classic Euler-Maruyama method to discretize the SDEs, along with a full truncation scheme to fix negative volatilities.

Empirical comparisons are conducted to the simulation schemes described above. With respect to Van Haastrecht and Pelsser's study [43], in the class of methods built on discretizing theories, Lord et al.'s scheme [40] outperforms other methods in the same class. While in the class of methods that focuses on the non-central chi-square distribution of the conditional volatility, Andersen's method [39] is claimed to be in the dominant place. Furthermore, simulation schemes in the latter class tend to give more robust results, and require less time steps than those in the former class.

In the case of the SSV model, the Euler-Maruyama method is used to discretize the SDE of temperature and volatility. We choose this method not only for its simplicity. According to Van Haastrecht and Pelsser [43], the simulation result of the Euler-Maruyama method can be maintained in an acceptable level with 32 time steps per year. The time increment of DAT simulation is one day, that is 365 time steps per year, which will certainly increase the preciseness of the simulation.

Meanwhile, instead of the full truncation method of Lord et al. [40], which fix the negative values of the volatility with zero, we replace negative volatilities with their absolute values. Such setting has been tested empirically along with the full truncation method, the result indicates that the absolute value of volatility is a more suitable option for the temperature simulation of Chinese cities. As a result, the discretized temperature and volatility can be expressed as:

$$\ln \hat{T}(t+\Delta) = \ln \hat{T}(t) - \frac{|\hat{V}(t)|\Delta}{2} + \sqrt{|\hat{V}(t)|} + Z_1\sqrt{\Delta}; \tag{3.13}$$

$$\hat{V}(t+\Delta) = \hat{V}(t) + \kappa(\theta - |\hat{V}(t)|) + \eta\sqrt{|\hat{V}(t)|}Z_2\sqrt{\Delta}, \tag{3.14}$$

where Z_1 and Z_2 are standard normal random variables that are independent from each other.

Thus, the Monte Carlo simulation of DATs under the SSV model can be implemented by: a) fix the starting data and obtain the initial value of DAT and volatility, b) set the time increment Δ to be one, c) generate the set of Z_1 and Z_2.

3.5 Summary

Considering the trade-off between the model complexity and its explanatory power, it is expected that a model with more parameters generates more accurate results than those with less parameters. Consequentially, in order to determine the most suitable temperature model, we need to answer the question whether additional costs of including stochastic volatility can be justified by its benefits. In the next chapter, we carry out in-sample and out-of-sample model comparison tests to compare the performance of the SSV model along with the performances of the Alaton model [1], the CAR model [2] and the Spline model [3].

Chapter 4

An empirical study on temperature models

As the major barrier of studying weather derivative modeling in China is due to the absence of real market data, one can only focus on the accuracy of temperature modeling rather than on the derivative pricing in order to examine the performances of different models. In this chapter, we utilize the DAT data described in the preceding Chapter to conduct empirical analyses on the stochastic seasonal variation (SSV) model along with three established empirical temperature and pricing models, i.e. the Alaton model [1], the continuous auto-regressive (CAR) model [2], and the Spline model [3]. We then compare heuristically the four temperature models, in terms of simulation results, residual normality, auto-correlation function (ACF), Akaike Information Criterion (AIC) and error measures, with the hope to find out the most suitable model for modeling and pricing temperature-based derivatives in China. Meanwhile, we look into the option prices generated by different models. The results show that the SSV model dominates the other three models by providing a more precise fitting of the temperature process. Further, the Spline model [3] displays inconsistencies when it is applied to Chinese temperature data. This model has the smallest relative errors, but the worst result for the normality of residuals.

There are three major contributions made in this chapter. First, we include a variety of characteristic temperature models that are suggested by the literatures, and apply them to thirty-year temperature data of twelve Chinese cities. With such amount of data included, we aim to gain a robust conclusion on the temperature modeling for China. Second, to the best of our knowledge, it is the first time that the Spline model [3] is applied to Chinese temperature data, and compared with other stochastic models. Third, we incorporate an elaborate analysis in order to gain a better understanding of temperature-based derivative modeling in China from different aspect, and to select the most suitable model for Chinese temperature data. With such a study, one can gain a comprehensive understanding of the temperature dynamics of Chinese cities in different regions, thus to adapt the fundamental theories of temperature-based weather derivative modeling to Chinese market from a practical point of view.

The chapter proceeds as follows. In the first section, we fit the Alaton model [1], the CAR model [2], and the Spline model [3] to the DAT data of twelve Chinese cities. We present the results of the parameter estimation for each model and city, with the hope to gain a general understanding to the models' performances. In the second section, we compare analytically the Alaton model [1], the CAR model [2], the Spline model [3] and the SSV model. The empirical results of the comparison consists of residual normality, auto-correlation function (ACF), Akaike Information Criterion (AIC), relative error, Monte Carlo simulation and option pricing as well as implications of the results. In the last section, we look into the price behaviors of the four temperature models through the prices of cooling degree-day, heating degree-day, and growth degree-day options.

4.1 Parameter estimation of the empirical models

4.1.1 Alaton model [1]

In the literature review, we explain mathematically how the Alaton model [1] captures the temperature evolution, and derives approximate temperature-based contract prices in the incomplete market. In this section, we apply the model analytically to the real DAT data of Chinese cities.

We start off with estimating the parameters of the Alaton model [1] in Eq. 2.39 and 2.42. We use the ordinary least squares (OLS) approach to estimate the parameters in the mean seasonality function, A, B, C and φ. We employ the results of the SSV model in Section 3.2 directly, as the OU processes of the models are identical. Table 3.2 (see Section 3.2) gives the estimated values of the four parameters of the Chinese cities.

After fitting the mean function to the temperature data, we are then able to compute the volatility σ^2. According to Alaton et al. [1], the temperature volatility is monthly constant and equals to the mean value of the temperature quadratic variation and its regressed estimator (see Eq. 4.2). For a given month p, the quadratic variation is defined as:

$$\sigma_p^2 = \frac{1}{N_p} \sum_{j=0}^{N_p-1} (T_{j+1} - T_j)^2, \tag{4.1}$$

where:
σ_p denotes the quadratic standard deviation of month p;
N_p denotes the number of days in month p;
T_j denotes the temperature of day j during the month.

According to Alaton et al. (2002), the volatility estimator under the regressing method is expressed as:

$$T(t) = (T(s) - \mu(s))e^{-\alpha(t-s)} + \mu(t) + \int_s^t e^{-\alpha(t-\tau)}\sigma_\tau \, dW_\tau, t > s. \tag{4.2}$$

where:

$$\widetilde{T}_j = T_j - (T_j^m - T_j^{m-1}). \tag{4.3}$$

N_p denotes the total number of days in month p.

Table 4.1 gives the result of the estimated monthly volatilities of the Alaton model [1].

Table 4.1: Estimated values of volatility for the Alaton model [1] of twelve cities in mainland China

	Jan.	Feb.	Mar.	Apr.	May	Jun.	Jul.	Aug.	Sep.	Oct.	Nov.	Dec.
Harbin	3.67	3.41	3.40	3.51	3.11	2.50	1.79	1.80	2.48	3.39	3.97	3.87
Changchun	3.81	3.72	3.61	3.73	3.09	2.38	1.75	1.87	2.64	3.76	4.24	4.16
Beijing	2.11	2.26	2.58	2.61	2.44	2.19	1.99	1.64	1.84	2.17	2.52	2.35
Tianjin	1.86	2.07	2.54	2.72	2.51	2.15	1.85	1.58	1.86	2.21	2.33	1.94
Shanghai	2.38	2.96	2.82	2.86	2.17	2.23	1.66	1.39	1.79	1.68	2.66	2.71
Hangzhou	2.25	2.57	2.88	2.71	2.36	2.03	1.71	1.48	1.75	1.83	2.29	2.36
Nanjing	2.19	2.41	2.76	2.65	2.29	1.97	1.72	1.55	1.73	1.90	2.34	2.37
Guangzhou	2.29	2.56	2.13	2.67	1.65	1.31	1.30	1.21	1.32	1.58	2.04	2.24
Hainan	1.72	1.81	2.02	1.64	1.24	0.98	0.84	0.91	0.91	1.04	1.46	1.70
Kunming	1.97	2.02	2.19	1.95	2.05	1.50	1.13	1.33	1.48	1.71	1.72	1.87
Lahsa	2.27	2.19	2.02	1.83	1.97	1.90	1.62	1.47	1.32	1.46	1.58	1.94
Urumchi	2.84	2.70	2.97	3.50	3.46	2.76	2.55	2.80	2.87	2.87	3.08	3.16

With the mean estimators of monthly volatilities, the mean reverting parameter α has its estimator given by [1]:

$$\alpha = -\log\left(\frac{\sum_{i=1}^n \frac{T_{i-1}^m - T_{i-1}}{\sigma_{i-1}^2}\left(T_i - T_i^m\right)}{\sum_{i=1}^n \frac{T_{i-1}^m - T_{i-1}}{\sigma_{i-1}^2}\left(T_{i-1} - T_{i-1}^m\right)}\right), \tag{4.4}$$

Therefore, Table 4.2 gives the result of α of the twelve cities.

4.1.2 CAR model [2]

To estimate the parameters involved in the CAR model [2], we need to utilize the convertibility between an auto-regress (AR) process and a CAR process. Recall that the CAR model [2] defines the temperature process $T(t)$ as:

$$T(t) = \mu(t) + X(t), \tag{4.5}$$

Table 4.2: Estimated value of α of twelve cities in mainland China

	α
Harbin	0.2821
Changchun	0.3091
Beijing	0.3121
Tianjin	0.2800
Shanghai	0.3008
Hangzhou	0.2636
Nanjing	0.2515
Guangzhou	0.2279
Hainan	0.1954
Kunming	0.2911
Lahsa	0.2616
Urumchi	0.1977

where $\mu(t)$ is defined by Eq. 2.39, and $X(t)$ is the CAR(p) process which is given by Eq. 2.47 and 2.48.

We replace the CAR process $X(t)$ with an AR process $y(t)$ that follows:

$$y_{i+p} = \sum_{j=i}^{p} b_j y_{i+p-j} + \sigma_i \epsilon_i, \tag{4.6}$$

where ϵ_i are independent, standard normally distributed random variables. As it is proved by Benth et al. [2] that the optimal order of the AR (CAR) process is three, we follow his approach. Hence, we have:

$$y_{i+3} = b_1 y_{i+2} + b_2 y_{i+1} + b_3 y_i + \sigma_i \epsilon_i. \tag{4.7}$$

Finally, we transfer the AR(3) process into a CAR(3) process by using Benth et al.'s solution [2]:

$$3 - a_1 = b_1,$$

$$2a_1 - a_2 - 3 = b_2,$$

$$a_2 + 1 - (a_1 + a_3) = b_3.$$

Table 4.3 lists the estimated values of AR(3) and CAR(3) process. Note that the mean seasonality function $\mu(t)$ in Eq. 4.5 remains identical from that in the Alaton model [1]. Thus, we employ the estimation results of $\mu(t)$ directly from the previous section.

Different from the Alaton model [1], Benth et al. [2] propose a truncated

Table 4.3: Estimated parameters of AR(3) and CAR(3) process

	b_1	b_2	b_3	α_1	α_2	α_3
Haerbing	0.8444	-0.2094	0.1204	2.1556	1.5206	0.4854
Changchun	0.8645	-0.2714	0.1322	2.1355	1.5424	0.5391
Beijing	0.7726	-0.1165	0.0900	2.2274	1.5713	0.4339
Tianjin	0.8788	-0.2568	0.1337	2.1212	1.4992	0.5117
Hangzhou	0.9492	-0.3187	0.1003	2.0508	1.4203	0.4698
Nanjing	0.9488	-0.3174	0.1025	2.0512	1.4198	0.4711
Shanghai	0.8781	-0.28	0.1065	2.1219	1.5328	0.2954
Guangzhou	1.0782	-0.3993	0.0956	1.9218	1.2429	0.4167
Hainan	1.0393	-0.3105	0.0780	1.9607	1.2319	0.3492
Kunming	0.8117	-0.1538	0.0901	2.1883	1.5304	0.4322
Lahsa	0.7896	-0.0926	0.0811	2.2104	1.5134	0.3841
Urumchi	0.9953	-0.2622	0.0627	2.0047	1.2716	0.3296

Fourier series as a functional volatility $\sigma_i = \sigma(i)$ to model the observed seasonal heteroskedasticity of residuals after removing seasonal component and AR(3) process:

$$\sigma^2(t) = c_1 + \sum_{k=1}^{4}(c_{2k}cos(2k\pi t/365) + c_{2k+1}sin(2k\pi t/365)). \tag{4.8}$$

In the study on the Stockholm temperature data, Benth et al. [28] find the optimum orders for the truncated Fourier series equals to four. In our study on the DATs of the Chinese cities, we keep the same specification as they are shown to be suitable for Chinese temperature data in Zong and Ender's study [7]. Table 4.4 gives the result of the parameters c_1 to c_9 estimated using the least squares method.

Table 4.4: Estimated parameters of seasonal volatility function of the CAR model

	c_1	c_2	c_3	c_4	c_5	c_6	c_7	c_8	c_9
Haerbing	7.8542	4.0041	1.2152	0.5701	-1.9496	0.4113	0.1414	0.0758	0.3161
Changchun	8.7863	4.9923	1.2327	0.0051	-2.1259	0.1087	-0.2900	0.0609	0.2408
Beijing	3.9743	0.3922	0.9666	0.0708	-0.7373	-0.0986	-0.3272	0.0492	-0.0163
Tianjin	3.5554	-0.1899	0.9953	-0.3571	-0.8115	-0.0290	-0.1305	0.0380	0.0365
Hangzhou	3.7754	0.6239	1.7720	-0.4665	-0.2793	-0.0153	-0.2585	0.0455	-0.2055
Nanjing	3.4677	0.6274	1.1431	-0.1427	-0.5266	-0.0220	-0.2949	0.0069	-0.0939
Shanghai	3.6615	1.2009	1.5928	-0.0453	0.2622	-0.2355	-0.5166	0.0348	-0.2897
Guangzhou	2.7028	1.1581	1.1987	-0.1467	0.2805	-0.1051	-0.2850	0.0896	-0.1150
Hainan	1.5156	0.7415	0.7582	-0.0767	0.1460	0.0474	-0.1332	0.0339	-0.0839
Kunming	2.5353	0.7192	1.0103	-0.2222	-0.2884	-0.0394	0.2453	-0.0713	-0.0399
Lahsa	2.7588	0.4149	1.0084	0.6218	0.2384	0.1368	0.2000	0.0408	-0.1436
Urumchi	6.6512	0.1391	0.8918	0.1284	-0.9269	1.6059	0.5340	-0.1125	0.2341

4.1.3 Spline model [3]

To fit the DAT process described by the Spline model [3], we start off with the determination of the tensor product splines of the seasonal mean and the seasonal

variation of DAT series. Analogues to Eq. 2.57, let $S_{Dd,Kd}$ denote the vector space of all splines with degree Dd and knot sequence Kd in the day direction and correspondingly $S_{Dy,Ky}$ in the year direction. The mean temperature μ follows:

$$\mu_{d,y} = S_{Dd,Kd} \otimes S_{Dy,Ky}. \tag{4.9}$$

As it is specified by Schiller et al. [3], a cubic spline with breaks approximately every 60 days is used in the day direction. In the year direction, a linear trend with breaks on the first and on the last year of the measured time is used to represent the global warming. Following their specification, we obtain the knot sequences respectively in the day and year direction according to the spline orders:

$$Kd = \{1, 1, 1, 1, 61, 122, 183, 203, 244, 305, 365, 365, 365, 365\}; \tag{4.10}$$

$$Ky = \{1, 1, 30, 30\}. \tag{4.11}$$

After the mean seasonal components are removed from the DAT series of the twelve Chinese cities, there exists a similar seasonal trend in the squared residuals, which is interpreted as the DAT variation. Hence, we construct another spline surface following the Schiller et al.'s method [3]. The method remains the same as the construction of the mean seasonality surfaces. Due to the high volatility of Chinese temperature data, we reduce the number of breaks and make them more centralized at the peak and the bottom of the cubic spline in order to get a smooth surface. The specified break sequences for the spline of the variances are respectively $Kd = 1, 183, 203, 365$ in the day direction and $Ky = 1, 30$ in the year direction. The new break sequences are modified regarding to the plots of the twelve Chinese cities in our study.

Figure 4.1 and 4.2 give respectively the estimated smooth spline surfaces of the DATs and the DAT variances using the least square method. As it is shown in Figure 3, the tensor product spline is capable of capturing the DAT seasonality. However, modeling the DAT variances of Chinese cities with a cubic spline in the day direction may not be the most suitable case. Instead of a smooth pulse shaped curve, the modeled variance in the day direction tends to create waves at the knots during the interpolation. From this result, we infer that applying a stochastic process is a better solution for the variance modeling for Chinese cities.

Finally, we estimate the parameters in the AROMA process (see Eq. 2.58 and 2.59) of the residuals after the mean and the variance are determined. The specifications on the parameters are listed in Table 4.5 in accordance to Schiller et al.'s study [3]. The least square method are used to implement the regression.

Table 4.5: Parameter specifications of the AROMA process

r	m_1	m_2	m_3	m_4
4	1	2	$\leqslant 35$	$\leqslant 35$

Figure 4.1: Estimated spline surface of DATs (Year: 1983-2012. X-axis: days. Y-axis: years. Z-axis: temperature.).

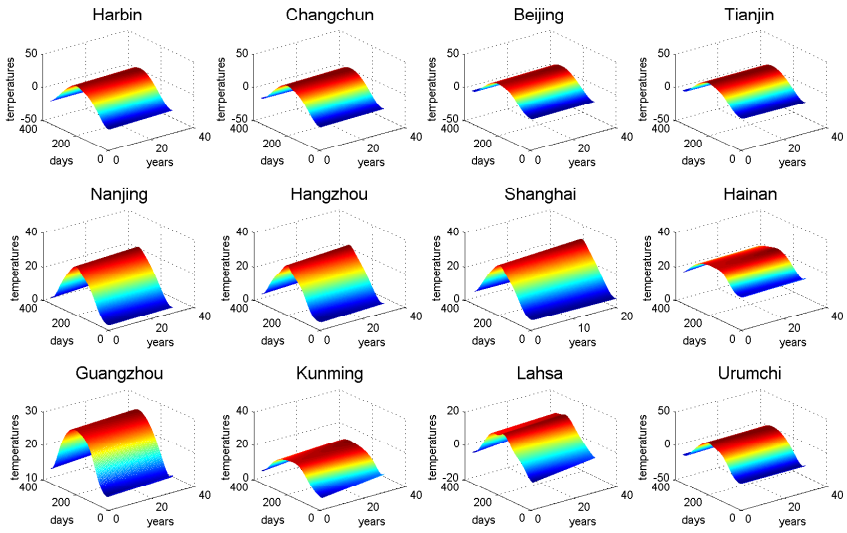

Table 4.6 gives the estimated parameters of the AROMA process. In Table 4.6, the values of m_3 exclusively equal to three for all the twelve Chinese cities. This is strong evidence supporting the assumption that the value of m_3 constantly equals to three of all the cities in mainland China.

4.2 Simulation results

4.2.1 Alaton model [1]

Figure 4.3 presents the simulated DAT using the Alaton model [1] against the real DAT data. The simulation reveals the fundamental drawback of Alaton et al.'s method [1] which neglects the seasonal variation of the temperature dynamic. This observation directs us to the modeling of the temperature volatility in order to structure a more precise model.

4.2.2 CAR model [2]

In the study on Stockholm temperature data, Benth et al. [2] find the optimum order for the CAR(p) process and the truncated Fourier series respectively equals to three and four. In our study on the DAT of Chinese cities, we keep the same specifications as they are shown to be suitable for Chinese temperature data in Zong and Ender's study [7]. Figure 4.4 gives the simulated DAT (black) using the CAR

Figure 4.2: Estimated spline surface of DAT variance (Year: 1983-2012. X-axis: days. Y-axis: years. Z-axis: temperature variance).

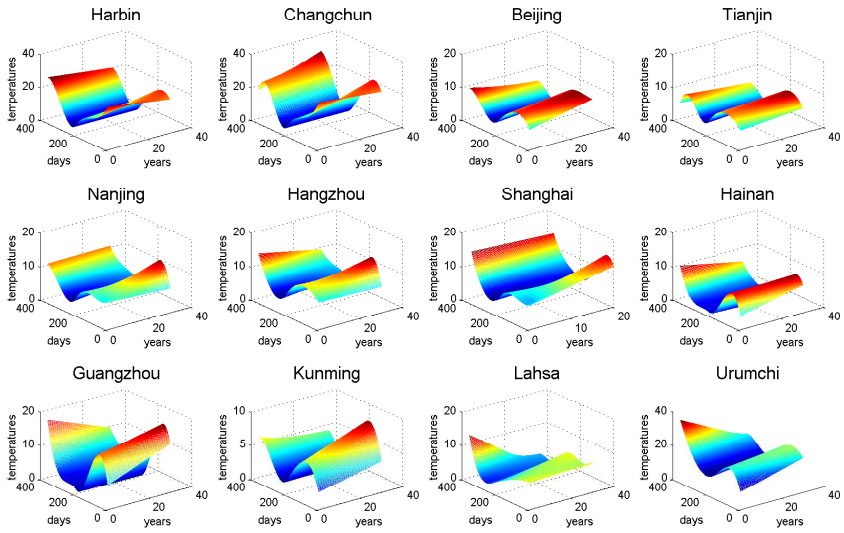

model [2] against the real DAT data (blue). Generally, the simulated temperature shows similarity with the real data. However, it is also noticed that the temperature dynamics of the CAR model [2] shows a tendency of underestimating the volatility, as the real temperature data seems to fluctuate in a more volatile manner.

4.2.3 Spline model [3]

Figure 4.5 gives the real temperature data (blue) and the simulated DATs of 2012 using the Spline model [3] (black). The simulated temperature shows an excellent fit to the real data. We suspect that it is mainly contributed by the AROMA process of the residual in the in-sample simulation. That is to say, the temperature model corrects the estimation of today's temperature with the real temperature in the near past via the AROMA process.

4.2.4 SSV model

Figure 4.6 shows the mean squared residuals on an annual scale and its corresponding estimated Fourier series. As it appears in Figure 6, the truncated Fourier series seems to be a suitable option to capture the seasonal trend of the temperature variation for all the twelve cities.

Figure 4.7 presents the simulated temperature variation with piecewise volatility. The simulated variation displays good fits to the real data. Further, from Figure 4.7,

Table 4.6: Estimated parameters of the AROMA process

City	ϕ_1	ϕ_2	ϕ_3	ϕ_4	m_3	m_4
Harbin	1.0130	-0.5578	0.2011	0.1102	3	34
Changchun	1.0834	-0.7016	0.2658	0.1001	3	34
Beijing	0.8695	-0.3787	0.1802	0.0865	3	34
Tianjin	1.0795	-0.6794	0.2791	0.0862	3	35
Nanjing	1.2266	-0.8037	0.3664	-0.0851	3	4
Hangzhou	1.2475	-0.8223	0.3616	-0.0788	3	4
Shanghai	1.1063	-0.6695	0.2312	0.0429	3	10
Guangzhou	1.1320	-0.4990	0.0940	0.0616	3	35
Hainan	1.2571	-0.6879	0.1311	0.0241	3	11
Lhasa	0.9262	-0.4404	0.1895	0.0658	3	35
Kunming	0.8152	-0.2391	0.1245	0.0693	3	24
Urumchi	1.2438	-0.6135	0.0831	0.0433	3	8

a warm/cold season division of the year looks to be sufficient while being applied to the estimation of volatilities of temperature variations.

With the simulated temperature volatility, we can simulate the DAT process which follows Eq. 4.2. Figure 4.8 shows the simulated DAT using the SSV model against the original DAT data. The simulated temperature data shows a close performance to the observed data, with the highest goodness-of-fit to temperature fluctuations compared to the Alaton model [1] and the CAR model [2].

4.3 Model comparison

4.3.1 Methodology

In order to gain a comprehensive understanding of the models' behaviors, four comparison criteria, including residual normality, auto-correlation function (ACF), Akaike Information Criterion (AIC) and monthly relative error (MRE), are introduced in this section.

Residual normality

The residual normality reflects the model's explanatory power towards temperature evolutions. Normally-distributed residuals play not only a crucial role in the exposition of the model's goodness-of-fit, but also in the computation of accurate derivative prices. As the random processes of the four models are formed based on the Brownian motion (or the AROMA process, which contains a independent identically normally distributed random variable), the residuals, after removing all the other components, should hypothetically follow a normal distribution. There exists a number of temperature-based weather derivative studies based on the argument of normal residuals, which includes Benth et al.'s study [2] [30], and Goncu's

Figure 4.3: Original DAT data and simulated DAT using the Alaton model [1] (Year: 2012).

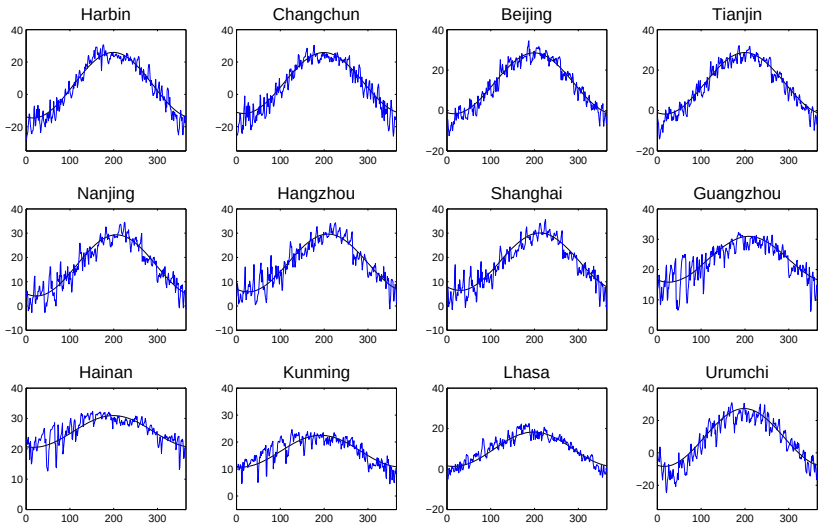

study [29]. In this section, we perform three different normality tests, i.e. the Kolmogorov-Smirnov test, the Jarque-Bera test and the Lilliefors test, to the residuals. We acknowledge normality as long as the residuals of the model are accepted by one of the three tests. Further, we present the histograms and the Q-Q plots of the residuals in order to examine the performance of each model further.

Autocorrelation function (ACF) of residuals and squared residuals

Autocorrelation functions are widely used in the modeling of time series, especially as a mathematical tool in the determination of time lags of autoregressive models. It displays the pattern of inter-dependencies and seasonalities of the observed data.

In our investigation where the ACF serves as a model comparison criterion, we present the ACF plots of model residuals and squared model residuals. The purpose is to understand the evolutions and inter-dependencies of the residual and the squared residual, thus to gain some indications on the models' performances. Generally, the ACF of residuals gives an exposition of the modeling power towards the long-term seasonality of the temperature process, and the ACF of squared residuals reflects the modeling of the volatility process.

Akaike Information Criterion (AIC)

The AIC serves as a model comparison criterion that takes into account the trade-off between the size of the model and its goodness-of-fit. Give a model with K unknown

Figure 4.4: Original DAT data and simulated DAT using the CAR model [2] (Year: 2012).

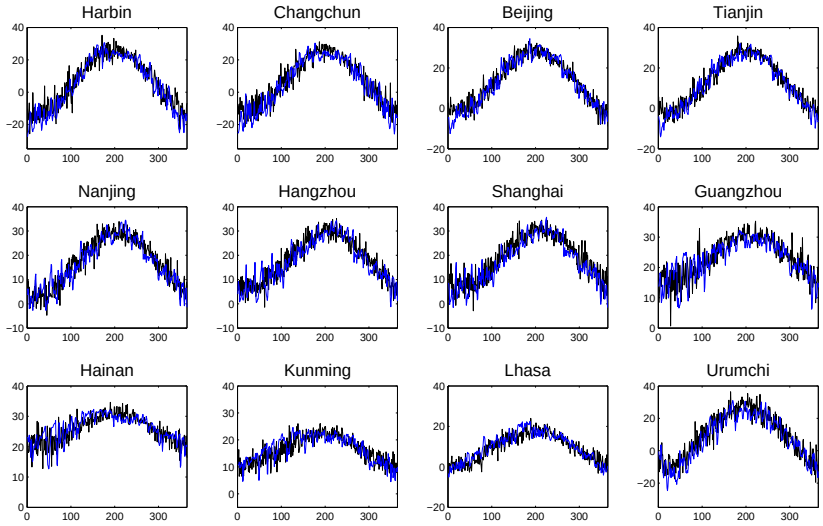

parameters, its AIC is originally defined as:

$$AIC = -2\log(\mathcal{L}(\hat{\theta}|x)) + 2K, \tag{4.12}$$

where $\mathcal{L}(\hat{\theta}|x)$ is the optimized likelihood function of the model regarding to its parameter estimation. In a more peculiar case where the least square method is applied, AIC can be expressed in the form:

$$AIC = \log(\hat{\sigma}^2) + 2\frac{K}{N}, \tag{4.13}$$

where $\hat{\sigma}^2$ is the variance of estimated residuals, and N is the number of observations.

In the model selection, one could gain an general inference on the parsimony of different models regarding their AICs. Specifically, models with a lower AIC is preferable as they display a higher level of parsimony.

Monthly relative error (MRE)

In addition to the investigation of residuals, error measures are considered to be necessary criteria as they serve as the indication of the model's accuracy. In this sense, we apply the MRE as our third model comparison criterion, which is defined as [35]:

Figure 4.5: Original DAT data and simulated DAT using the Spline model [3] (Year: 2012

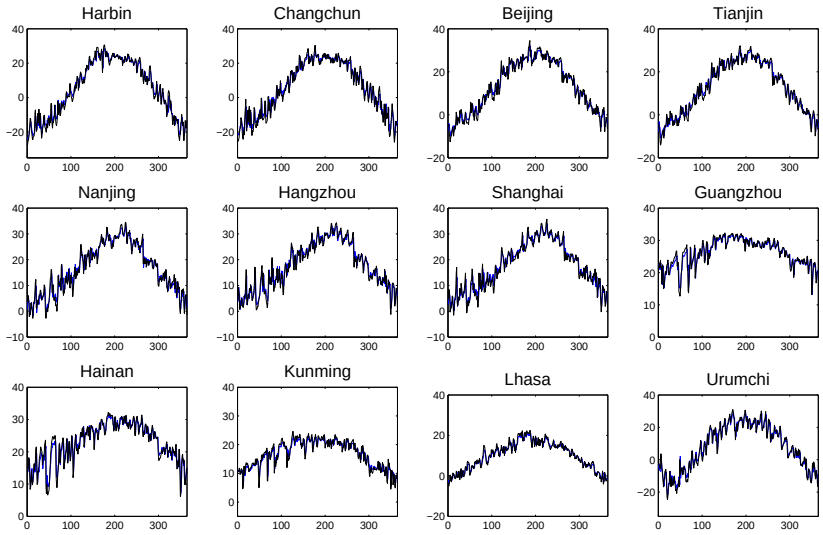

$$ER_{relative} = \frac{T_{estimated} - T_{observed}}{T_{observed}}. \tag{4.14}$$

We select relative errors rather than mean squared errors for the reason that the former one presents not only the size of the fitting error, but also the scale of the error compared to the observed data. Both in-sample and out-of-sample MREs are compared among the temperature models in this section, with the aim to gain comprehensive insights of the model's goodness-of-fit and forecasting power.

4.3.2 Results and implications

In this section, we present the model comparison results among the Alaton model [1], the CAR model [2], the Spline model [3] and the SSV model. The four selective criteria, i.e. residual normality, ACF, AIC and MRE, are discussed on a empirical base.

Residual normality

Table 7.1 in the Appendix gives the final results of the residual tests for each city and each model. In the table, we also present the proportions of acceptance out of the three normality tests.

From Table 7.1, we can see that the SSV model dominates the Alaton model [1], the CAR model [2] and the Spline model [3] with accepted normality for eleven cities' residuals. Second to the SSV model, the CAR model has five cities with

Figure 4.6: Empirical temperature variation and its estimated Fourier series.

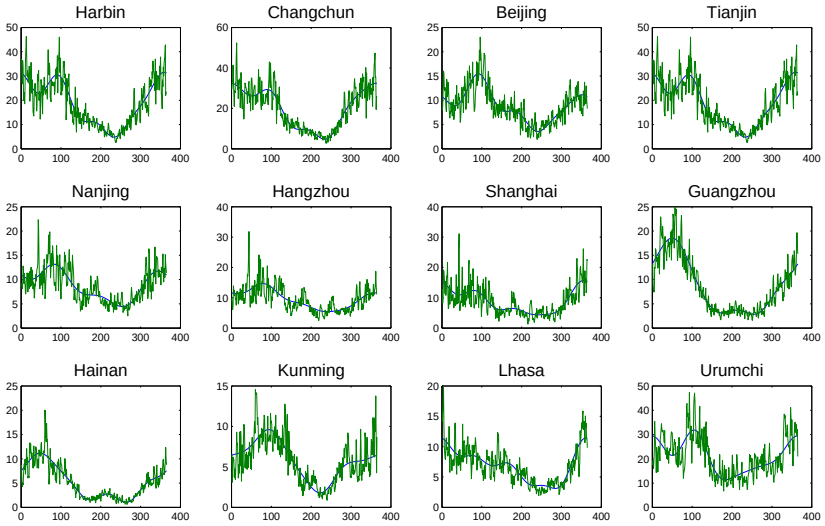

normal residuals. These five cities, namely Beijing, Tianjin, Hangzhou, Nanjing and Shanghai, exclusively cover the climatic zone II and III. Following the CAR model [2], the Alaton model [1] shows a slight weakness. Three cities' residuals are accepted by the normality tests, respectively Tianjin from climatic zone II, Nanjing from climatic zone III and Lhasa from climatic zone VI. Despite of the outstanding performance of modeling the US temperature data [3], the Spline model is the weakest model in the residual normality tests while it is applied to Chinese data.

As it is displayed in Table 7.1, the residuals of Nanjing always follow a normal distribution. We infer that the temperature models capture the DATs of the cities from climatic zone II and III in a better way, as they show a higher frequency of normal residuals.

In Figure 7.1 - 7.4 in the Appendix, the histograms of the residuals' distributions and their corresponding normal distributions are shown. From the histograms, we observe an obvious difference between the Spline model and the other three models. Especially for the cities from climatic zone IV, V, VI and VII, namely Hainan, Guangzhou, Lhasa, Kunming and Urumchi, the residuals obtained from the Spline model tend to display strong bias against the normal distributions. Agreeing with the results of normality tests, the residuals obtained from the SSV model show rather close fits to the normal distribution across cities. Although the normality tests suggest that the CAR model [2] is better than the Alaton model [1], the differences between them are very limited in the histograms.

In the Q-Q plots shown in Figure 7.5 - 7.8 in the Appendix, the results consid-

Figure 4.7: Empirical and simulated temperature variations.

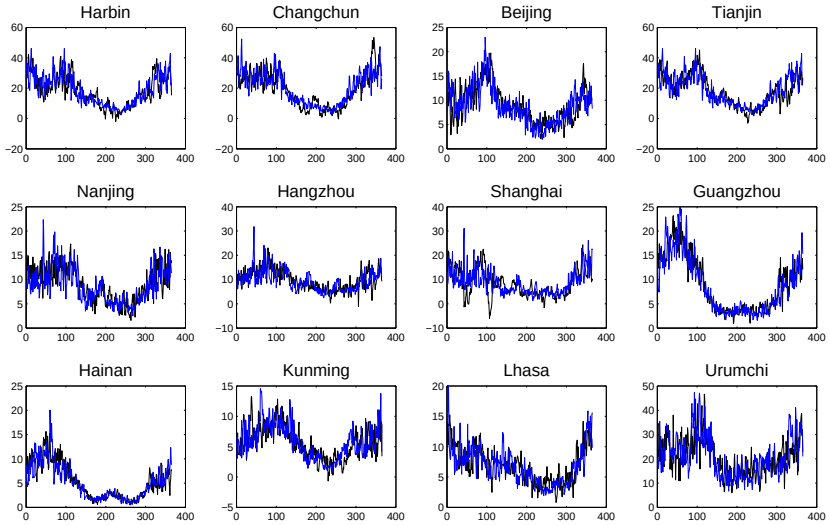

erably translate into the conclusion we draw from normality tests and histograms. To be noted here, we can observe that the residuals' distributions from the Alaton model [1], the CAR model [2] and the Spline model [3] tend to show a bias at the end of the quantile line against the standard normal quantiles in the Q-Q plots. The bias is caused by a steeper trend in the Q-Q plot which indicates that the residuals' distributions are more dispersed compared to the standard normal distribution. Obviously, the unfavorable dispersions of the residual distributions obtained by the Spline model [3] are drastically more intense than those obtained by the Alaton model [1] and the CAR model [2]. In accordance to the histograms, the residual Q-Q plots from the Alaton model [1] and the CAR model [2] give very similar results. The residual distributions of the SSV model show very similar quantiles compared to the standard normal distribution.

ACF of residuals and squared residuals

Figure 7.9-7.12 show the ACF plots of residuals obtained from the Alaton model [1], the CAR model [2], the Spline model [3] and the SSV model. According to the results, residuals of the SSV model and the Spline model [3] fluctuate in more steady manners without any observable seasonality in all the twelve cities. On the other hand, the Alaton model [1] and the CAR model [2] reveal their weaknesses in their residual ACF plots, where both of the two models show significant seasonal patterns.

Since the ACF of residuals provides indications on the general modeling of long-term evolutions of the time series, we infer that despite of the fact that the mean

Figure 4.8: Original DAT data and simulated DAT using the SSV model (Year: 2012).

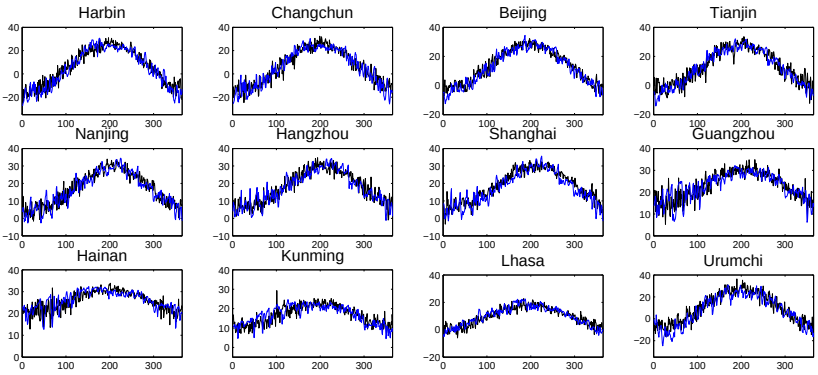

functions of the Alaton model [1], the CAR model [2] and the SSV model are identical (see Eq. 2.39 and 3.2), the stochastic volatility process attributes a higher level of fitting power to the SSV model. Further, from the ACF result of the Spline model [3], we believe that the method of employing tensor product splines to model the mean temperature evolution is appropriate.

The ACF plots of squared residuals are provided in Figure 7.13-7.16. Opposite to the results based on residuals, squared residuals of the CAR model [2] turn to be more robust in their ACF plots, while those of the Spline model tend to show seasonality. This observation indicates that truncated fourier series are more suitable than tensor product splines while being applied to model the temperature volatility. Additioanlly, squared residuals of the Alaton model [1] and the SSV model display consistency with their residuals in the ACF plot.

With respect to the investigation of ACFs, it is concluded that the SSV model outperforms the other three temperature models by capturing both the long-term evolution and the volatility of the temperature process, while the Alaton model [1] is the weakest while being applied to Chinese temperature data as it fails in both aspects.

AIC

According to Eq. 4.12 and 4.13, the model size K needs to be determined before looking into its AIC. Table 4.7 gives the number of estimated parameters in each of the four temperature models. Note that in the Spline model [3], we count the tensor products μ and σ^2 as two parameters.

As the parameters of all the four models are estimated based on the least-square method, AICs can be obtained by applying Eq. 4.13. Results are listed in Table 4.8, from which three major observations can be made.

First, the Alaton model [1] produces the highest AICs among all the four temperature models. That is to say, although the Alaton model [1] has the smallest number

Table 4.7: The number of parameters in Alaton et al.'s model (2002), the CAR model (Benth et al., 2007), the Spline model (Schiller et al., 2012) and the SSV model.

Alaton et al.'s model	CAR model	Spline model	SSV model
6	16	8	16

Table 4.8: AICs of Alaton et al.'s model (2002), the CAR model (Benth et al., 2007), the Spline model (Schiller et al., 2012) and the SSV model.

	Alaton et al.'s model	CAR model	Spline model	SSV model
Harbin	3.67	0.04	2.04	-0.07
Changchun	3.71	0.03	2.16	-0.07
Beijing	2.92	0.04	1.37	-0.10
Tianjin	2.92	0.03	1.26	-0.13
Nanjing	2.99	0.04	1.24	-0.15
Hangzhou	2.95	0.03	1.33	-0.14
Shanghai	3.02	0.02	1.30	-0.14
Guangzhou	2.88	0.03	0.42	-0.16
Hainan	2.38	0.04	1.00	-0.05
Kunming	2.51	0.03	0.92	-0.12
Lhasa	2.66	0.02	1.00	-0.15
Urumchi	3.83	0.02	1.88	-0.09

of parameters, its poor fitting to the temperature heteroskedasticity and the seasonal volatility brings up the AIC, and makes it the least parsimonious model.

Second, the Spline model [3] produces lower AICs than the Alaton model [1], which indicates an increase of the model parsimony. However, it is still arguable of the treatment which assumes the tensor product spline to be one parameter. As a matter of fact, the number and the order of least-square estimated polynomials that construct the spline depend on the order of the spline and the number of knots. In this sense, the parameter counts of the Spline model can be rather high, so does the AIC.

Last, although the CAR model [2] and the SSV model contain the largest number of parameters, they manage to produce lower AICs compared to the Alaton model [1] and the Spline model [3] in all the twelve cities. Further, as the only model that generates negative AICs, the SSV model is the most preferable model as it shows the greatest level of parsimony.

MRE

In this section, the model MREs are compared on both the in-sample and the out-of-sample bases. The out-of-sample MRE is an informative factor in the model comparison as it reflects the model's forecasting power.

Figure 7.17 - 7.20 in the Appendix show the bar plots of the in-sample MREs based on the simulated temperatures of the Alaton model [1], the CAR model [2], the Spline model [3] and the SSV model. As it is shown in the figures, the simulated DATs using the SSV model produce very close MREs with the Alaton model [1] and the CAR model [2]. Inconsistent to the results of the residual normality check, the Spline model [3] prevails over the other three models as it generates the smallest error terms. As it is discussed in the previous section, the major concern here is that the high goodness-of-fit stems from the in-sample simulation of the AROMA

process. Regardless of this argument, the Spline model [3] is the most accurate model to capture the temperature dynamics in terms of error measures. Further, it is consistent among all the four models that the monthly relative errors tend to show a seasonal pattern. To be precise, the large relative errors appear during cold season while in warm season the relative errors are generally very small. In other words, the SSV model cannot fully capture the seasonal variation of the Chinese DAT data as well as the other three models.

Table 4.9 gives the total numbers of months in which the in-sample relative errors of the Alaton model [1] and of the SSV model are smaller than those of the CAR model [2]. The SSV model has more often smaller errors than the Alaton model [1] and the CAR model [2] while the CAR model [2] shows a slightly better performance than the Alaton model [1].

Table 4.9: Total number of months that the Alaton model [1] and the SSV model have smaller MREs than the CAR model [2] in the in-sample simulation.

	Alaton model	SSV model
Harbin	5	5
Changchun	4	5
Beijing	3	8
Tianjin	2	7
Nanjing	5	6
Hangzhou	5	6
Shanghai	5	8
Guangzhou	5	7
Hainan	8	7
Kunming	5	6
Lhasa	3	6
Urumchi	3	6

In Table 4.10, we respectively give the total numbers of months in which the Spline model [3] produces smaller in-sample relative errors than the Alaton model [1], the CAR model [2] and the SSV model. The Spline model [3] has an exclusively better performance than the three stochastic models in terms of the relative errors across all the cities in the study. Additionally, from Table 4.10, we also notice that differences among Alaton et al.'s model [1], the CAR model [2] and the SSV model while being compared with the Spline model [3] are very minor.

Table 4.10: Total number of months that the Spline model [3] has smaller MREs than the Alaton model [1], the CAR model [2] and the SSV model in the in-sample simulation.

	Alaton model	CAR model	SSV model
Harbin	11	11	11
Changchun	11	11	11
Beijing	12	11	11
Tianjin	12	12	12
Nanjing	11	12	12
Hangzhou	11	11	11
Shanghai	11	11	11
Guangzhou	12	11	12
Hainan	11	11	11
Kunming	11	11	11
Lhasa	11	11	11
Urumchi	12	12	12

Meanwhile, Figure 7.21 - 7.24 in the Appendix give the out-of-sample monthly relative errors of each city and each model. Similar with the in-sample MRE dia-

grams, one can observe strong seasonal patterns of the out-of-sample MREs for all the cities and models.

In order to investigate the out-of-sample MREs of the stochastic models, the total numbers of months in which the Alaton model [1] and of the SSV model have smaller relative errors than the CAR model [2] are listed in Table 4.11. Similar with the in-sample results in Table 4.9, the difference of the MREs between the three stochastic models is minor. However, the results of the out-of-sample comparison distribute in a more volatile way. For instance, in the comparison between the Alaton model [1] and the CAR model [2] for the city of Lhasa, there are only two months in a year when the CAR model [2] has smaller MREs than the Alaton model [1]. A similar case exists in the comparison between the SSV model and the CAR model [2] for Urumchi. The small size of DATs employed in the out-of-sample tests might be the cause of this instability.

Table 4.11: Total number of months that the Alaton model [1] and the SSV model have smaller MREs than the CAR model [2] in the out-of-sample simulation.

	Alaton model	SSV model
Harbin	7	7
Changchun	5	7
Beijing	5	6
Tianjin	6	6
Nanjing	5	6
Hangzhou	5	7
Shanghai	2	6
Guangzhou	8	5
Hainan	5	4
Kunming	7	6
Lhasa	2	8
Urumchi	9	3

Table 4.12 presents the out-of-sample comparison between the Spline model [3] and the stochastic models. In the case of Shanghai and Hainan, the Spline model shows a consistent dominant performance with lower MREs. However, apart from these two cities, the Spline model generates similar out-of-sample results of MREs compared to the stochastic models.

Table 4.12: Total number of months that the Spline model [3] has smaller MREs than the Alaton model [1], the CAR model [2] and the SSV model in the out-of-sample simulation.

	Alaton model	CAR model	SSV model
Harbin	5	6	5
Changchun	5	6	6
Beijing	6	6	5
Tianjin	5	6	4
Nanjing	7	7	7
Hangzhou	7	7	6
Shanghai	10	11	10
Guangzhou	3	2	3
Hainan	12	12	12
Kunming	7	8	7
Lhasa	6	5	6
Urumchi	4	6	7

Summary of model comparison results

With the hope to show the model comparison results from an overall perspective, we make an attempt to rank the models' performances in a quantified way. Table 4.13 shows the order and the summation of the orders of each temperature model in each criterion discussed in the preceding sections. Models with lower summation of orders are more preferable.

In conclusion, the SSV model occupies a dominant place in the model comparison. It gives the best performance among the four models for all the criteria except the MRE. Additionally, the SSV model has the lowest summation of orders, which indicates the best model performance.

The same summations of orders given by the CAR model [2] and the Spline model [3] indicate a similarity between the two models' performances. The CAR model tends to produce more normally-distributed residuals and to be more parsimonious, while the Spline model tends to have a better forecasting power towards the temperature evolution. In this sense, we infer that the CAR model is more suitable for temperature-based derivative pricing due to its noise behaviors, while the latter one is more suitable to be used as a temperature forecasting tool.

Finally, the Alaton model [1] is the least preferred model when it is applied to Chinese temperature data. We infer that the weakness of the Alaton model [1] is mainly due to its constant volatility.

Table 4.13: Ranking scores of Alaton et al.'s model [1], the CAR model [2], the Spline model [3] and the SSV model.

	Residual normality	ACF	AIC	MRE	Total
Alaton model	3	4	4	4	15
CAR model	2	3	2	4	11
Spline model	4	3	3	1	11
SSV model	1	1	1	4	7

4.4 Temperature-based option pricing

4.4.1 General settings

In the following sections, we present European option prices obtained from Monte Carlo simulations of the four models considered in this study and computed with the approximation formulae of the Alaton model [1] in Eq. 2.45 and the CAR model [2] in Eq. 2.55. Technically, the Monte Carlo simulated prices are capable of offering adequate information for the purpose of model comparison given that there are no real market data of temperature-based derivatives in China yet. Nevertheless, we strongly recommend the derivation of pricing formulae for the Spline model [3] and the SSV model for future research.

In order to price temperature-based derivatives, the market price of risk (MPR) is required as the underlyings, temperature indices, are not tradable. However, without the real market data, one cannot determine the value or the dynamics of

the MPR. Instead, specifications need to be given carefully before studying the pricing of temperature-based derivatives. In this section, we assume that the value of the MPR is zero (Goncu, 2011).

4.4.2 CDD and HDD call option prices

In Tables 4.14 and 4.15, the prices of HDD and CDD call options are respectively listed. The tick size is assumed to be one unit of currency per degree-day index. From Tables 4.14 and 4.15, three major aspects are discussed.

Table 4.14: HDD call options pricing using Monte Carlo simulation (MC) and approximation formulae (Contract Period: Jan. 2010).

Climatic zone	City	Strike price /RMB	Option price Alaton model	Option price Alaton model (MC)	Option price CAR model	Option price CAR model (MC)	Option price Spline model (MC)	Option price SSV model (MC)
I	Harbin	750	319.64	320.94	281.22	274.54	312.32	238.63
	Changchun		259.21	261.62	203.27	201.68	250.25	148.54
II	Beijing	500	182.16	182.10	115.17	120.74	165.75	76.70
	Tianjin		204.69	204.73	128.75	126.12	188.18	112.41
III	Nanjing	200	244.22	244.45	233.03	233.97	229.97	160.98
	Hangzhou		176.79	175.26	167.09	168.71	175.38	194.12
	Shanghai		187.60	188.59	145.98	144.88	194.86	169.82
IV	Guangzhou	50	56.17	57.60	37.30	39.15	58.72	40.09
	Hainan		0	0	0	0	0	0
V	Kunming	100	117.41	117.48	81.90	79.68	109.60	155.23
VI	Lhasa	400	160.53	161.54	131.43	130.13	142.10	106.69
VII	Urumchi	600	264.81	261.58	225.35	225.56	349.26	196.06

Table 4.15: CDD call options pricing using Monte Carlo simulation (MC) and approximation formulae (Contract Period: Jul. 2010).

Climatic zone	City	Strike price /RMB	Option price Alaton model	Option price Alaton model (MC)	Option price CAR model	Option price CAR model (MC)	Option price Spline model (MC)	Option price SSV model (MC)
I	Harbin	100	87.95	88.48	139.49	138.47	81.35	140.98
	Changchun		79.44	77.56	136.81	138.06	69.23	135.58
II	Beijing	150	172.01	172.58	164.03	163.08	162.46	191.48
	Tianjin		155.23	156.23	155.60	160.66	146.52	164.70
III	Nanjing	200	124.57	123.94	136.06	139.04	124.27	142.60
	Hangzhou		138.30	138.74	153.29	159.08	140.72	169.24
	Shanghai		137.18	137.88	165.97	169.2	133.35	148.54
IV	Guangzhou	250	114.65	115.42	136.58	137.55	107.02	109.30
	Hainan		130.09	130.12	157.69	161.41	124.21	139.90
V	Kunming	50	60.27	60.07	76.98	88.92	50.40	84.75
VI	Lhasa	20	5.74	7.36	8.95	10.62	0	2.31
VII	Urumchi	100	102.42	99.64	114.13	109.98	91.89	140.76

First, there are significant discrepancies among the prices obtained from different models. In detail, the option prices obtained from the Alaton model [1] and from the Spline model [3] are comparatively close while the CAR model [2] and the SSV model generate close option prices. Moreover, the option prices of the CAR model [2] and the SSV model exhibit an up to 20 percent variation from the prices of the other two models. Further, compared with the prices of the Alaton model [1] and of the Spline model [3], the prices obtained from the CAR model [2] and the SSV model are lower/higher in the cold/warm season. Lastly, although the option prices of the Alaton model [1] and the Spline model [3] seem to be close, the Alaton model [1] tends to give higher prices for both HDD and CDD contracts. Due to the absence of real market prices, we cannot judge which model is the best one in

terms of temperature-based derivatives pricing. Nevertheless, from the results of our study, we infer that model risk exists.

Second, the two pricing approaches, i.e. the approximation formula and the Monte Carlo simulation, generate very similar results using the Alaton model [1] and the CAR model [2]. For further research, we suggest to derive the approximation formula for the SSV model, thereby to conduct a more comprehensive analysis between the two approaches.

Third, from Table 4.14 and 4.15, we notice that for all the four models involved, the option prices of the cities from the same climatic zones stay close. Given that the CDD/HDD call option contract specifications are consistent for the cities from a same climatic zone, we infer that it is realistic to design a climatic zone-based contract which is capable of hedging temperature risks for all the cities in one climatic zone.

4.5 Summary

In this chapter, we analyzed the performances of the SSV model along with other three empirical models, i.e. the Alaton model [1], the CAR model, and the Spline model [3], in terms of temperature modeling.

With respect to the results of the study, the SSV model is primarily recommended to be hired to model temperature data of Chinese cities. Despite of its complexity, the SSV model dominates the other three empirical models with higher rates of residual normality, which indicates an essential improvement on the modeling. According to the results, we infer that it is necessary to include a stochastic process to model the volatility of the DATs of Chinese cities.

On the other hand, although the CAR model [2] provides weaker performance than the SSV model in terms of temperature modeling, it produces generally robust results throughout the study. Especially in the pricing section, the CAR model gives close price results between the Monte Carlo simulation and the approximation formula. Further, option prices obtained from the CAR model and from the Monte Carlo simulation under the SSV model are very close as well. Thus, we would recommend the CAR model to be another reliable model for temperature-based derivative pricing in China.

Further, as a more basic stochastic temperature model, the Alaton model [1] tends to provide the least precise results throughout the study. Thus, we infer that the Alaton model [1] is generally not an appropriate model for Chinese temperature-based derivative modeling and pricing.

In particular, the Spline model [3] shows an excellent performance in reducing error terms of temperature modeling. As a result, we recommend to apply the Spline model to implement temperature forecasts for Chinese cities. However, due to its weak performance in producing normal residuals, it is rather risky to employ the Spline model [3] as an pricing tool.

Chapter 5

Optimal growth degree-day index design: agricultural risk management in China

The yield farmers can harvest from their fields is heavily influenced by the weather during crops' growing seasons. Adverse weather conditions like excess rain, drought, frost, extreme high temperatures, hail, storms, etc. can cause crop losses with negative impact on farmers' income [44]. Especially in developing countries with limited access to the financial system, bad harvests have severe consequences for small scale farmers and their families. Possible measures are off-farm employment, selling of farm assets, withdrawal of their children from school, taking money from dubious money lenders, etc. [45, 46]. The situation will be worse if weather fluctuations increase due to climate change. To stabilize farmers' income and to facilitate adaptation to climate change, the introduction of financial hedging instruments like insurance is seen as one part of action plans worldwide [47].

This chapter explores the practical value of temperature-based weather derivatives as a risk hedging tool in the agricultural sector of China. Temperature-based indices are investigated both on the city and on the climatic zone scale. There are two major objectives of this chapter. In the first place, we make an attempt to increase the risk hedging power of temperature-based derivative contracts by introducing new forms of temperature indices. In the second place, we aim to reduce the model dimension of cross-regional contract valuation by designing a climatic zone-based GDD contract, which provides identical prices to all cities covered by the same climatic zone. There are four major advantages of model dimension reduction. First, it is more time-saving for issuers of the climatic zone-based contract to implement the modeling and the pricing, as only an unique price is rendered by each contract for all cities in one climatic zone. Second, in addition to modern cities, the climatic zone-based contract can also cover small suburban regions where no observed temperature data can be collected. Third, from the issuer's point of view, with more regions covered in the contract, the climatic zone-based contract is impaired with lower transaction costs and higher profits, with increased number

of transactions. Last, replacing individual local weather contracts with the climatic zone-based contract increases the liquidity of the market.

The remaining part of the chapter is organized as follows. In the next section, we provide a brief review of the research background and the motivation. Section 5.2 gives an overview of the temperature and the yield data used on this study. Section 5.3 explains the novelly introduced GDD indices. And Section 5.4 describes the efficiency test that is conducted to the indices in detail.

5.1 Application of temperature-based derivatives in agricultural risk management

The primary concern of agricultural producers is the weather risks embedded in the industry. Second to the USA, China has become one of the largest market for agricultural insurance with its great potential demand [48]. Among all the agricultural risk hedging instruments discussed so far, weather insurances and derivatives are the most widely studied in the literature. Despite that traditional damaged-based insurance contracts are one kind of financial hedging instruments, some disadvantages are inherent in those contracts. Farmers have to prove their damage before they get any indemnity which leads to high administration costs on both sides [45, 49]. Moreover, traditional insurance bears the problem of asymmetric information, in particular adverse selection and moral hazard. This means that farmers have better information about their production risk and behavior than insurers. To overcome this imbalance additional costs arise [45, 49]. To increase efficiency of farmers' money and public funding, alternative instruments for risk transfer like weather index insurance or weather derivatives should be included in the portfolio. That those instruments are feasible, even in developing countries is shown by several examples all over the world: e.g. Malawi, Ethiopia, India, Vietnam, Thailand, Mongolia, Mexico, Central America, Brazil, and Ukraine [55].

Given the size and importance of China, studies of efficiency of weather index insurance or weather derivatives are comparatively scarce for China. According to Heimfarth and Musshoff [9], 70% of the Chinese population are farm households who are heavily affected by yield variations caused by weather uncertainty. Second to the USA, China has become one of the largest markets for agricultural insurance with a great potential demand [48]. Existing studies indicate that weather derivatives can reduce agricultural risks associated with yield variations. Sun et al. [51] analyzed the efficiency of weather derivatives written on precipitation and temperature indices. They measured the risk reduction power for corn production in Northeast China using the mean root square loss (MRSL). The results of Sun et al. [51] indicated that weather derivatives will only be efficient when the yield variation can be explained by the weather index to a certain degree. Pelka et al. [52] found that precipitation-based weather derivatives can reduce yield risk of maize based on data of eight Chinese provinces. Ender and Zhang [10] studied the risk hedging power of weather options written on growth degree-day (GDD) indices using efficiency tests

proposed by Vedenov and Barnett [12]. They applied wheat and rice yield data from Beijing and Shanghai. By comparing the distributions of farmers' revenues with and without GDD put options, the authors concluded that GDD options can reduce the fluctuations of farmers' income.

In reality, risk hedging for farm households is still systematically underdeveloped in China. The difficulty in launching weather derivatives for Chinese farmers is twofold. First, the willingness of farmers to purchase such risk hedging instruments is comparatively low, due to destitution and the lack of education. According to Kong et al.'s study [53] of willingness to pay for weather insurance on Chinese farm households , the authors concluded that the demand of Chinese farmers for such insurance is elastic and highly correlated with price and compensation. Turvey and Kong [8] suggested to cut the prices for Chinese farmers and to launch subsidies if necessary as a result from their survey. Second, the derivative market in China is still in a piloting stage without a fully developed regulating system [52, 54]. Despite the fact that agricultural insurance has been authorized by the China Insurance Regulatory Commission in 2004 [53], there is still a long way to go to achieve greater market penetration. By the year 2007, only 0.2% of the gross domestic product (GDP) of agriculture was insured [56]. In the same year, existing agricultural insurance schemes launched by the Chinese government were identified by the World Bank to be over-priced [54].

Additionally to problems arising from the current economic situation in China, designing an efficient type of weather derivative contracts is another challenge for launching weather derivatives in China. To be specific, prices of weather derivative contracts are derived from weather processes which are highly localized. As a result, the prices should theoretically vary from place to place with otherwise unchanged contract specifications. But for the conventional city-based contracts, it is very time consuming to implement the valuation city by city. Increased transaction costs, low liquidity and inaccessible weather data are the major disadvantages of city-based contracts. Goncu and Zong [15] proposed to reduce the model dimension of cross-regional contract pricing in China by using a basket option covering multiple cities.

5.2 Data overview

In this study, we select eleven Chinese cities regarding to the Standard of Climatic Zone Partition of China which is a typical partition method used by Chinese architects for the purpose of distinguishing construction standards among regions with different climate characteristics. According to the standard, mainland China is divided into seven climatic zones according to the climatic patterns of different regions.

The representative cities in this study are chosen as they are the capital cities of the nine most agricultural productive provinces. This approach ensures that the locations of representative cities are distributed evenly, and that the result is relevant for the highest possible number of inhabitants. Table 1 gives an overview of the cities included in the study, and their corresponding agricultural districts and

climatic zones.Table 5.1 gives an overview of the cities included in the study, and their corresponding agricultural districts and climatic zones.

Table 5.1: Agricultural cities

Climatic zone	City	District
I	Harbin	Heilongjiang
I	Changchun	Jilin
II	Beijing	Municipality
II	Shijiazhuang	Hebei
II	Ji'nan	Shangdong
II	Zhengzhou	He'nan
III	Nanjing	Jiangsu
III	Hefei	Anhui
III	Wuhan	Hubei
III	Hangzhou	Zhejiang
III	Nanchang	Jiangxi

In order to calculate GDD indices and option prices, thirty years (from Jan. 1984 to Dec. 2013) of daily average temperature data collected from the China Meteorological Data Sharing Service System is used. Additionally, twenty-four years (from Jan. 1984 to Dec. 2007) of annual yield data collected from the China Agricultural Data Sharing System are used to conduct the efficiency tests. Note that we apply the yield data rather than the production data as production also depends on the crop acreage which changes from year to year.

5.3 Optimal city-based growth degree-day (GDD) index and climatic zone-based GDD contract design

Traditionally, the growth degree-day index is defined to be equal to the offset part of daily average temperature T_t that exceeds the optimal growth temperature $T^{optimal}$ of a particular crop, which can be expressed as[1]:

$$GDD_t = max[T_t - T^{optimal}, 0]. \tag{5.1}$$

Given that the purpose is to manage yield variation risks due to the temperature change, the aforementioned definition of the GDD can be rather unprecise and of low-efficiency. The reason is that it by assumption only considers the impact of higher temperature on the crop yields, which, in reality, is not true. As a matter of fact, different species of crops have different responses to temperature changes. During the growing phase, some crops might be benefited from higher temperature,

[1]Note: GDD indices are only considered on a city basis in this section of the thesis.

while some might prefer lower temperature. In this section, we define three different functional growth degree-day (GDD) indices. We then apply the continuous auto-regressive (CAR) model [2] to model the temperature evolution and to compute the prices of European call options that are written on the GDD indices. At last, an efficiency comparison is conducted among the GDD indices basing on their option prices.

According to the result of Chapter 4, the stochastic seasonal variation (SSV) model provides a dominant performance, compared to the Alaton model [1], the CAR model [2] and the Spline model [3], on the temperature modeling basis. However, due to the fact that there is no benchmarking market data of temperature-based derivative contract prices, we can hardly be sure about the SSV model's accuracy level in terms of derivative pricing as only the Monte Carlo simulation can be applied when it comes to pricing. On the other hand, the CAR model [2] exhibits a similarity with the SSV model throughout the study, with comparatively robust price results in both the approximation formulae and the Monte Carlo simulation (See Section 4.3 for more details). Thus, we choose the CAR model in the following chapter as the pricing mechanism for GDD contracts.

5.3.1 Designing the optimal city-based GDD index

Absolute deviation-based GDD index

We name the first type of city-based GDD indices the absolute deviation-based GDD, by which we assume that positive and negative deviations of daily average temperature (DAT) from the optimal growth temperature have same impacts on the crop yield. In consequence, given the optimal growth temperature of a particular crop $T^{optimal}$, the GDD index of day t equals to the absolute value of deviations from $T^{optimal}$, which can be analytically expressed as:

$$GDD_{abs}(t) = abs(T(t) - T^{optimal}), \tag{5.2}$$

where $T(t)$ denotes the DAT of day t.

Considering a GDD contingent claim with contract period (t_1, t_2), its accumulated GDD index equals to the summation of daily indices, which follows:

$$GDD_{abs}(t_1, t_2) = \sum_{s=t_1}^{t_2} GDD_{abs}(s). \tag{5.3}$$

In a more general case, for all types of daily GDD indices, the corresponding accumulated GDD in the time interval (t_1, t_2) satisfies:

$$GDD(t_1, t_2) = \sum_{s=t_1}^{t_2} GDD(s). \tag{5.4}$$

Correlation-adjusted GDD index

As well as the absolute deviation-based GDD index, the correlation-adjusted GDD is defined by temperature deviations from the optimal growth temperature. However, signs of deviations are taken into account in this case, in order to reflect different impacts of temperature on the crop yield. Three possible forms of correlation-adjusted GDD on day t are defined below.

- GDD based on the absolute deviation

$$GDD_{corad}(t) = abs(T(t) - T^{optimal}); \tag{5.5}$$

- GDD based on the positive deviation

$$GDD_{corad}(t) = max[T(t) - T^{optimal}, 0]; \tag{5.6}$$

- GDD based on the negative deviation

$$GDD_{corad}(t) = min[T(t) - T^{optimal}, 0], \tag{5.7}$$

where $T(t)$ is the DAT on day t.

The first form in Eq. 5.5 replicates the situation introduced by the absolute deviation-based GDD index in Section 5.3.1. Meanwhile, the second (i.e GDD based on the positive deviation)/third (i.e GDD based on the negative deviation) form assumes that only the positive/ negative skewness affects the crop yield. Based on the city scale, the form of correlation-adjusted GDD indices is selected to maximize the correlation between the annual accumulated GDD and the annual yield. Note that the annual accumulated GDD is computed from the summation of daily GDD indices during the crop's growing phase in the year.

GDD indicator function

We define the last type of the city-based GDD with an indicator function. Denote the optimal growth temperature to be $T^{optimal}$, the GDD indicator function of day t follows:

$$GDD_{indf}(t) = A(T(t)-T^{optimal}) \times 1_{\{T(t) \geqslant T^{optimal}\}} + B(T(t)-T^{optimal}) \times 1_{\{T(t)<T^{optimal}\}}, \tag{5.8}$$

where $T(t)$ is the DAT on day t. Meanwhile, Eq. 5.8 can be also written as:

$$GDD_{indf}(t) = A \times max[T(t) - T^{optimal}, 0] + B \times min[T(t) - T^{optimal}, 0]. \tag{5.9}$$

Note that Eq. 5.9 expresses the GDD index on a daily scale. Give the contract period (t_1, t_2), the accumulated GDD $GDD_i(t_1, t_2)$ follows Eq. 5.4.

The GDD indicator function assumes that both the positive and the negative deviations from the optimal growth temperature affect the crop yield, but with different levels of impact. The scaling parameters A and B respectively represent the impact of higher and of lower temperature that deviates from the optimal growth temperature, which can be estimated via the optimization mechanism:

$$\underset{A,B}{\operatorname{argmax}} |corr[GDD_k^{indf}, Y_k]|, \tag{5.10}$$

where Y_k denotes the time series of annual yields in k years, and GDD_k^{indf} refers to the time series of corresponding annual GDD indices that are computed from accumulations of daily GDDs during the crop's growing phase.

5.3.2 Designing climatic zone-based GDD contracts

The standard of climatic zone partition divides mainland China into seven parts according to the climatic patterns of different regions. Due to the large land area of China, a well-designed climatic zone-based temperature contract can be particularly economic and of great convenience. As the climatic zone-based GDD produces an unique temperature index for all the cities in the same climatic zone, one of the most outstanding advantage of such an index is cost reduction. To be specific, a spatially standardized index saves the computational time of the modeling. Further, it brings down the transaction cost when an unique index is traded in all the cities in the climatic zone. As a result, such contract is beneficial for a variety of sectors that are exposed under weather risks, such as agriculture-related industries, banking sector, insurance companies, reinsurance, government, agricultural insurance schemes, etc. The second advantage of the climatic zone-based weighted quadratic index is that it incorporates the idea of spatial aggregation which is claimed to be able to reduce the basis risk of temperature-based derivatives.

In this section, we introduce a new class of GDD contracts which is based on a climatic zone scale. Three different approaches of calculating climatic zone-based GDD indices are listed. In the empirical study, we valuate a range of European option contracts written on the proposed indices using the CAR model [2]. Next, efficiency comparisons are conducted both between the climatic zone-based and city-based GDD indices and among the three types of climatic zone-based indices.

Average climatic zone-based GDD contracts

To calculate the climatic zone-based GDD, we first select a certain number of representative cities that distribute evenly in the climatic zone. Let $GDD_i(t)$ denote the GDD index of representative city i, the climatic zone-based index can be expressed as a weighted function of city-based indices, which follows:

$$GDD(w,t) = \sum_{i=1}^{n} w_i \times GDD_i(t), \tag{5.11}$$

where n is the total number of representative cities selected from the climatic zone, and $w = w_i, i = 1, 2, ..., n$ is the set of weight parameters of the representative cities. Therefore, it is crucial to find an suitable way to define the weight, as the index value $GDD(w, t)$ changes accordingly, as well as the contract efficiency.

In the first definition of weights, we let the weight parameter have equal values in all the representative cities from the same climatic zone. Given the total number of representative cities in the climatic zone n, the climatic zone-based weight is expressed as:

$$w_i = \frac{1}{n}. \tag{5.12}$$

In this case, the climatic zone-based GDD is simply the average value of GDD indices of representative cities. Therefore, we name this type of climatic zone-based GDD index the average climatic zone-based GDD.

Analogue to the accumulated city-based index , the accumulated climatic zone-based index $GDD(w, t_1, t_2)$ is given by:

$$GDD(w, t_1, t_2) = \sum_{s=t_1}^{t_2} GDD(w, s). \tag{5.13}$$

Yield-weighted climatic zone-based GDD contracts

Different from the average climatic zone-based GDD, we define the second type of climatic zone-based weights with the yield that a particular crop grows in the representative city. Specifically, considering a particular crop, we let w_i be the proportion that is expressed by the crop's annual yield in city i over the total annual yield of all the representative cities from the climatic zone. Thus, w_i follows:

$$w_i(t) = \frac{Y_i(t)}{\sum_{s=1}^{n} Y_s(t)}, \tag{5.14}$$

where $Y_i(t)$ is the crop yield in city i at year t.

Optimal-weighted climatic zone-based GDD contracts

The third type of climatic zone-based GDD weights are designed to maximize the absolute value of the correlation between the climatic zone-based GDD index and the total yield. Let Y_i be the set of annual crop yields in city i during time interval Ω, w_i satisfies:

$$w = argmax|corr[GDD(w, \Omega), \sum_{s=1}^{n} Y_s]|, \tag{5.15}$$

with the constraint equality:

$$\sum_{s=1}^{n} w_s = 1. \tag{5.16}$$

5.4 Efficiency comparison among GDD contracts

5.4.1 GDD Contract Optimalisation

In this part, we propose a method to find out the optimal tick size for the GDD contracts under the framework of Vedenov and Barnett's work [12]. Despite that the majority of empirical studies choose to neglect the discussion on the tick size of the weather contracts, the tick size is a crucial factor in terms of contract designing and optimalisation. Let $\bar{Y}$ denote the long-term average yield of a crop, and Y_t^{det} denote the annual time-detrended yield of year t, which follows:

$$Y_t^{det} = Y_t \frac{Y_t^{tr}}{Y_{t_0}^{tr}}. \tag{5.17}$$

where Y_t^{tr} expresses the deterministic component of the annual yield Y_t, which can be estimated by regressing the following equation:

$$\log(Y_t) = a_0 + a_1(t - t_0). \tag{5.18}$$

Thus, the optimal tick size λ of a GDD contract can be solved by minimizing Eq. 5.19:

$$\sum_t max[\bar{Y} - (Y_t^{det} + \lambda * P - \lambda * P_0), 0]^2. \tag{5.19}$$

where P is the option prices under a CAR model [2] and P_0 is the corresponding payoffs. Under this condition, the tick size minimizes the aggregated semi-variance of the loss [12, 57].

5.4.2 An empirical efficiency test

In order to compare the efficiency of the city-based and the climatic zone-based GDD contracts in terms of risk reduction for farm households, we look into the annual revenues of a certain crop with and without the considered GDD contracts. According to Vedenov and Barnett [12], the revenue without the GDD contract equals to the gross income of selling the commodity, which follows:

$$R_t = pY_t^{det}, \quad t = 1, ..., T, \tag{5.20}$$

while the revenue with the GDD contract is given by:

$$R_t' = pY_t^{det} + contract\ payoff - contract\ price, \quad t = 1, ..., T, \tag{5.21}$$

where p is the commodity price of the corresponding crop, and Y_t^{det} is the time-detrended yield.

We apply three test criteria used by Vedenov and Barnett [12] in order to gain some implications on the efficiency of weather contracts analytically. The definition and the mathematical expressions of the test criteria are given below:

- The mean root square loss (MRSL).

$$MRSL = \sqrt{\frac{1}{T}\sum_{t=1}^{T}[max(p\bar{Y} - R_t, 0)]^2}. \tag{5.22}$$

- The value-at-risk (VaR).

$$Pr(R < VaR_\alpha) = \alpha. \tag{5.23}$$

- The certainty-equivalent revenues (CERs).

$$U = 1 - exp(-\gamma R). \tag{5.24}$$

The first criterion, the MRSL, measures the semi-variance of the revenue distribution. A smaller MRSL indicates a lower level of revenue variation, thus less pronounced yield risks. Meanwhile, the VaR is an inverse function of the cumulative density function of the return distribution which measures the value of return at a given risk level. By computing the VaR at different risk values, one can gain a general understanding about the return distribution. Last, the CERs compute expected revenues with a given level of risk aversion. Both the VaR and the CERs assess the risk hedging power of an weather contract in different ways with the MRSL, in which case a smaller value refers to a lower degree of risk exposition.

Remark that in the case of the CERs, we estimate the risk aversion level γ [58] by the following equation:

$$E[U(R)] = U((1 - \theta) * E[R]). \tag{5.25}$$

We then compute the value of γ in Eq.5.24 with different risk premiums θ, i.e. 0%, 5% and 10%. However, we find that with the yield data of Chinese cities, the results across cities and risk premiums exclusively tend to 1. Under this condition, the values of the CERs of a given city shall be proportional to the corresponding values of the risk premiums. Thus, in Table 5.4 and 5.5, only the CERs with risk premium 5% are given.

Our investigation of city-based and climatic zone-based GDD contracts can be split into two consecutive efficiency tests. In the first efficiency test, we look into the risk hedging performances of European call options written on the three city-based indices. Two scenarios are considered when different city-based GDD indices are compared. The first one (Case 1) is an ideal situation in which weather contract

transactions take place in all the representative cities, while the second situation (Case 2) is more practical which only allows one trading spot in each climatic zone. In Case 2, the trading spots of each climatic zone are Changchun (Climatic zone I), Shijiazhuang (Climatic zone I), and Hefei (Climatic zone I). The trading spots are selected as they are located in the center of other representative cities in their climatic zone. After the most efficient city-based index is determined, we conduct the second efficiency test on the climatic zone-based GDD contracts, aiming to find the best way to define weight parameters. Eventually, we compare the risk hedging power of the city-based and the climatic zone-based GDD contracts, in order to understand the practical value of the climatic zone-based contracts.

5.5 Results and Discussion

5.5.1 Efficiency analysis of city-based GDD indices

In this section, we present analytical results of the efficiency test on the city-based GDD indices. The three city-based indices, i.e. the absolute deviation-based GDD, the correlation-adjusted GDD, and the GDD indicator function, are compared in terms of the mean root square loss (MRSL), the value-at-risk (VaR) and the certainty-equivalent revenues (CERs). Discussions on the performances of different GDD indices are made, with the purpose to determine the most suitable and efficient hedging underlying for agricultural risk reduction in China.

The MRSLs

Table 5.2 and 5.3 display the values of four types of MRSLs, which are obtained from farmers'revenues without any GDD contracts, and with GDD call options respectively written on the three different city-based GDD indices.

Table 5.2 describes a situation where accesses to GDD derivative transactions exist in all the representative cities. As the MRSL measures the semi-variance of the loss distribution, a smaller MRSL indicates a less risky situation. Three observations are made from Table 5.2.

Table 5.2: Efficiency comparison among city-based GDD contracts: MRSL (Case 1).

City	Climatic zone	Without contract	Absolute deviation	Change	Correlation-adjusted	Change	Indicator function	Change
Haerbin	I	318.60	294.28	-0.08	303.82	-0.05	274.68	-0.14
Changchun		217.16	203.46	-0.06	212.50	-0.02	178.97	-0.18
Beijing	II	153.10	95.85	-0.37	136.26	-0.11	100.53	-0.34
Shijiazhuang		294.83	161.37	-0.45	268.30	-0.09	267.17	-0.09
Ji'nan		309.45	160.51	-0.48	265.63	-0.14	295.06	-0.05
Zhengzhou		339.69	189.87	-0.44	286.00	-0.16	228.01	-0.33
Nanjing	III	136.33	123.51	-0.09	129.91	-0.05	135.18	-0.01
Hefei		288.25	268.97	-0.07	260.87	-0.09	288.21	0.00
Wuhan		62.96	60.78	-0.03	59.69	-0.05	61.92	-0.02
Hangzhou		202.99	187.46	-0.08	180.27	-0.11	200.06	-0.01
Nanchang		182.02	178.00	-0.02	158.04	-0.13	180.42	-0.01

The first observation is that given a particular type of GDD indices, its MRSL-reduction levels change from place to place. For instance, for the cities in climatic

zone II, absolute deviation-based GDDs provide an outstanding performance with significantly lower MRSLs, which indicate a lower level of revenue fluctuations, compared to the correlation-adjusted GDD and the GDD indicator function. However, when it comes to the cities in climatic zone I, the GDD indicator function gives the best result among the three GDD indices. Similarly, in climatic zone III, MRSLs obtained from the GDD indicator function have the highest values than those obtained from the absolute deviation-based GDD and the correlation-adjusted GDD.

The second observation is that MRSLs obtained from a given type of GDD indices tend to stay close to each other in the same climatic zone. Typical examples can be found in climatic zone II when the absolute deviation-based GDD is applied, and in climatic zone III when the GDD indicator function is applied. As a matter of fact, the only exception of the pre-described phenomenon is in the case of the GDD indicator function, with which MRSLs have huge variances in climatic zone II.

Last, compared with correlation-adjusted GDDs and GDD indicator functions, absolute deviation-based GDDs tend to provide the most stable and acceptable results in reducing MRSLs. To be specific, MRSLs obtained from absolute deviation-based GDDs have either the lowest values (in climatic zone II), or the second lowest values with limited differences from the lowest (in climatic zone I and III). On the other hand, the correlation-adjusted GDD falls behind in the MRSL comparison in climatic zone I and II, while in climatic zone III, it gives close result with the absolute deviation-based GDD. Meanwhile, the GDD indicator function only outperforms the other two GDDs in climatic zone I, while in climatic zone III, it give the poorest performance with highest MRSLs among the three types of GDD indices.

In Table 5.3, only one representative city is allowed to operate GDD contract exchanges in each climatic zone. The findings from Table 5.3 are threefold.

Table 5.3: Efficiency comparison among city-based GDD contracts: MRSL (Case 2).

City	Climatic zone	Without contract	Absolute deviation	Change	Correlation-adjusted	Change	Indicator function	Change
Haerbin	I	318.60	301.32	-0.05	308.28	-0.03	262.86	-0.17
Changchun*		217.16	203.46	-0.06	212.50	-0.02	178.97	-0.18
Beijing	II	153.10	96.73	-0.37	139.26	-0.09	144.71	-0.05
Shijiazhuang*		294.83	161.37	-0.45	268.30	-0.09	267.17	-0.09
Ji'nan		309.45	165.88	-0.46	280.98	-0.09	276.69	-0.11
Zhengzhou		339.69	191.60	-0.44	309.04	-0.09	304.38	-0.10
Nanjing	III	136.33	125.44	-0.08	124.76	-0.08	136.33	0.00
Hefei*		288.25	268.97	-0.07	260.87	-0.09	288.21	0.00
Wuhan		62.96	60.82	-0.03	59.25	-0.06	62.86	0.00
Hangzhou		202.99	188.19	-0.07	174.83	-0.14	202.80	0.00
Nanchang		182.02	169.26	-0.07	155.86	-0.14	181.34	0.00

First, the assumption that only allows one trading spot in the climatic zone causes small changes in the MRSL. Contracts written on the GDD index of another location in the same climatic zone (Case 2) tend to have lower risk hedging efficiency compared with those written on their local GDD index (Case 1). However, it is not always the case that the efficiency will be reduced if the GDD contract is not written on the local DAT index. For instance, MRSLs of the cities in climatic zone III decrease exclusively in Case 2 when the correlation-adjusted GDD is applied.

Second, climatic zone-based patterns can be observed from different angles of MRSLs. As it has been already discussed in the previous paragraphs, MRSLs of

the cities from the same climatic zone have close values when the type of GDD indices is fixed. Moreover, from Case 1 to Case 2, MRSLs change in the same manner (decrease or increase) for the cities in the same climatic zone for a given type of GDD indices. One typical example is when the correlation-adjusted GDD is applied, all the cities from climatic zone II and III display a lower MRSL in Case 2.

Third, the order of risk hedging powers of the three GDD indices remains the same in Case 2. Even when only one exchange spot is allowed in each climatic zone, the absolute deviation-based GDD still outperforms the other two types of GDD indices.

The VaRs

Table 7.3 and 7.4 in the Appendix list VaRs respectively at risk levels 5%, 10% and 20%, along with the increase of the VaR by holding a corresponding GDD contract. Table 7.3 gives the VaR result in Case 1, which assumes that there are GDD contract transactions in all the representative cities, while Table 7.4 displays the VaRs in Case 2, which only allows one trading spot in each climatic zone.

We can find mainly two similarities between the result of the MRSL and the VaR measures. First, inconsistency exists in the performances of a given type of GDD index. For example, at risk level 5%, the absolute deviation-based GDD provides the highest VaRs in climatic zone II, but the lowest in climatic zone I. Second, the more realistic situation, in which there is only one trading spot among the representative cities in the climatic zone, results in lower risk hedging efficiency of GDD contracts. The major reason is due to the geographical risk caused by purchasing contracts written on GDD indices of a different location. However, different from the result of MRSLs, climatic zone-based pattern becomes less pronounced in the case of the VaR. To be specific, given the type of GDD indices, larger variances can be observed in the VaRs in the same climatic zones. Further, signs of VaR changes, that are caused by switching from Case 1 to Case 2, vary from city to city in the climatic zone.

Besides the observations discussed above, one can also notice that the performances of GDD indices vary at different risk levels. For instance, the absolute deviation-based GDD shows a higher level of risk reduction at risk level 5% compared to the correlation-adjusted GDD and the GDD indicator function. However, at risk level 20%, such superiority of the absolute deviation-based GDD dims as the correlation-adjusted GDD tends to produces higher VaRs for the cities from climatic zone III. Nevertheless, according to Table 7.3 and 7.4, we still consider the absolute deviation-based GDD to be the most preferable index taking in to account that the information at risk level 5% is more valuable in the case of risk management for Chinese farmers who are highly risk-averse. Additionally, the absolute deviation-based GDD tends to produce the most stable performances among all the three types of GDD indices.

The CERs

In Table 5.4 and 5.5, CERs with risk premium 5% are given respectively in Case 1 and Case 2.

Table 5.4: Efficiency comparison among city-based GDD contracts: CER (Case 1).

City	Climatic zone	Without contract	Absolute deviation	Change	Correlation-adjusted	Change	Indicator function	Change
Haerbin	I	535.77	570	0.06	559.06	0.04	591.72	0.10
Changchun		1001.27	1020.60	0.02	1013.07	0.01	1045.49	0.04
Beijing	II	523.33	584.58	0.12	547.32	0.05	573.39	0.10
Shijiazhuang		236.90	367.49	0.55	269.15	0.14	271.23	0.14
Ji'nan		298.11	440.09	0.48	350.06	0.17	315.26	0.06
Zhengzhou		209.80	359.60	0.71	270.84	0.29	328.58	0.57
Nanjing	III	674.57	688.7	0.02	98.82	-0.85	675.95	0.00
Hefei		405.35	427.2	0.05	441.80	0.09	405.58	0.00
Wuhan		524.97	529.53	0.01	531.23	0.01	524.91	0.00
Hangzhou		346.47	365.10	0.05	372.55	0.08	349.14	0.01
Nanchang		76.07	80.16	0.05	101.85	0.34	77.79	0.02

Table 5.5: Efficiency comparison among city-based GDD contracts: CER (Case 2).

City	Climatic zone	Without contract	Absolute deviation	Change	Correlation-adjusted	Change	Indicator function	Change
Haerbin	I	535.77	562.46	0.05	553.91	0.03	600.62	0.12
Changchun		1001.27	1020.14	0.02	1013.07	0.01	1045.49	0.04
Beijing	II	523.33	585.37	0.12	540.07	0.03	537.09	0.03
Shijiazhuang		236.90	367.22	0.55	269.15	0.14	271.23	0.14
Ji'nan		298.11	436.11	0.46	332.32	0.11	336.27	0.13
Zhengzhou		209.80	357.97	0.71	247.01	0.18	251.33	0.20
Nanjing	III	674.57	685.79	0.02	93.87	-0.86	674.54	0.00
Hefei		405.35	427.05	0.05	441.80	0.09	405.58	0.00
Wuhan		524.97	528.99	0.01	531.40	0.01	524.83	0.00
Hangzhou		346.47	362.46	0.05	377.13	0.09	346.88	0.00
Nanchang		76.07	90.15	0.19	104.02	0.37	76.82	0.01

The result of the CER measure supports the conclusion made from the previous sections. Further, great similarities exist between the CERs and the MRSLs. Typical expositions of the similarity are in climatic zone II when absolute deviation-based GDDs are considered and in climatic zone III when GDD indicator functions are considered. The former combination of climatic zones and GDD indices always produces the highest level of risk reduction among the three different types of GDDs, while the latter combination always produces the lowest level of risk reduction. Moreover, from Table 5.4 and 5.5, we can again find the climatic zone-based pattern that is described by MRSLs. Finally, despite that the performances of GDD indices displays an inconsistency from climatic zone to climatic zone, the absolute deviation-based GDD occupies the dominant place by producing comparatively better and more stable results. Such stability indicates reliability of the risk hedging power of the GDD index.

5.5.2 Efficiency analysis of climatic zone-based GDD contracts

According to the conclusion of the previous section, we hire the absolute deviation-based GDD index as the city-based index in this section. Subsequential, the climatic zone-based index is obtained regarding to the weight of each representative city in the climatic zone. Therefore, different types of weights lead to different values of

climatic zone-based indices. This section includes three different types of weights described in Section 5.3.2, i.e. the average weight, the yield-based weight and the optimized weight. We first compare the result of the efficiency test that is based on option contracts written on different climatic zone-based GDD indices. The objective is to find the most efficient definition of climatic zone-based weights. Next, we conduct an efficiency comparison between the climatic zone-based contract and the city-based contract[2], through which we hope to find out whether the climatic zone-based contract is capable of replacing the city-based contract as an agricultural risk management tool in China.

The MRSLs

Table 5.6 lists the MRSLs of climatic zone-based option contracts with respectively the average GDD (Weight: Case 1), the yield-weighted GDD (Weight: Case 2) and the optimal-weighted GDD (Weight: Case 3). The major observations from Table 5.6 are threefold.

First, the climatic zone-based GDD contract can be considered as an effective risk management tool in terms of hedging weather risks for Chinese farm households. As it is shown in Table 5.6, MRSLs are exclusively reduced by holding a climatic zone-based GDD contract in all the cities considered.

Second, the three different types of climatic zone-based GDD indices generate fairly close results in the MRSL measure, which indicates very similar performances in smoothing return fluctuations. Especially between the average GDD contract and the yield-weighted GDD contract, the percentages of the MRSL reduction stays the same in nine out of eleven cities.

Last, when the MRSLs of climatic zone-based contracts are compared with those of city-based contracts, there does not exist an unique way of defining the climatic zone-based index in order to achieve a better performance. According to Table 5.6, none of the three types of climatic zone-based indices manages to provide exclusively lower MRSLs than the city-based index. Namely, the average GDD and the yield-weighted GDD fail in Climatic zone I and III, while the optimal-weighted GDD fails in climatic zone II. Consequently, we have to leave the climatic zone-based weight flexible in order to adjust the performance of climatic zone-based contracts. In the case of the MRSL measure, we recommend the combination of hiring the average GDD index for cities in Climatic zone II, and hiring the optimal-weighted GDD for cities in Climatic zone I and III as it generates the best result. Specifically, the MRSLs obtained from the combination are always smaller than those obtained from city-based contracts in Case 2 [3]. Even in Case 1 [4], eight out of eleven cities have

[2]Note: City-based contracts in this section only refer to those city-based contracts written on the absolute deviation-based GDD index, as they are identified as the most suitable type of contract on the city scale for agricultural risk management in China (see Section 5.5.1).

[3]Note: Case 2 of city-based contracts describes a situation in which only one representative city is allowed to issue GDD derivative contracts in each climatic zone.

[4]Note: Case 1 of city-based contracts describes a situation in which all the representative city are allowed to issue GDD derivative contracts.

lower MRSLs by following the scheme described by the combination.

Table 5.6: Efficiency comparison among climatic zone-based GDD contracts: MRSL.

City	Climatic zone	Without contract	Weight: Case 1	Change	Weight: Case 2	Change	Weight: Case 3	Change
Haerbin	I	318.60	300	-0.06	300.65	-0.06	295.11	-0.07
Changchun		217.16	203	-0.06	203.55	-0.06	200.07	-0.08
Beijing	II	153.10	95.3	-0.38	94.9	-0.38	95.86	-0.37
Shijiazhuang		294.83	159	-0.46	159.38	-0.46	169.24	-0.43
Ji'nan		309.45	163	-0.47	163.36	-0.47	173.20	-0.44
Zhengzhou		339.69	189	-0.44	189.31	-0.44	200.43	-0.41
Nanjing	III	136.33	126	-0.08	125.13	-0.08	124.26	-0.09
Hefei		288.25	269	-0.07	267.91	-0.07	262.82	-0.09
Wuhan		62.96	61.8	-0.02	61.53	-0.02	61.54	-0.02
Hangzhou		202.99	191	-0.06	189.46	-0.07	186.96	-0.08
Nanchang		182.02	170	-0.07	168.28	-0.08	163.70	-0.10

The VaRs

Table 7.5 provides the VaRs of climatic zone-based contracts. Inconsistencies can be noticed between the result of the VaR measure and of the MRSL measure. The findings are discussed in the following.

First, despite that the VaR result tends to produce a higher level of deviations between different types of climatic zone-based indices than the MRSL, one can still observe similarity between the average GDD and the yield-weighted GDD. As it is shown in Table 7.5, for the same city, the VaRs obtained from the average GDD and the yield-weighted GDD tend to stay in a very close interval, while the VaR obtained from the optimal-weighted GDD tends to have larger difference with the other two types of VaRs.

Second, according to Table 7.5, climatic zone-based contracts increase the values of VaRs on the base of those without GDD contracts in most of the cities. It indicates a risk reduction that is resulted from purchasing the climatic zone-based GDD contract.

Third, the performance of climatic zone-based contracts becomes less promising in the VaR measure. According to the result of MRSLs, by combining different types of weighted GDD indices, the climatic zone-based contract can always have a higher degree of risk reducing efficiency than the city-based contract. However, it is no longer the case in the VaR measure. Taking the VaRs at risk level 5% in Case 2 (the more practical case!) as an example, all the three types of climatic zone-based contracts fail in the comparison with city-based contracts in four out of eleven cities, namely Changchun, Nanjing, Hefei and Hangzhou. That is to say, no matter which type of climatic zone-based contract is applied, the city-based contract is still a better risk hedging instrument in those four cities.

Last, the VaR result suggests that the average GDD contract and the yield-weighted GDD contract are better options than city-based contracts in Climatic zone II, as they produce higher VaRs for all the cities in the climatic zone. Under this circumstance, we recommend the average GDD contract considering its simplicity.

The CERs

The result of climatic zone-based CERs is shown in Table 5.7. Great similarity with the result of MRSLs can be found.

First of all, being consistent with the result of MRSLs and of VaRs, the CERs indicate that climatic zone-based contracts manage to reduce yield variations by producing greater CERs. Further, the CERs result reveals the similarity between the average GDD and the yield-weighted GDD as well as MRSLs and VaRs.

Furthermore, in the comparison with city-based contracts, the CERs result in rather close conclusion with the MRSL, that is in Climatic zone I and III, the optimal-weighted GDD contract outperforms all the other types of GDD contracts which includes both city-based and climatic zone-based contracts, while in Climatic zone II, the average GDD and the yield-weighted GDD contracts are the best choices.

Table 5.7: Efficiency comparison among climatic zone-based GDD contracts: CER.

City	Climatic zone	Without contract	Weight: Case 1	Change	Weight: Case 2	Change	Weight: Case 3	Change
Haerbin	I	535.77	563.7	0.05	562.99	0.05	568.88	0.06
Changchun		1001.27	1020.82	0.02	1020.40	0.02	1024.17	0.02
Beijing	II	523.33	586.53	0.12	586.70	0.12	584.71	0.12
Shijiazhuang		236.90	368.95	0.56	368.85	0.56	361.87	0.53
Ji'nan		298.11	438.02	0.47	437.87	0.47	430.86	0.45
Zhengzhou		209.80	360	0.72	359.81	0.72	351.77	0.68
Nanjing	III	674.57	685.29	0.02	686.19	0.02	688.20	0.02
Hefei		405.35	426.31	0.05	428.2	0.06	434.11	0.07
Wuhan		524.97	527.80	0.01	528.28	0.01	528.48	0.01
Hangzhou		346.47	360.4	0.04	362.12	0.05	365.67	0.06
Nanchang		76.07	89.48	0.18	90.97	0.20	95.40	0.25

5.6 Summary

In this section, we carry out efficiency tests in order to determine the optimal city-based and climatic zone-based GDD indices for agricultural risk management in China. Major conclusions are summarized in the following.

First, among all the three types of city-based GDDs, i.e. the absolute deviation-based GDD, the correlation-adjusted GDD, and the GDD indicator function, the

absolute deviation-based GDD is our primary recommendation as it provides overall more robust results than the other two types of indices.

Second, efficiency results obtained from climatic zone-based GDD indices suggests that climatic zone-based contracts can be a more efficient risk hedging instrument compared with city-based contracts. Further, we recommend market participants who are exposed to the yield risk to purchase the climatic zone-based contract written on the average GDD index, if he is located in climatic zone II; and to purchase the climatic zone-based contract written on the optimal-weighted GDD index, if he is located in climatic zone I or III.

Chapter 6

Conclusions

6.1 Research summary

The presented thesis constructed the fundamental modeling framework of temperature-based weather derivatives in China on the theoretical and empirical basis. In the first part of the thesis, existing temperature models and pricing approaches were discussed deliberately taking into account the reality of Chinese market. Three established temperature models respectively proposed by Alaton et al. [1], Benth et al. [2] and Schiller et al. [3] were applied to model the daily average temperature (DAT) data of twelve Chinese cities. Meanwhile, a novel temperature model contains stochastic volatility modeling, namely the stochastic seasonal variation (SSV) model, was introduced in order to achieve better goodness-of-fit and forecasting power. Model comparisons were conducted among the four temperature models. In the second part of the thesis, temperature-based derivative contracts were discussed from a more practical perspective, which put emphasis on its usage as an agricultural risk management tool. Three types of new temperature indices, namely the absolute deviation-based GDD, the correlation-adjusted GDD, and the GDD indicator function, were proposed with the purpose of achieving greater degrees of risk reduction. Further, temperature-based contracts on the climatic zone level were introduced for the sake of spatial aggregation. Finally, efficiency tests involved the mean root square loss (MRSL),the value-at-risk (VaR) and the certainty-equivalent revenues (CER) were implemented with the aim to investigate the risk hedging power of the proposed GDD indices.

Major findings of the study is summarized in the following.

First, there exists significant model risk in the temperature modeling. According to the result of model comparison in Chapter 4, deviations in different levels can be observed from the results of the four temperature models under investigation. Generally speaking, in the case of temperature modeling, the three stochastic models, i.e. the Alaton model [1], the CAR model [2] and the SSV model, follow comparatively close patterns. Especially in the error measure, monthly relative errors of the three stochastic models tend to stay on a similar scale. However, in the case of derivative pricing, huge deviations can be observed between the option prices obtained from

the Alaton model [1] and those from the CAR model [2] and the SSV model.

Second, stochastic volatility modeling provided by the SSV model makes essential improvements on both the goodness-of-fit and the forecasting power of temperature models. As a result, the SSV model is considered to be the primary option for temperature-based derivatives modeling and pricing in China. On the other hand, the Spline model [3] displays an outstanding performance in the error measure. However, due to its instability with the residual normality, we wouldn't recommend the Spline model for application. Moreover, although the result of our model comparison suggests that the CAR model [2] has weaker performance than the SSV model. As a classical stochastic temperature model, the CAR model provides rather robust results. Especially in the pricing section, the CAR model produces close contract prices between the Monte Carlo simulation and the approximation formula. Additionally, option prices obtained from the CAR model and those from the Monte Carlo simulation under the SSV model shows great similarity, which supports the reliability of the pricing result. Thus, we consider the CAR model to be another reliable model for temperature-based contract pricing.

Third, weather derivative contracts written on GDD indices are effective risk hedging tools for agricultural risks that are related with yield variations in China. Among all the three city-based GDD indices included in the study, namely the absolute deviation-based GDD, the correlation-adjusted GDD, and the GDD indicator function, the absolute deviation-based GDD is our primary recommendation as it offers an overall stable performance with pronouncing risk reduction.

Fourth, deliberately-used climatic zone-based GDD contracts can be a more efficient instrument for agricultural risk management than the city-based GDD contract. Sufficient result suggests that for cities in climatic zone I and III, climatic zone-based contracts written on the optimal-weighted GDD offers better risk reducing performances than city-based contracts, and for cities in climatic zone II, climatic zone-based contracts written on the average GDD and the yield-weighted GDD performs better than the city-based contract.

6.2 Future research

In this section, we list four recommendations for future work with respect to the results of this thesis.

First, considering the limited sample size of the out-of-sample test in the model comparison, we suggest a back-testing comparison among the four temperature models, for the purpose of gaining stable results of their forecasting power.

Second, more elaborate analyses on price behaviors should be conducted to learn more about the inherent model risk. Specifically, the major limitation of temperature-based derivative study in China is the lack of market data of contract prices, which give access to the market price of temperature risk. In this case, utility-based models could be applied in empirical analyzes in order to investigate the behavior of the market price of risk, thus take the entire research to another

depth.

Third, for the research of agricultural risk management, we intend a study focused on GDD distributions. As the CAR model [2] prices temperature-based derivatives with the assumption that the underlying indices are normally distributed, we assume that with a deeper understanding of the GDD distribution, more precise models for Chinese climatic-zone based GDD contracts can be derived.

Fourth, a temperature (weather)-yield regression model is recommended to be deduced and applied to Chinese data. The weather-yield model enables yield-forecast based on the forecasting result of temperature (or other weather factors), with which out-of-sample efficiency tests on GDD contracts can be then conducted.

Appendix A

Appendix of figures

Figure A.1: Histograms of in-sample residuals from the Alaton model [1] (Year: 1983-2012).

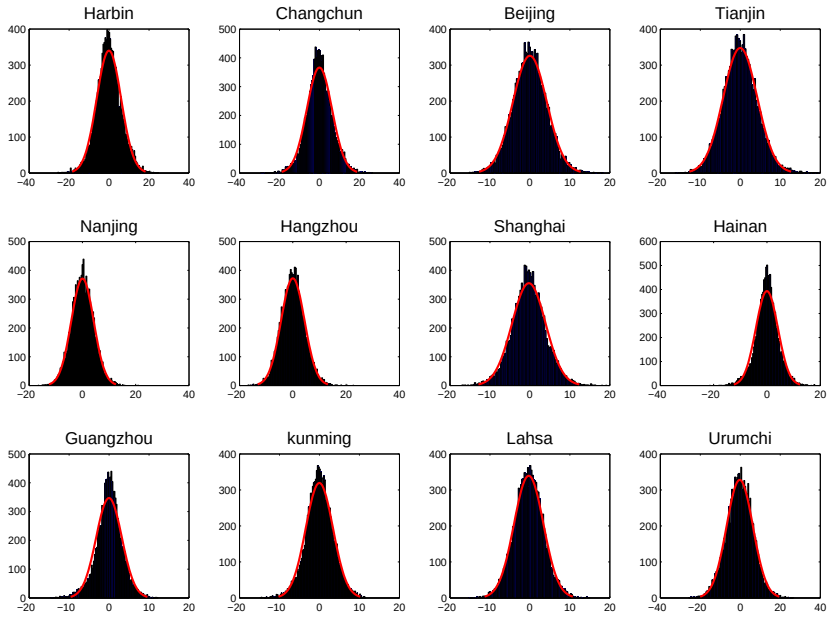

Figure A.2: Histograms of in-sample residuals from the CAR model [2] (Year: 1983-2012).

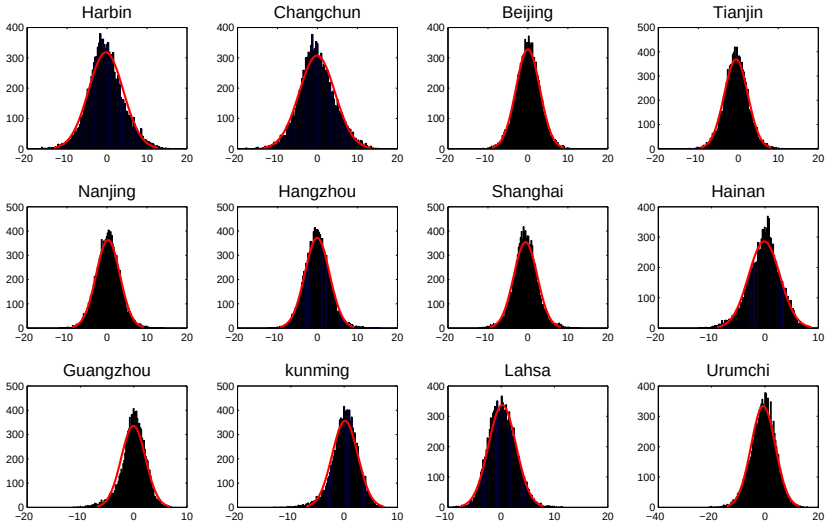

Figure A.3: Histograms of in-sample residuals from the Spline model [3] (Year: 1983-2012).

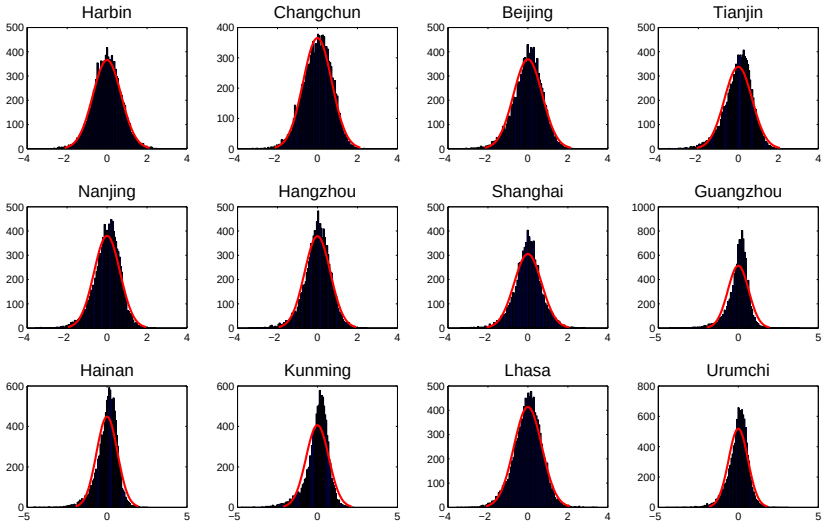

Figure A.4: Histograms of in-sample residuals from the SSV model (Year: 1983-2012).

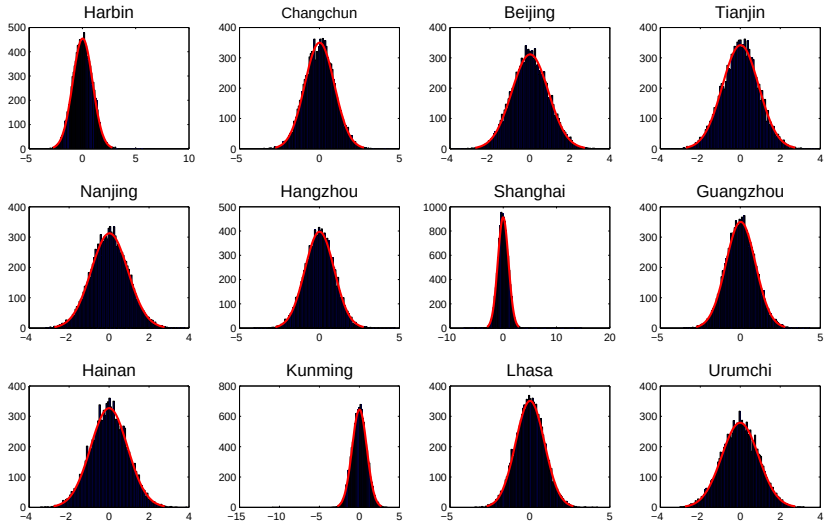

Figure A.5: Q-Q plots of in-sample residuals from the Alaton model [1] (Year: 1983-2012).

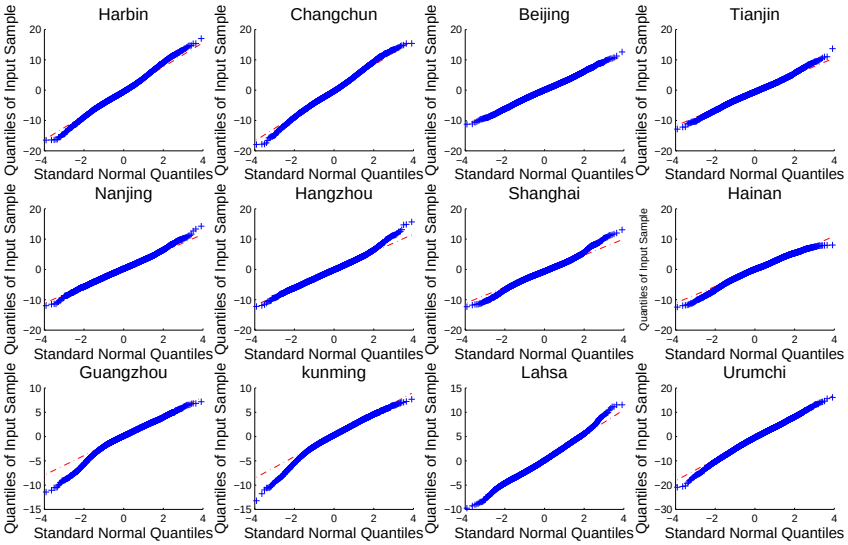

Figure A.6: Q-Q plots of in-sample residuals from the CAR model [2] (Year: 1983-2012).

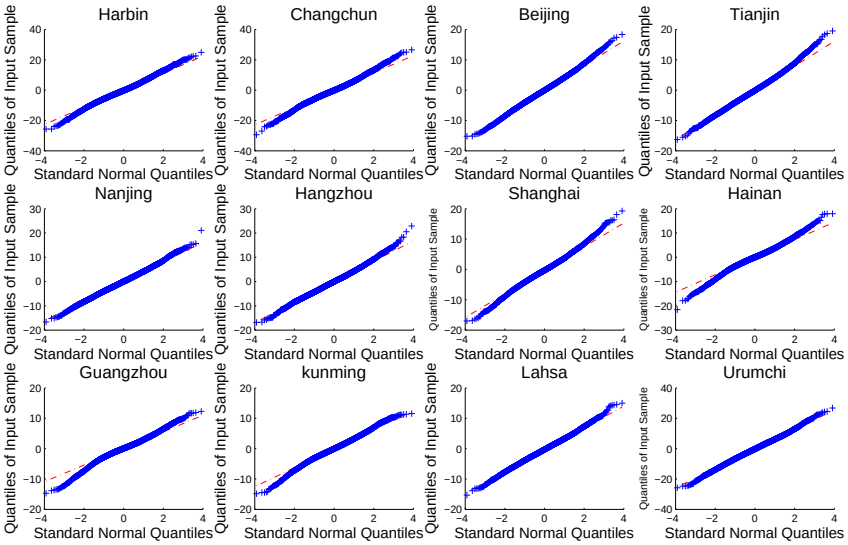

Figure A.7: Q-Q plots of in-sample residuals from the Spline model [3] (Year: 1983-2012).

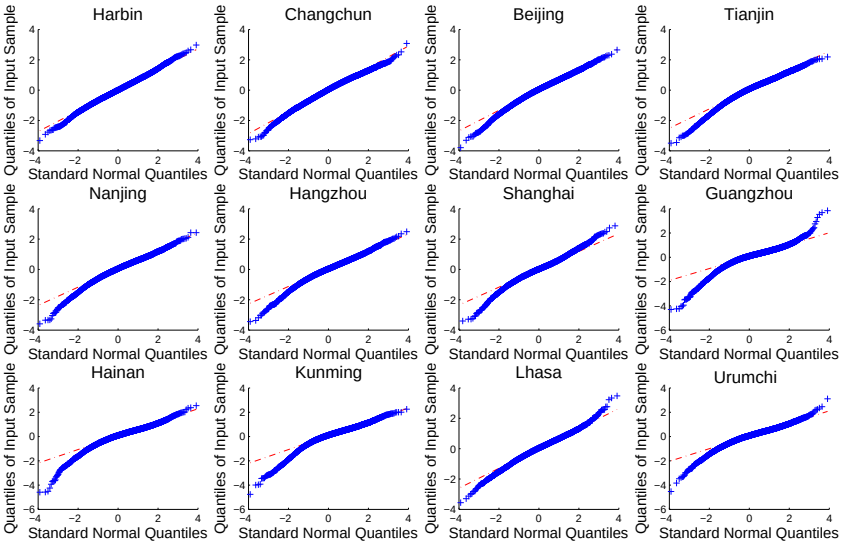

Figure A.8: Q-Q plots of in-sample residuals from the SSV model (Year: 1983-2012).

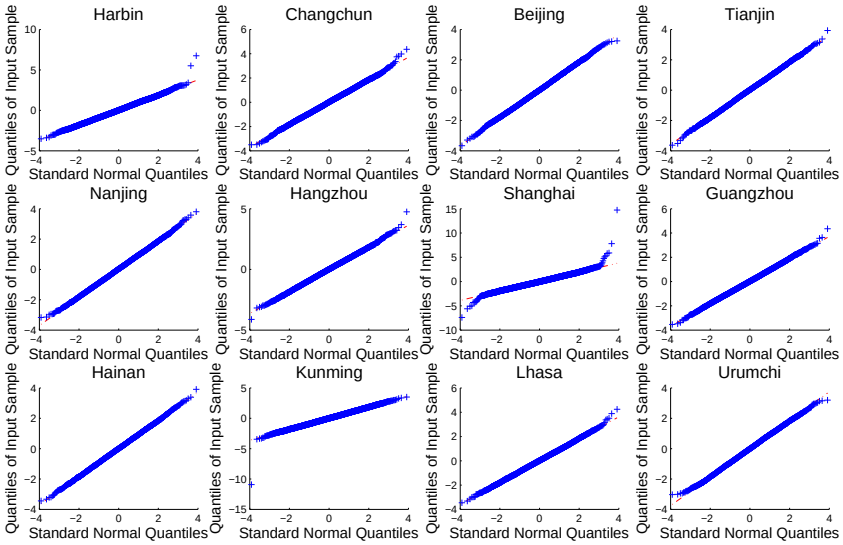

Figure A.9: ACF of residuals from the Alaton model [1] (Year: 1983-2012).

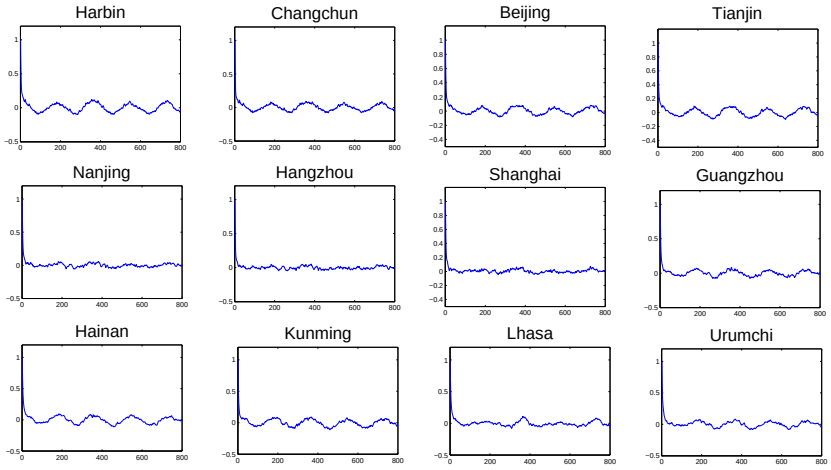

Figure A.10: ACF of residuals from the CAR model [2] (Year: 1983-2012).

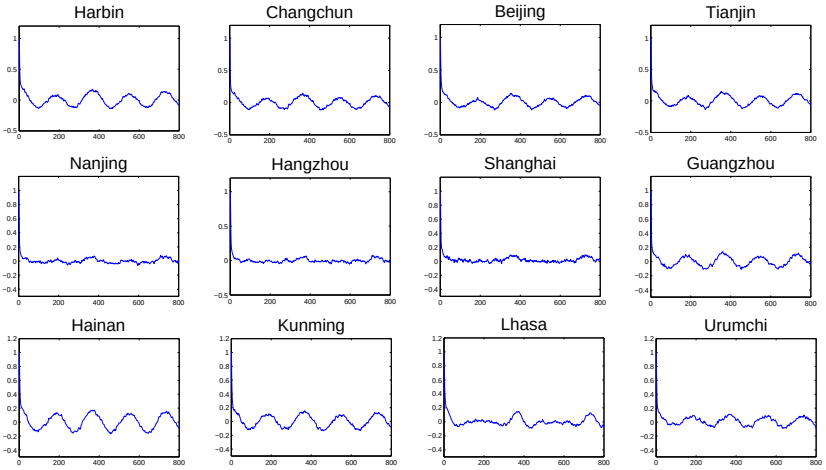

Figure A.11: ACF of residuals from the Spline model [3] (Year: 1983-2012).

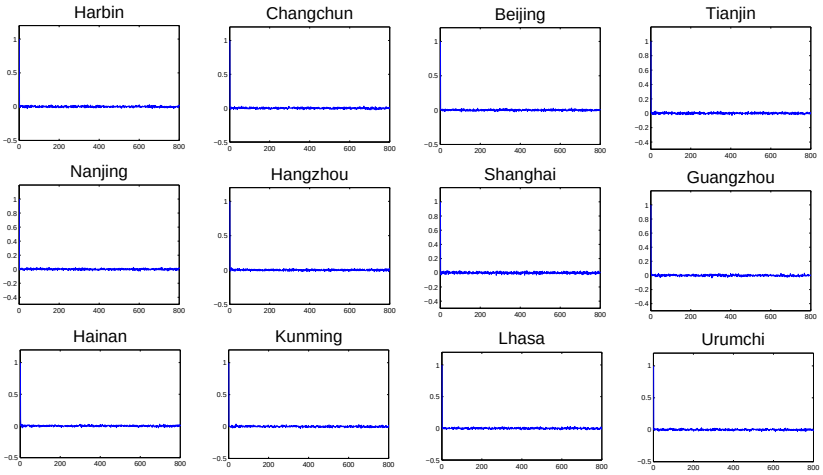

Figure A.12: ACF of residuals from the SSV model (Year: 1983-2012).

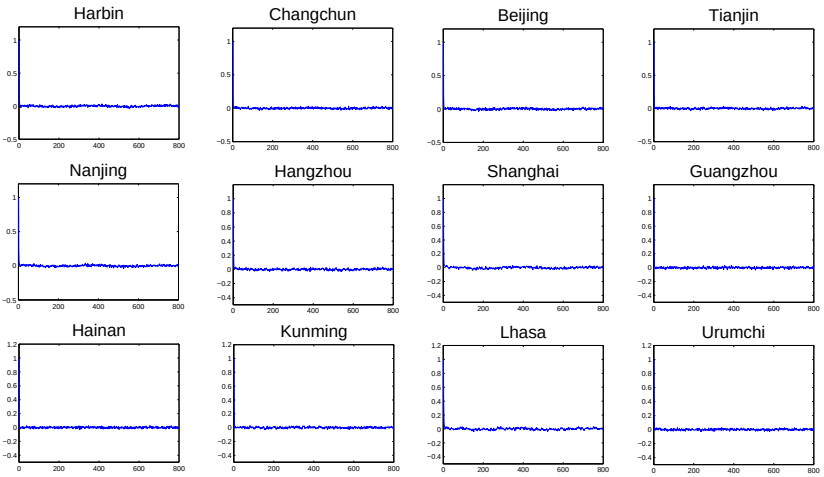

Figure A.13: ACF of squared residuals from the Alaton model [1] (Year: 1983-2012).

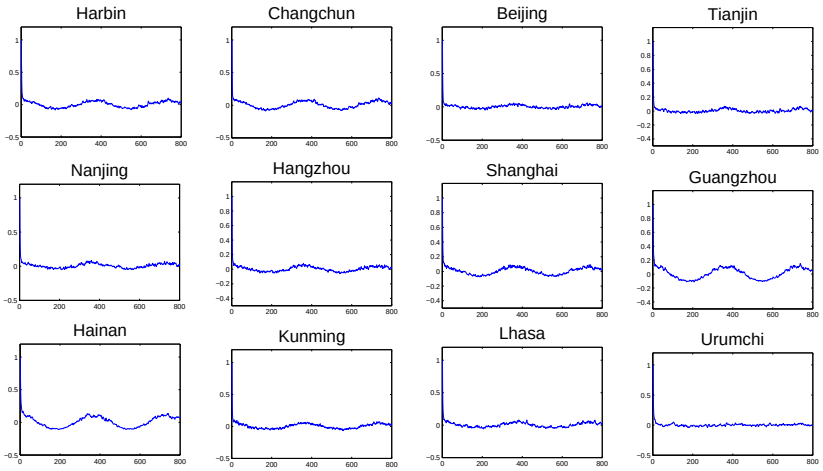

Figure A.14: ACF of squared residuals from the CAR model [2] (Year: 1983-2012).

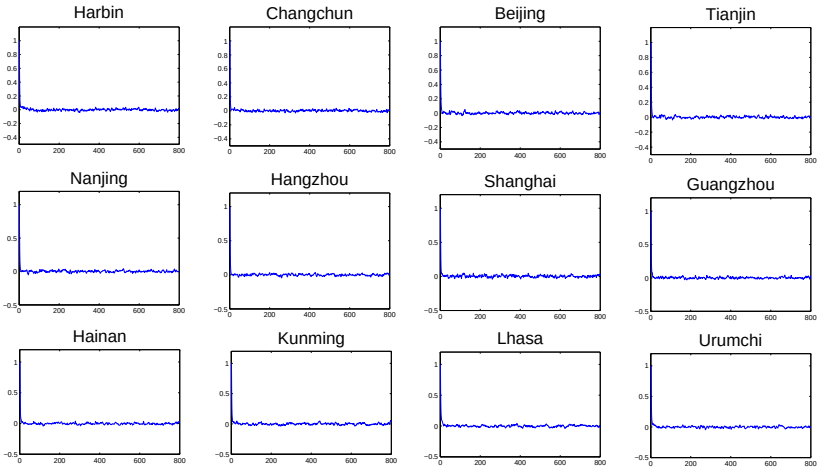

Figure A.15: ACF of squared residuals from the Spline model [3] (Year: 1983-2012).

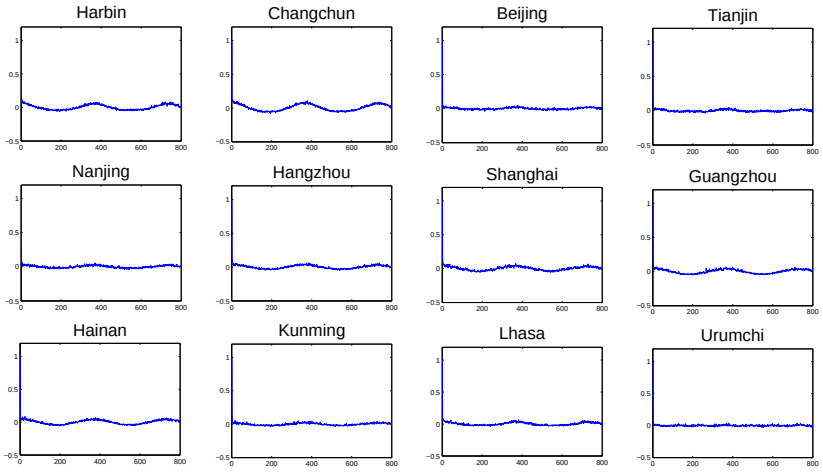

Figure A.16: ACF of squared residuals from the SSV model (Year: 1983-2012).

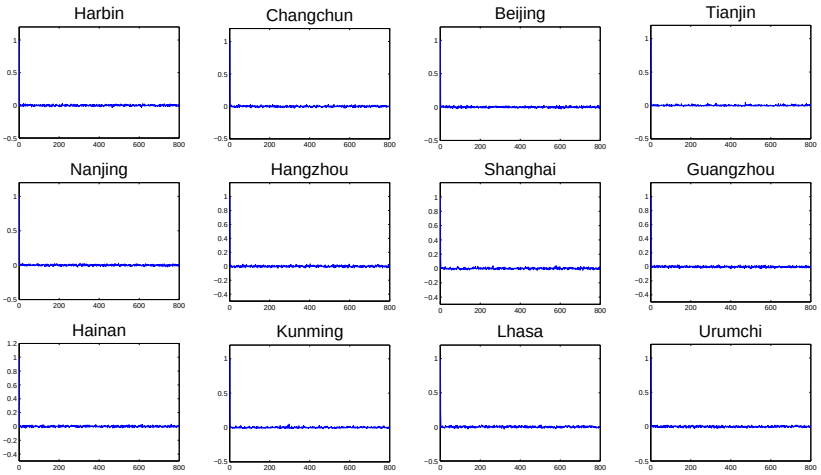

Figure A.17: In-sample MREs of the simulated DATs using the Alaton model [1] (Year: 1983-2012).

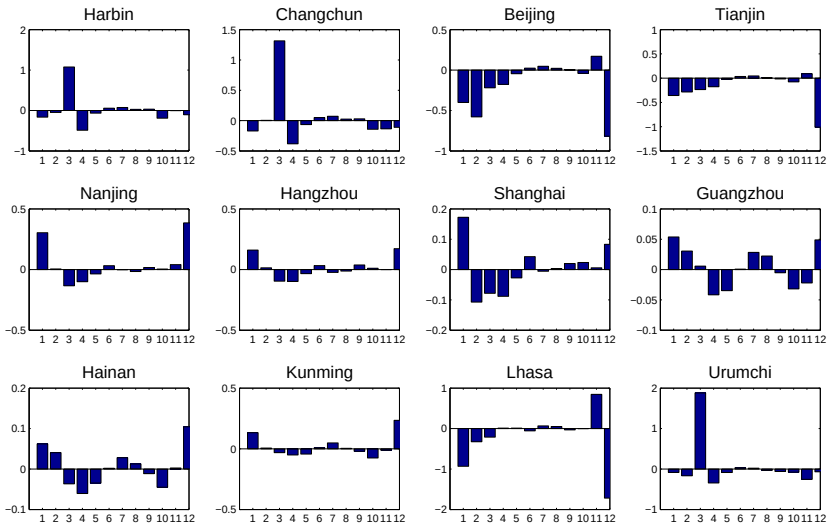

Figure A.18: In-sample MREs of the simulated DATs using the CAR model [2] (Year: 1983-2012).

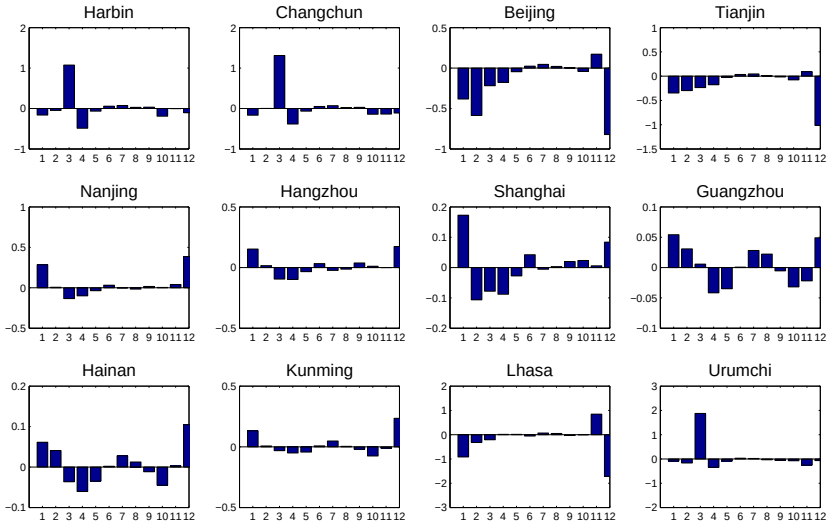

Figure A.19: In-sample MREs of the simulated DATs using the Spline model [3] (Year: 1983-2012).

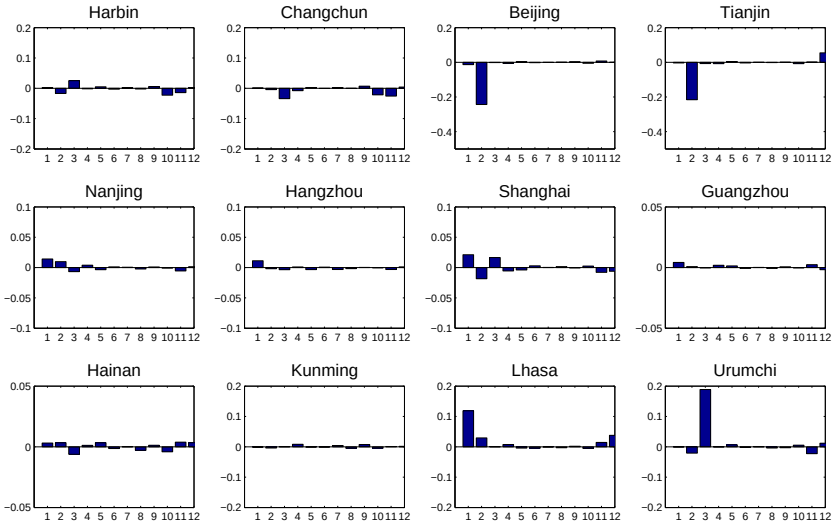

Figure A.20: In-sample MREs of the simulated DATs using the SSV model (Year: 1983-2012).

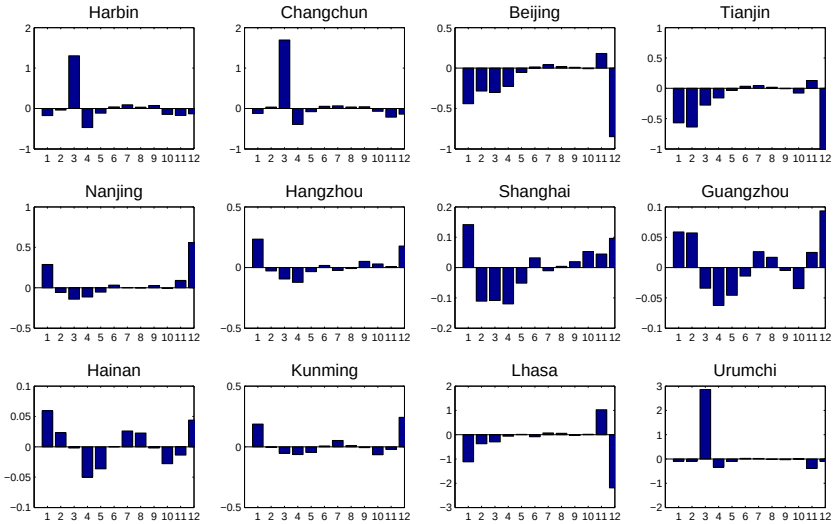

Figure A.21: Out-of-sample MREs of the simulated DATs using the Alaton model [1] (Year: 1983-2012).

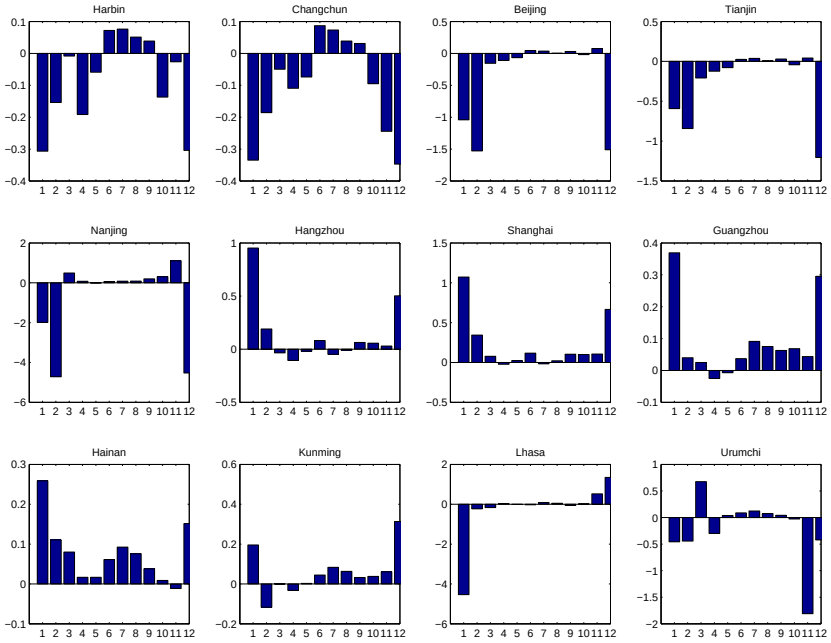

Figure A.22: Out-of-sample MREs of the simulated DATs using the CAR model [2] (Year: 1983-2012).

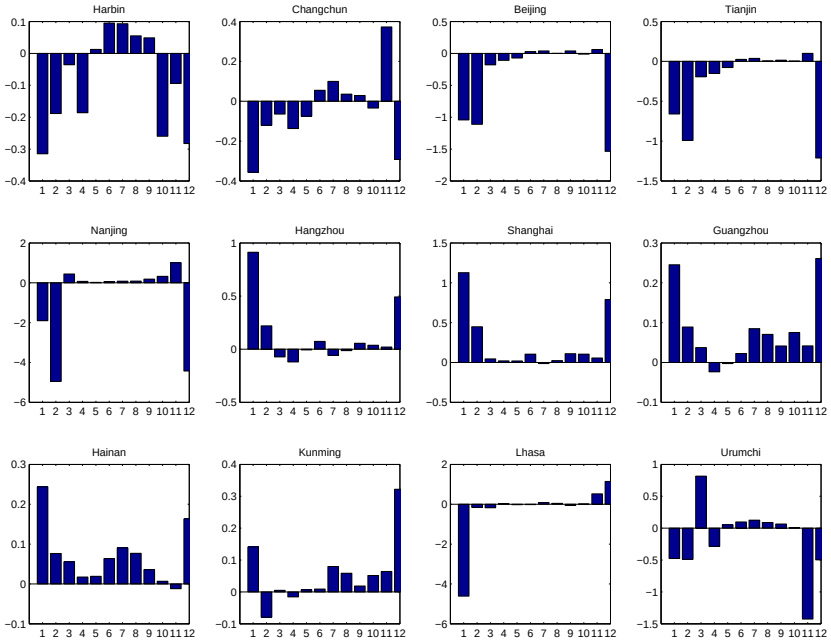

Figure A.23: Out-of-sample MREs of the simulated DATs using the Spline model [3] (Year: 1983-2012).

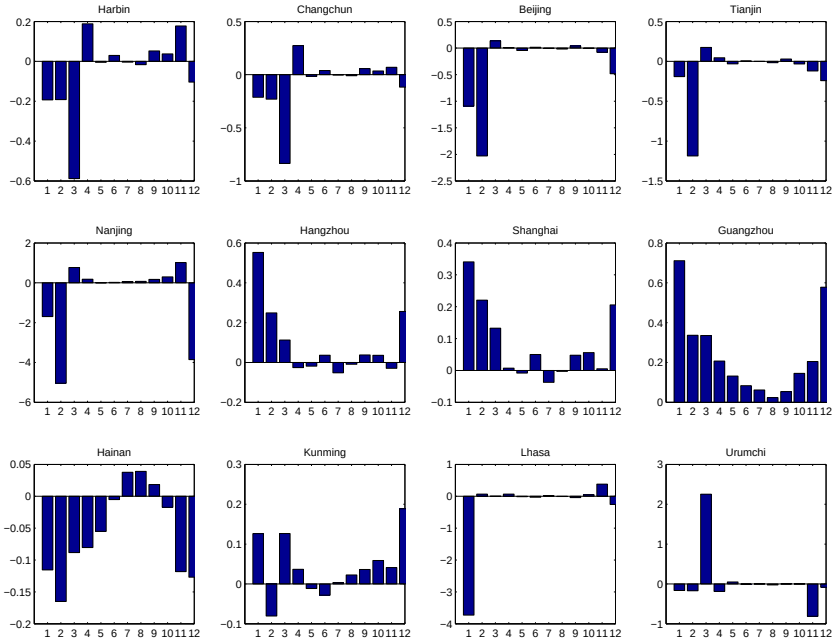

Figure A.24: Out-of-sample MREs of the simulated DATs using the SSV model (Year: 1983-2012).

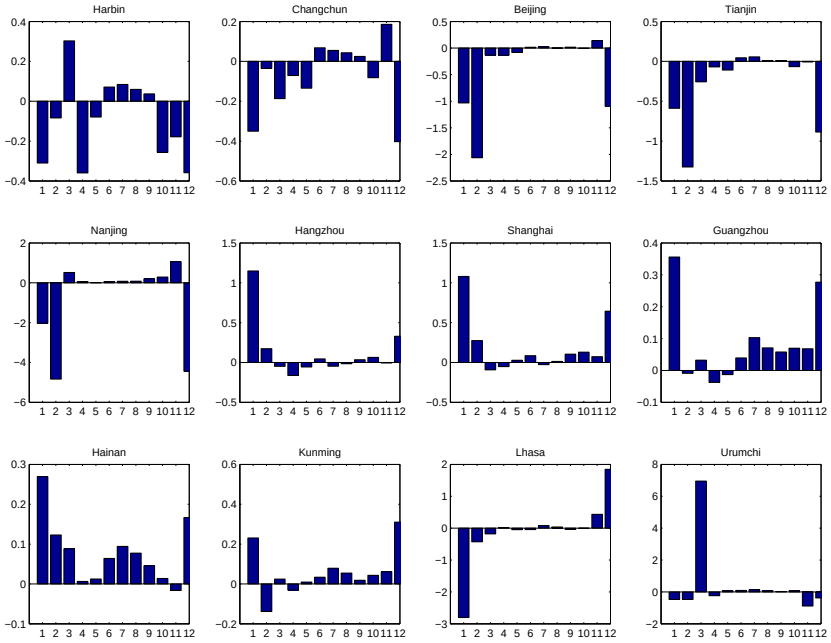

Appendix B

Appendix of tables

Table B.1: In-sample residual normality test for the Alaton model [1], CAR model [2] and the Spline model [3].

	Proportion (Alaton)	Final result (Alaton)	Proportion (CAR)	Final result (CAR)	Proportion (Spline)	Final result (Spline)	Proportion (SSV)	Final result (SSV)
Harbin	0	Rejected	0	Rejected	0	Rejected	2/3	Accepted
Changchun	0	Rejected	0	Rejected	0	Rejected	1/3	Accepted
Beijing	0	Rejected	2/3	Accepted	0	Rejected	1/3	Accepted
Tianjin	1/3	Accepted	2/3	Accepted	0	Rejected	2/3	Accepted
Hangzhou	0	Rejected	1/3	Accepted	3/3	Accepted	1/3	Accepted
Nanjing	2/3	Accepted	2/3	Accepted	2/3	Accepted	2/3	Accepted
Shanghai	0	Rejected	1/3	Accepted	0	Rejected	0	Rejected
Guangzhou	0	Rejected	0	Rejected	0	Rejected	2/3	Accepted
Hainan	0	Rejected	0	Rejected	0	Rejected	2/3	Accepted
Kunming	0	Rejected	0	Rejected	0	Rejected	2/3	Accepted
Lhasa	1/3	Accepted	0	Rejected	0	Rejected	1/3	Accepted
Urumchi	0	Rejected	0	Rejected	0	Rejected	1/3	Accepted

Table B.2: Out-of-sample residual normality test for the Alaton model [1], CAR model [2] and Spline model [3].

	Proportion (Alaton)	Final result (Alaton)	Proportion (CAR)	Final result (CAR)	Proportion (Spline)	Final result (Spline)	Proportion (SSV)	Final result (SSV)
Harbin	2/3	Accepted	2/3	Accepted	2/3	Accepted	3/3	Accepted
Changchun	2/3	Accepted	2/3	Accepted	2/3	Accepted	3/3	Accepted
Beijing	2/3	Accepted	2/3	Accepted	2/3	Accepted	1/3	Accepted
Tianjin	1/3	Accepted	2/3	Accepted	1/3	Accepted	2/3	Accepted
Hangzhou	2/3	Accepted	2/3	Accepted	0	Rejected	3/3	Accepted
Nanjing	1/3	Accepted	2/3	Accepted	1/3	Accepted	3/3	Accepted
Shanghai	0	Rejected	1/3	Accepted	0	Rejected	1/3	Accepted
Guangzhou	0	Rejected	2/3	Accepted	0	Rejected	3/3	Accepted
Hainan	0	Rejected	2/3	Accepted	0	Rejected	3/3	Accepted
Kunming	0	Rejected	2/3	Accepted	0	Rejected	3/3	Accepted
Lhasa	0	Rejected	2/3	Accepted	1/3	Accepted	3/3	Accepted
Urumchi	0	Rejected	2/3	Accepted	0	Rejected	3/3	Accepted

Table B.3: Efficiency comparison among city-based GDD contracts: VaR (Case 1).

City	Climatic zone	Without contract	Absolute deviation	Change	Correlation-adjusted	Change	Indicator function	Change
$VaR_{0.05}$								
Haerbin	I	307.59	312.68	5.08	314.83	7.24	342.92	35.32
Changchun		764.75	786.84	22.08	776.31	11.56	819.11	54.35
Beijing	II	394.05	470.93	76.88	413.07	19.02	489.35	95.30
Shijiazhuang		210.39	308.91	98.52	172.12	-38.27	159.86	-50.53
Ji'nan		231.54	400.90	169.36	207.33	-24.21	221.67	-9.87
Zhengzhou		153.25	264.35	111.10	144.79	-8.46	216.76	63.50
Nanjing	III	580.83	592.05	11.23	574.05	-6.78	581.10	0.27
Hefei		239.09	277.08	37.99	227.42	-11.67	238.42	-0.67
Wuhan		455.55	462.45	6.89	462.64	7.09	457.87	2.32
Hangzhou		274.96	280.34	5.39	280.26	5.30	281.26	6.30
Nanchang		48.52	54.42	5.90	46.96	-1.56	47.69	-0.83
$VaR_{0.1}$								
Haerbin	I	364.83	362.22	-2.62	364.06	-0.77	391.54	26.71
Changchun		838.16	855.54	17.37	837.21	-0.96	888.42	50.26
Beijing	II	430.57	500.90	70.34	440.40	9.83	510.50	79.94
Shijiazhuang		216.70	328.45	111.75	192.51	-24.20	180.97	-35.73
Ji'nan		250.06	414.56	164.51	246.83	-3.23	245.03	-5.03
Zhengzhou		168.44	292.49	124.05	170.85	2.41	244.62	76.18
Nanjing	III	614.00	612.12	-1.87	612.76	-1.24	613.80	-0.20
Hefei		304.69	329.77	25.08	300.76	-3.93	304.39	-0.30
Wuhan		490.54	496.97	6.43	497.63	7.09	491.70	1.16
Hangzhou		297.91	298.19	0.28	308.62	10.71	301.25	3.34
Nanchang		55.38	60.43	5.05	61.80	6.42	54.85	-0.53
$VaR_{0.2}$								
Haerbin	I	422.08	436.53	14.45	437.91	15.84	464.48	42.40
Changchun		923.81	947.14	23.33	922.46	-1.35	969.29	45.48
Beijing	II	467.08	542.87	75.79	488.22	21.14	542.23	75.15
Shijiazhuang		225.12	347.99	122.87	218.00	-7.13	212.65	-12.48
Ji'nan		272.28	433.69	161.41	292.92	20.64	277.73	5.45
Zhengzhou		186.66	325.32	138.66	209.95	23.28	283.62	96.96
Nanjing	III	656.64	668.32	11.67	675.66	19.02	655.83	-0.81
Hefei		362.09	373.68	11.59	374.11	12.02	362.12	0.03
Wuhan		516.78	522.87	6.09	523.86	7.08	517.07	0.29
Hangzhou		320.85	329.42	8.57	353.20	32.35	327.91	7.06
Nanchang		63.62	69.43	5.82	76.64	13.02	64.87	1.25

Table B.4: Efficiency comparison among city-based GDD contracts: VaR (Case 2).

City	Climatic zone	Without contract	Absolute deviation	Change	Correlation-adjusted	Change	Indicator function	Change
				$VaR_{0.05}$				
				$VAR_{0.05}$				
Haerbin	I	307.59	297.92	-9.67	303.79	-3.80	350.63	43.04
Changchun		764.75	786.84	22.09	776.31	11.56	819.11	54.35
Beijing	II	394.05	471.94	77.89	420.56	26.51	397.18	3.13
Shijiazhuang		210.39	308.91	98.52	172.12	-38.27	159.86	-50.53
Ji'nan		231.54	379.57	148.03	218.46	-13.08	211.48	-20.06
Zhengzhou		153.25	262.20	108.95	142.61	-10.64	120.40	-32.86
Nanjing	III	580.83	589.46	8.63	580.28	-0.55	580.78	-0.05
Hefei		239.09	277.08	37.99	227.42	-11.67	238.42	-0.67
Wuhan		455.55	462.84	7.29	460.61	5.06	460.39	4.84
Hangzhou		274.96	286.19	11.23	287.00	12.04	273.80	-1.16
Nanchang		48.52	36.97	-11.55	57.24	8.72	46.90	-1.62
				$VaR_{0.1}$				
Haerbin	I	364.83	362.23	-2.61	352.99	-11.84	414.02	49.19
Changchun		838.16	855.54	17.37	837.21	-0.95	888.42	50.26
Beijing	II	430.57	501.79	71.22	449.55	18.98	429.05	-1.52
Shijiazhuang		216.70	328.45	111.75	192.51	-24.19	180.97	-35.73
Ji'nan		250.06	398.12	148.06	243.02	-7.04	241.47	-8.59
Zhengzhou		168.44	286.60	118.16	171.52	3.08	151.55	-16.89
Nanjing	III	614.00	615.83	1.84	619.21	5.21	613.97	-0.03
Hefei		304.69	329.77	25.08	300.76	-3.93	304.39	-0.30
Wuhan		490.54	497.81	7.27	498.78	8.24	490.83	0.29
Hangzhou		297.91	298.98	1.07	317.71	19.80	297.11	-0.80
Nanchang		55.38	48.82	-6.56	69.94	14.56	53.60	-1.78
				$VaR_{0.2}$				
Haerbin	I	422.08	439.40	17.33	426.79	4.71	490.08	68.01
Changchun		923.81	947.14	23.33	922.46	-1.35	969.29	45.48
Beijing	II	467.08	543.57	76.48	490.14	23.05	480.06	12.97
Shijiazhuang		225.12	347.99	122.87	218.00	-7.13	212.65	-12.48
Ji'nan		272.28	432.58	160.30	279.85	7.57	277.46	5.18
Zhengzhou		186.66	320.77	134.10	206.21	19.55	188.94	2.27
Nanjing	III	656.64	664.17	7.53	669.25	12.61	656.64	0.00
Hefei		362.09	373.68	11.59	374.11	12.02	362.12	0.03
Wuhan		516.78	519.67	2.89	524.22	7.44	516.93	0.15
Hangzhou		320.85	329.99	9.14	367.60	46.75	320.42	-0.43
Nanchang		63.62	65.42	1.80	85.17	21.55	64.32	0.70

Table B.5: Efficiency comparison among climatic zone-based GDD contracts: VaR.

City	Climatic zone	Without contract	Weight: Case 1	VaR Increase	Weight: Case 2	VaR Increase	Weight: Case 3	VaR Increase
$VaR_{0.05}$								
Haerbin	I	307.59	294.03	-13.57	302.39	-5.2	311.74	4.15
Changchun		764.75	783.93	19.18	784	19.24	785.55	20.80
Beijing	II	394.05	474.33	80.28	475.15	81.1	471.65	77.60
Shijiazhuang		210.39	314.74	104.35	311.04	100.66	288.10	77.71
Ji'nan		231.54	392.6	161.06	391.56	160.01	357.54	126.00
Zhengzhou		153.25	271.37	118.11	268.51	115.25	246.12	92.86
Nanjing	III	580.83	588.33	7.5	588.9	8.07	586.25	5.42
Hefei		239.09	248.37	9.28	252.92	13.83	253.40	14.31
Wuhan		455.55	463.1	7.54	464.01	8.46	465.31	9.76
Hangzhou		274.96	282.84	7.88	281.77	6.82	279.70	4.74
Nanchang		48.52	41.46	-7.05	38.74	-9.78	45.40	-3.12
$VaR_{0.1}$								
Haerbin	I	364.83	357.59	-7.24	353.69	-11.14	373.35	8.51
Changchun		838.16	853.44	15.27	853.38	15.21	855.16	17.00
Beijing	II	430.57	503.79	73.22	504.57	74.01	501.27	70.70
Shijiazhuang		216.70	330.21	113.51	329.98	113.28	310.05	93.34
Ji'nan		250.06	409.36	159.3	411.14	161.08	379.13	129.08
Zhengzhou		168.44	294.67	126.23	292.17	123.73	277.79	109.35
Nanjing	III	614	613.19	-0.81	613.04	-0.95	615.17	1.17
Hefei		304.69	318.42	13.73	323.71	19.02	316.26	11.57
Wuhan		490.54	498.21	7.67	495.03	4.49	496.49	5.95
Hangzhou		297.91	300.91	3.01	300.69	2.79	301.36	3.45
Nanchang		55.38	52.87	-2.51	50.92	-4.46	57.39	2.01
$VaR_{0.2}$								
Haerbin	I	422.08	433.87	11.79	430.64	8.56	447.27	25.20
Changchun		923.81	946.11	22.3	945.88	22.07	947.97	24.16
Beijing	II	467.08	539.13	72.05	539.88	72.8	542.74	75.66
Shijiazhuang		225.12	351.87	126.75	348.92	123.8	335.65	110.53
Ji'nan		272.28	431.7	159.42	430.71	158.43	422.33	150.05
Zhengzhou		186.66	327.29	140.62	325.3	138.63	309.47	122.80
Nanjing	III	656.64	662.92	6.28	665.36	8.72	668.18	11.54
Hefei		362.09	370.96	8.87	376.81	14.72	379.12	17.03
Wuhan		516.78	520.15	3.37	521.62	4.84	523.21	6.43
Hangzhou		320.85	326.21	5.36	327.17	6.32	331.68	10.83
Nanchang		63.62	66.57	2.95	65.54	1.92	71.77	8.15

Bibliography

[1] Alaton, P., Djehiche, B., and Stillberger, D. (2002), *On Modeling and Pricing Weather Derivatives*, Applied Mathematical Finance, vol.9, no.88, 1-20.

[2] Benth, F.E., Saltyte Benth, J. and Koekebakker, S. (2007), *Putting a Price on Temperature*, Scandinavian Journal of Statistics, vol. 34, no. 4, 746-767.

[3] Schiller, F., Seidler, G. and Wimmer, M. (2012), *Temperature Models for Pricing Weather Derivatives*, Quantitative Finance, vol.12, no.3, 489-500.

[4] Weather Risk Management Association (2011), *Weather Risk Derivative Survey*, May 2011.

[5] Jewson, S., Brix, A. and Ziehmann, C., 2005. *Weather Derivative Valuation: The Meterological, Statistical, Financial and Mathematical Foundations*, Cambridge University Press, Cambridge, England.

[6] Liu, X., 2006. *Weather Derivatives: A Contemporary Review and Its Application in China*. Master Thesis, University of Nottingham, England.

[7] Zong, L. and Ender, M. (2014), *Model Comparison for Temperature-based Weather Derivatives in Mainland China*, Emerging Markets Finance and Trade, vol.50, no.5, 68-86.

[8] Turvey, C G. and Kong, R. (2010), *Weather Risk and the Viability of Weather Insurance in China's Gansu, Shaanxi, and Henan Provinces*, China Agricultural Economic Review, vol.2, no.1, 5-24.

[9] Heimfarth, L. and Musshoff, O. (2011), *Weather index-based Insurances for Farmers in the North China Plain: An Analysis of Risk Reduction Potential and basis Risk*, Agricultural Finance Review, vol.71, no.2, 218-239.

[10] Ender, M. and Zhang, R. Y. (2014), *Efficiency of Weather Derivatives for Chinese Agriculture Industry*, Accepted for publication in: China Agricultural Economic Review.

[11] China News Service Website (Webpage). *Population of Mainland China at the end of 2014*.
(URL): http://www.chinanews.com/gn/2015/02-26/7080280.shtml
Accessed [02/26/2015]

[12] Vedenov, D. V. and Barnett,B. J. (2004), *Efficiency of Weather Derivatives as Primary Crop Insurance Instruments*, Journal of Agricultural and Resource Economics, vol.29, 387-403.

[13] Pelka, N. and Musshoff, O. (2013), *Hedging Effectiveness of Weather Derivatives in Arable Farming - Is There a Need for Mixed Indices?*, Agricultural Finance Review, vol.73, no.2, 358-372.

[14] Weather China (Webpage). *Daily average temperature*. (URL): http://baike.weather.com.cn/index.php?doc-view-1648.php Accessed [08/30/2011]

[15] Goncu, A. and Zong, L (2013), *Pricing Futures and Options on a Basket of Temperature Indices*, Review of Futures Markets, vol.1, no.1, 9-18.

[16] Woodard, J. D. and Garcia, P. (2008), *Basis Risk and Weather Hedging Effectiveness*, Agricultural Finance Review, vol.68, no.1, 99-117.

[17] Platen, E. and West, J. (2004), *A Fair Pricing Approach to Weather Derivatives*, Asia-Pacific Financial Markets, vol.11, no.1, 23-53.

[18] Cao, M. and Wei, J. (2004), *Weather Derivatives Valuation and Market Price of Weather Risk*, ournal of Future Markets, vol.24, no.11, 1065-1089.

[19] Lucas, R. E. (1978), *Asset Prices in an Exchange Economy*, Econometrica, vol.46, 1429-1445.

[20] Davis, M. (2001), *Pricing Weather Derivatives by Marginal Value*, Quantitative Finance, vol.1, 1-4.

[21] Platen, E. (2002), *Arbitrage in Continuous Complete Markets*, Advances in Applied Probability, vol.34, no.3, 540-558.

[22] Dornier, F. and Queruel, M. (2000), *Caution to the Wind*, Energy and Power Risk Management, Weather Risk Special Report, August, 30-32.

[23] Brody, D.C., Syroka, J. and Zervos, M. (2002), *Dynamical Pricing of Weather Derivatives*, Quantitative Finance, vol.2, no.3, 189-198.

[24] Benth, F.E. and Saltyte Benth, J. (2011), *Weather Derivatives and Stochastic Modelling of Temperature*, International Journal of Stochastic Analysis, vol.2011.

[25] Caballero, R., Jewson, S. and Brix, A. (2002), *Long Memory in Surface Air Temperature: Detection, Modeling, and Application to Weather Derivative Valuation*, Climate Research, vol. 21, 127-140.

[26] Jewson, S. and Caballero, R. (2003), *Seasonality in the Statistics of Surface Air Temperature and Pricing of Weather Derivatives*, Meteorological Applications, vol.10, no.4, 367-376.

[27] Campbell, S. D. and Diebold F. X. (2005), *Weather forecasting for weather derivatives*, Journal of the American Statistical Association, vol.100, 6-16 .

[28] Benth, F.E., Saltyte Benth, J. and Koekebakker, S., 2008. *Stochastic Modelling of Electricity and related Markets*, World Scientific Publishing, Singapore.

[29] Goncu, A. (2011), *Pricing Temperature-based Weather Derivatives in China*, Journal of Risk Finance, vol.13, no.1, 32-44.

[30] Benth, F. E., Hardle, W. K. and Cabrera, B. L., 2011. *Pricing of Asian temperature risk*. Tools for Finance and Insurance, Springer Berlin Heidelberg, 163-199.

[31] Sun, B. and Van Kooten, G. C. (2015), *Financial Weather Derivatives for Corn Production in Northern China: A Comparison of Pricing Methods*, Journal of Empirical Finance.

[32] Goncu, A. (2013), *Modeling and Pricing Precipitation-based Weather Derivatives*, Financial Mathematics and Applications, vol.21, 151-171.

[33] Zhu, J., Pollanen, M., Abdella, K., and Cater, B. (2012), *Modeling Drought Option Contracts*, ISRN Applied Mathematics, 1-16.

[34] Lou, W. and Sun, S. (2003), *Design of Agricultural Insurance Policy for Tea Tree Freezing Damage in Zhejiang Province, China*, Theoretical and Applied Climatology, vol.111, no.3-4, 713-728.

[35] Mraoua, M. and Bari, D. (2005), *Temperature Stochastic Modeling and Weather Derivatives Pricing: Empirical Study With Moroccan Data*, Afrika Statistika, vol.2, no.1, 22-43.

[36] Broni-Mensah, E. K., 2012. *Numerical Solutions of Weather Derivaties and Other Incomplete Market Problems*. Ph.D. Thesis, University of Manchester, England.

[37] Broadie, M. and Kaya, O. (2006), *Exact Simulation of Stochastic Volatility and Other Affine Jump Diffusion Processes*, Operations Research, vol.54, no.2, 217-231.

[38] Kahl, C. and Jackel, P. (2006), *Fast Strong Approximation Monte Carlo Schemes for Stochastic Volatility Models*, Quantitative Finance, vol.6, no.6, 513-536.

[39] Andersen, L. (2007), *Efficient Simulation of the Heston Stochastic Volatility Model*, SSRN eLibrary.

[40] Lord, R., Koekkoek, R. and Dijk, D. V. (2010), *A Comparison of Biased Simulation Schemes for Stochastic Volatility Models*, Quantitative Finance, vol.10, no.2, 177-194.

[41] Heston, S. (1993), *A Closed-Form Solutions for Options with Stochastic Volatility with Applications to Bond and Currency Options*, Review of Financial Studies, vol.6, 327-343.

[42] Milstein, G. N., Platen, E. and Schurz, H. (1998), *Balanced Implicit Methods for Stiff Stochastic Systems*, SIAM Journal on Numerical Analysis, vol.38, no.3, 1010-1019.

[43] Van Haastrecht, A. and Pelsser, A. (2010), *Efficient, Almost Exact Simulation of the Heston Stochastic Volatility Model*, International Journal of Theoretical and Applied Finance, vol.13, no.1, 1-43.

[44] Rosenzweig, C., Iglesias, A., Yang, X. B., Epstein, P. R. and Chivian, E. (2001), *Climate change and extreme weather events; implications for food production, plant diseases, and pests*, Global change and Human Health, vol.2, no.2, 90-104.

[45] Hess, U., Richter, K. and Stoppa, A., 2002. *Weather risk management for agriculture and agri-business in developing countries*. Dischel, Robert, Ed..

[46] Arnold, M., 2008. *The role of risk transfer and insurance in disaster risk reduction and climate change adaptation*. Stockholm: Commission on Climate Change and Development, Tech Report.

[47] Linnerooth-Bayer, J. and Mechler, R. (2006), *Insurance for assisting adaptation to climate change in developing countries: a proposed strategy*, Climate policy, vol.6, no.6, 621-636.

[48] Mahul, O. and Stutley, C. J., 2010. *Government Support to Agricultural Insurance: Challenges and Options for Developing Countries*. World Bank Publications, Washington, DC, Tech Report.

[49] Skees, J. R., Barnett, B. J. and Collier, B., 2008. *Skees, J. R., Barnett, B. J. and Collier, B.*. Prepared for the OECD Expert Workshop on Economic Aspects of Adaptation.

[50] Hellmuth, M. E., Osgood, D. E., Hess, U., Moorhead, A. and Bhojwani, H., 2009. *Index insurance and climate risk: Prospects for development and disaster management*. Climate and Society No. 2. International Research Institute for Climate and Society (IRI), Columbia University, New York, USA, Tech Report.

[51] Sun, B., Guo, C. and van Kooten, G. C. (2014), *Hedging Weather Risk for Corn Production in Northestern China*, Agricultural Finance Review, vol.74, no.4, 555-572.

[52] Pelka, N., Musshoff, O. and Finger, R. (2014), *Hedging Effectiveness of Weather Index-based Insurance in China*, China Agricultural Economic Review, vol.6, no.2, 212-228.

[53] Kong, R., Turvey, C. G., He, G., Ma, J. and Meagher, P. (2011), *Factors Influencing Shaanxi and Gansu Farmers' Willingness to Purchase Weather Insurance*, China Agricultural Economic Review, vol.3, no.4, 423-440.

[54] Okhrin, O., Odening, M. and Wei, X. (2013), *Systematic Weather Risk and Crop Insurance: the Case of China*, The Journal of Risk and Insurance, vol.80, no.2, 351-372.

[55] Hellmuth, M. E., Osgood, D. E., Hess, U., Moorhead, A. and Bhojwani, H., 2009. *Index insurance and climate risk: Prospects for development and disaster management*. Climate and Society No. 2. International Research Institute for Climate and Society (IRI), Columbia University, New York, USA, Tech Report.

[56] Swiss Re, 2009. *An Insurance Recipe for the Chinese Food and Agricultural Industry*. Techincal Publishing, Swiss Re, Tech Report.

[57] Markowitz, H. M., 1991. *Portfolio Selection: Efficiency Diversification of Investments*, 2nd ed. Cambridge, MA: Basil Blackwell.

[58] Babcock, B. A., Choi, E. K. and Feinerman, E. (1993), *Risk and Probability Premiums for CARA Utility Functions*, Journal of Agricultural and Resource Economics, vol.18, no.1, 17-24.